

Electronic Supporting Information

Water as a monomer: synthesis of an aliphatic polyethersulfone from divinyl sulfone and water

Karin Ratzenböck, Mir Mehraj Ud Din, Susanne M. Fischer, Ema Žagar, David Pahovnik,
A. Daniel Boese, Daniel Rettenwander and Christian Slugovc

Table of Contents

1. General Information	2
2. General Procedures for Reaction Screening	4
3. Synthesis	6
a. Poly(oxy-1,2-ethanediylsulfonyl-1,2-ethanediyl) (PES)	
b. 1,4-oxathiane 4,4-dioxide (1)	
4. MALDI-TOF MS	13
5. Reaction Progress	18
6. Synthesis	25
a. PES in solution	
b. Bis-(2-methanesulfonyl-ethyl) ether	
c. PES with D ₂ O	
7. Computational Details	37
8. SEC chromatogram with Different Detectors	40
9. Bulk NMR Experiments	41
10. Properties	48
11. Electrochemical Application	50
12. References	56

1. General Information

All experiments were performed under ambient conditions. Chemicals were purchased from Alfa Aesar, Acros Organics, Sigma Aldrich or TCI and were used as received.

NMR spectroscopy: ^1H - and ^{13}C -NMR spectra were recorded on a Bruker Avance 300 MHz spectrometer (^1H : 300.36 MHz; ^{13}C : 75.53 MHz), a Bruker Avance NEO 400 MHz spectrometer (^1H : 400.14 MHz) or a Varian Inova 500 MHz instrument (^1H : 499.84 MHz; ^{13}C : 125.69 MHz) at 25 °C. Chemical shifts δ are given in ppm relative to residual protons and carbon signals of the deuterated solvent. Deuterated solvents were obtained from Cambridge Isotope Laboratories Inc.

Matrix-assisted laser desorption/ionization time-of-flight mass spectrometry (MALDI-TOF MS) measurements were performed using a Bruker UltrafleXtreme MALDI-TOF mass spectrometer (Bruker Daltonik). Samples were dissolved in HFIP (10 mg mL⁻¹) and mixed with a solution of matrix, 2,6-dihydroxyacetophenone in THF (30 mg mL⁻¹), and sodium trifluoroacetate in THF (10 mg mL⁻¹), at a volume ratio of 1:10:3. The solution (0.5 μL) was spotted onto the target plate (dried-droplet method). The reflective positive ion mode was used to record the mass spectra of the samples. Calibration was done externally with the poly(methyl methacrylate) standards (MALDI validation set PMMA, Fluka Analytical) using the nearest-neighbor position method.

The molar mass characteristics were determined by **size-exclusion chromatography (SEC)** coupled with an Optilab differential Refractive Index detector (RI, Wyatt Technology Corporation, USA). Separations of samples were performed at 50 °C in dimethyl sulfoxide (DMSO; purity $\geq 99.8\%$, Acros Organics, Belgium) containing 0.1 M LiBr (purity $\geq 99\%$, Honeywell, USA) using an Agilent 1260 HPLC chromatograph (Agilent Technologies, USA) and Polar Gel-M (7.5 \times 300 mm, 8 μm) analytical column with precolumn (Varian, USA). For kinetics measurement, Polar Gel-L SEC (7.5 \times 300 mm, 8 μm ; Agilent Laboratories, USA) analytical column with precolumn was used. The nominal flow rate of the eluent on both columns was 0.7 mL min⁻¹. The Polar Gel-M and Polar Gel-L SEC columns were calibrated with 18 and 10 poly(methyl methacrylate) standards (Agilent Technologies, USA), respectively, with narrow molar mass distribution and dissolved in the same solvent. The concentrations of samples and standards were typically 10 mg mL⁻¹, while the corresponding injected masses on the column were typically 1 mg. Astra 8.0.1.21 software with conventional calibration module (Wyatt Technology Corporation, USA) was used for data acquisition and evaluation.

Low resolution mass spectra were acquired by an Expression CMS L compact mass spectrometer from Advion. The spectrometer was equipped with an APCI (atmospheric-pressure chemical ionisation) ionisation source and quadrupole mass analyzer (range 10-2000 m/z).

IR spectra were recorded on a Bruker ALPHA FT-IR spectrometer from 4000-400 cm^{-1} with a resolution of 2 cm^{-1} and a sample scan time of 24 scans per spectrum.

For **powder X-ray diffractometric measurements (XRD)**, a Rigaku MiniFlex diffractometer operating with $\text{Cu K}\alpha$ radiation with a wavelength of 0.15418 nm was used. Data was collected at angles of 2θ ranging from 10° to 80° .

Thermogravimetric analysis (TGA) was performed with a Netzsch simultaneous thermal analyzer STA 449C (crucibles: aluminum from Netzsch). The heating rate was $10^\circ\text{C}/\text{min}$ until a final temperature of 550°C was reached. A helium flow of $20\text{ mL}\cdot\text{min}^{-1}$ was used in combination with a protective flow of helium of $10\text{ mL}\cdot\text{min}^{-1}$.

Differential scanning calorimetry (DSC) measurements were performed on a PerkinElmer DSC 8500 instrument using aluminum sealed pans. A temperature range from -30 to 120°C with a heating and cooling rate of $20^\circ\text{C}/\text{min}$ for the first and second run and $40^\circ\text{C}/\text{min}$ for the third run was chosen. The glass-transition temperature (T_g) was determined from the second heating run ($20^\circ\text{C}/\text{min}$) and the third heating run ($40^\circ\text{C}/\text{min}$).

In all experiments, deionized water was used; for easier readability deionized water is simply referred to as water in the manuscript.

2. General Procedures for Reaction Screening

General procedure for catalyst screening:

A 4 mL reaction vessel was charged with 5 mol% of the respective catalyst (**Table 1**). 10 equiv. deionized H₂O (152 mg, 8.44 mmol) and 1 equiv. (100 mg, 0.846 mmol) divinyl sulfone were added subsequently. The reaction mixture was stirred at rt under air atmosphere. The reaction progress was monitored by ¹H-NMR spectroscopy after 1 h and 24 h. The polymer precipitated and an off-white, brittle solid which is insoluble in all common solvents except for DMSO was isolated.

General procedure for screening of reaction parameters:

A 4 mL reaction vessel was charged with the respective catalyst (2, 5 or 10 mol%) (**Table 2**). Deionized H₂O (10, 20 or 100 equiv.) and 1 equiv. (100 mg, 0.846 mmol) divinyl sulfone were added subsequently. The reaction mixture was stirred at rt (or lowered or elevated temperature if noted) under air atmosphere. The reaction progress was monitored by ¹H-NMR spectroscopy after 1 h and 24 h.

Calculation of double bond conversion:

The double bond conversion of divinyl sulfone was calculated as follows:

(6.21 ppm -CH=CH₂ end group, 3.97 ppm -O-CH₂-cyclic, 3.81 ppm -O-CH₂-repeating unit)

Double bond conversion [%]

$$= \frac{\int -O-CH_2\text{-repeating unit} + \int -O-CH_2\text{-cyclic}}{\int -CH=CH_2\text{ end group} + \int -O-CH_2\text{-repeating unit} + \int -O-CH_2\text{-cyclic}} * 100$$

For further peak assignment see “Synthesis of **PES**”.

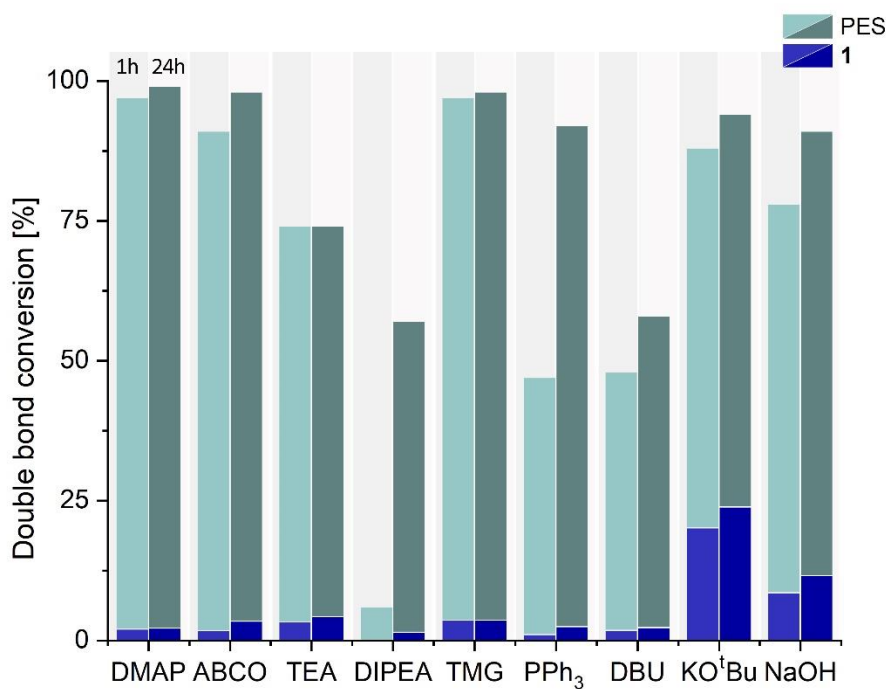


Figure S1. Figure representing data in **Table 1**; double bond conversion after 1 h and 24 h in the catalyst screening and the distribution of the product divided in **PES** and **1**.

Exemplary spectra for screening:

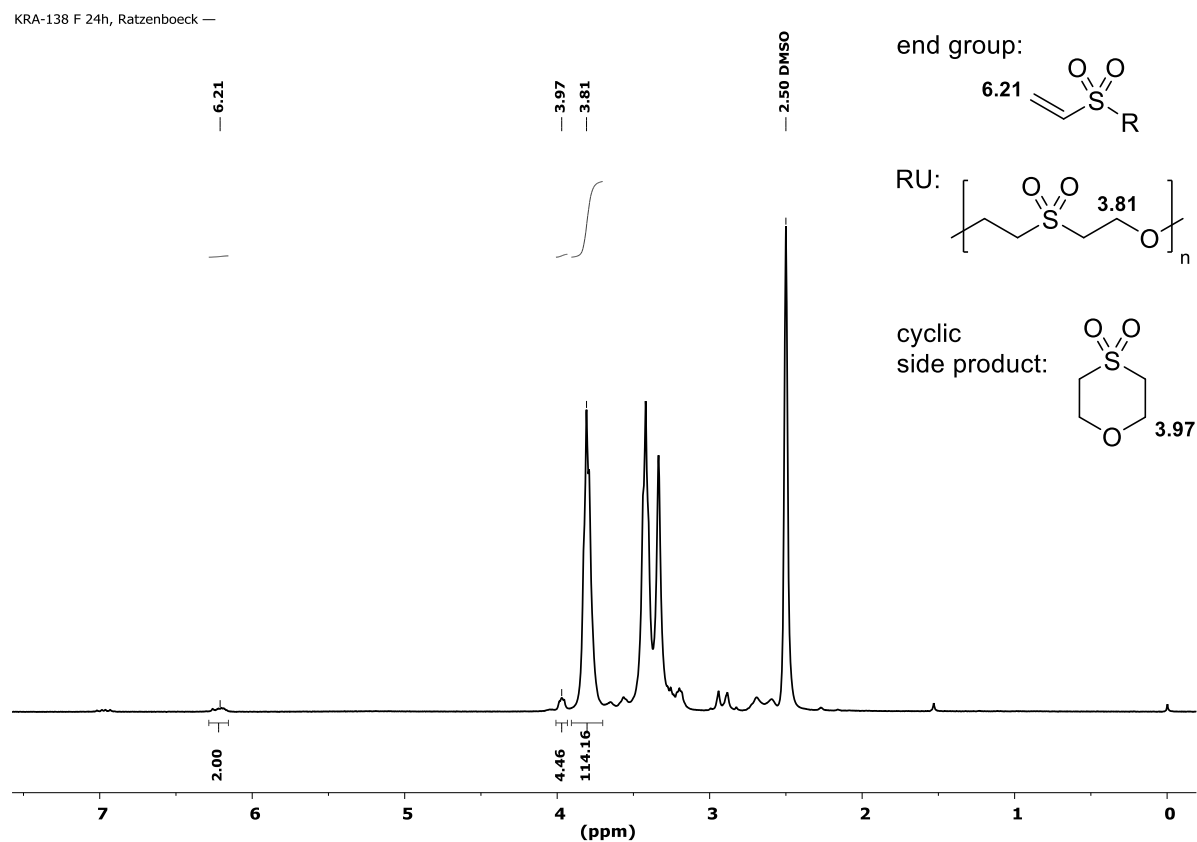


Figure S2. Exemplary ¹H-NMR spectrum of **entry 5** in **Table 1** (5 mol% TMG, 10 equiv. H₂O, rt) after 24 h reaction time in DMSO-*d*₆ with a calculated double bond conversion of 98%; 3.33 ppm residual water.

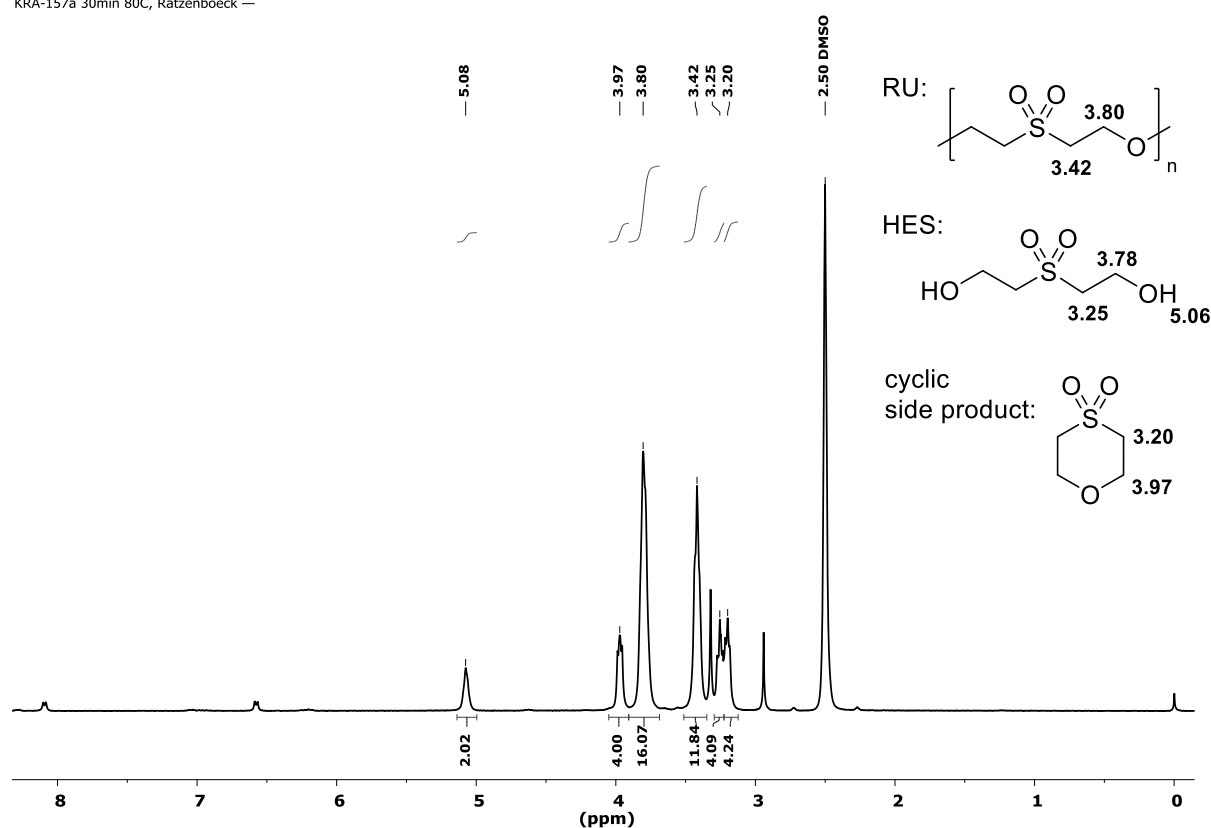


Figure S3. ^1H -NMR spectrum of **entry 14 in Table 2** (5 mol% DMAP, 10 equiv. H_2O , 80 °C) after 30 min reaction time in $\text{DMSO}-d_6$; 3.33 ppm residual water.

Bis(2-hydroxyethyl) sulfone (HES)

^1H -NMR (300 MHz, $\text{DMSO}-d_6$): δ = 5.06 (s, 2H), 3.78 (t, 4H), 3.25 (t, 4H) ppm.

3. Synthesis

Poly(oxy-1,2-ethanediylsulfonyl-1,2-ethanediyl) (PES)

In a 4 mL reaction vessel 4.9 mol% (15.2 mg, 0.124 mmol) DMAP was dissolved in 448 mg (24.9 mmol, 10 equiv.) deionized H_2O . After the addition of 297 mg (2.52 mmol, 1 equiv.) divinyl sulfone, the reaction mixture was stirred at room temperature for 1 h. The polymer precipitated as an off-white product from the reaction mixture (Figure S4). Either the crude polymer was used or the reaction was quenched by the addition of 200 μL 1 M HCl. Thereafter, the product was filtered, washed with deionized H_2O (3 x 0.5 mL) and dried in vacuo. As pure product a brittle, off-white polymer (311.1 mg, 87 %) was isolated (Figure S7).

IR (cm^{-1}): ν = 1279 (s, S=O), 1120 (s, S=O), 1097 (s, C-O)

^1H -NMR (500 MHz, $\text{DMSO-}d_6$): δ = 8.28 (d, J = 7.6 Hz, $-\text{CH-}$ DMAP $^+$ end group), 8.09 (residual DMAP), 7.04 (d, J = 7.0 Hz, $-\text{CH-}$ DMAP $^+$ end group), 7.00 – 6.94 (m, $-\text{CH=CH}_2$ end group), 6.58 (residual DMAP), 6.25 – 6.19 (m, $-\text{CH=CH}_2$ end group), 4.63 (t, J = 6.5 Hz, $-\text{N-CH}_2-$ DMAP $^+$ end group), 3.97 (s, $-\text{O-CH}_2-$ cyclic), **3.81** (t, **$-\text{O-CH}_2-$**), 3.78 (m, $-\text{CH}_2\text{-OH}$ end group), **3.42** (t, **$-\text{CH}_2\text{-SO}_2-$**), 3.26 (m, $-\text{CH}_2\text{-CH}_2\text{-OH}$ end group), 3.19 (s, $-\text{CH}_2\text{-SO}_2-$ cyclic and $-\text{CH}_3$ DMAP $^+$ end group), 2.94 (residual DMAP) ppm.

^{13}C -NMR (76 MHz, $\text{DMSO-}d_6$): δ = 156.0 (C_q DMAP $^+$ end group), 153.9 (C_q , residual DMAP), 149.3 (CH, residual DMAP), 142.4 (CH DMAP $^+$ end group), 137.9 ($-\text{CH=CH}_2$ end group), 129.0 ($-\text{CH=CH}_2$ end group), 107.4 (CH DMAP $^+$ end group), 106.7 (CH, residual DMAP), 65.8 ($-\text{O-CH}_2-$ cyclic), **63.9** (**$-\text{O-CH}_2-$**), 56.2 ($-\text{CH}_2\text{-CH}_2\text{-OH}$ end group), 55.0 ($-\text{CH}_2\text{-CH}_2\text{-OH}$ end group), **53.5** (**$-\text{CH}_2\text{-SO}_2-$**), 52.1 ($-\text{CH}_2\text{-SO}_2-$ cyclic), 38.6 (CH_3 , DMAP) ppm.

Ratzenboeck, KRA-124 DRY, — konzentrierte Lsg —

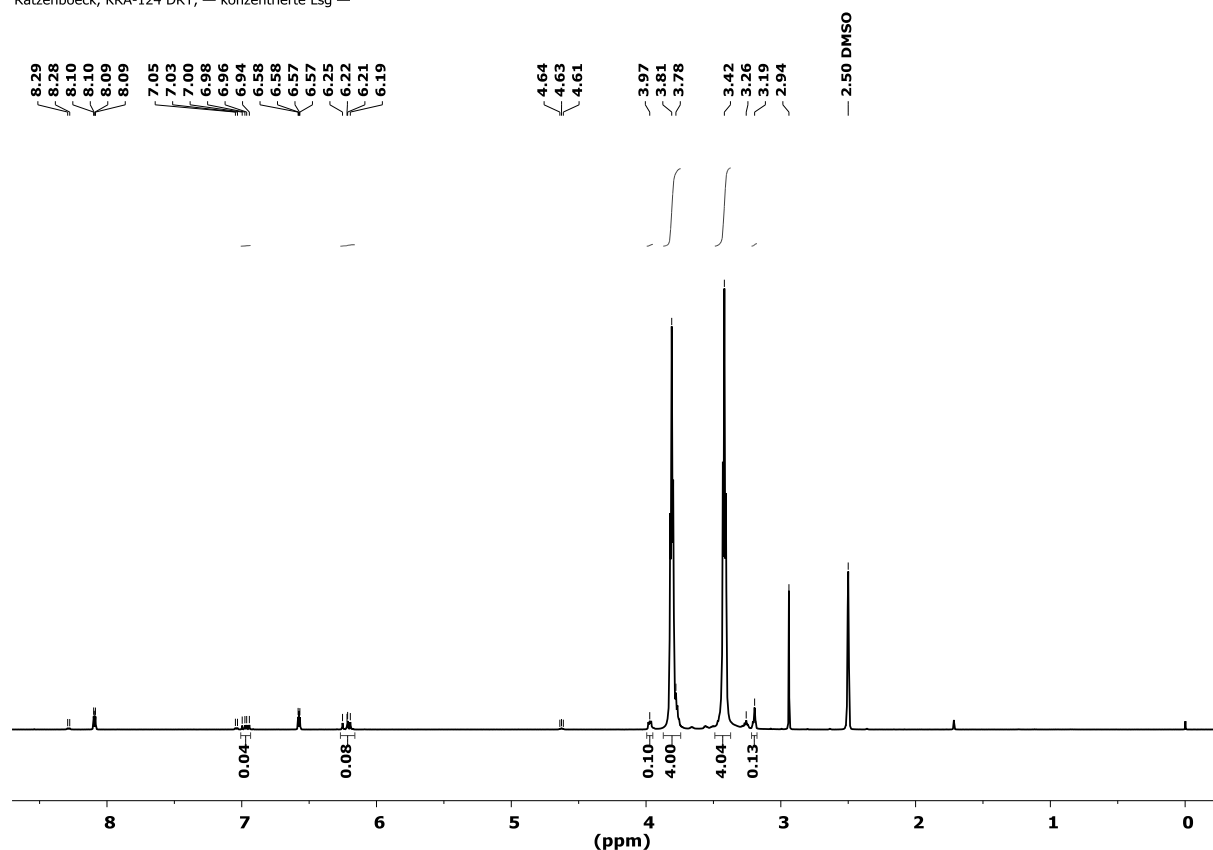
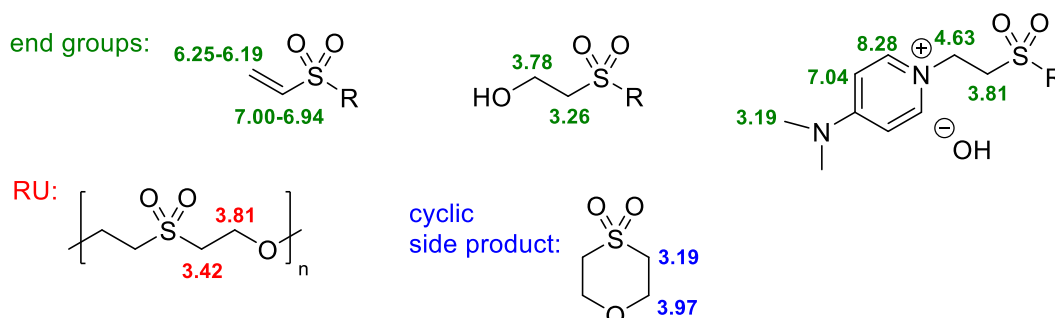


Figure S4. ^1H -NMR spectrum of **PES** (catalyzed by DMAP) under optimized reaction conditions in $\text{DMSO-}d_6$.



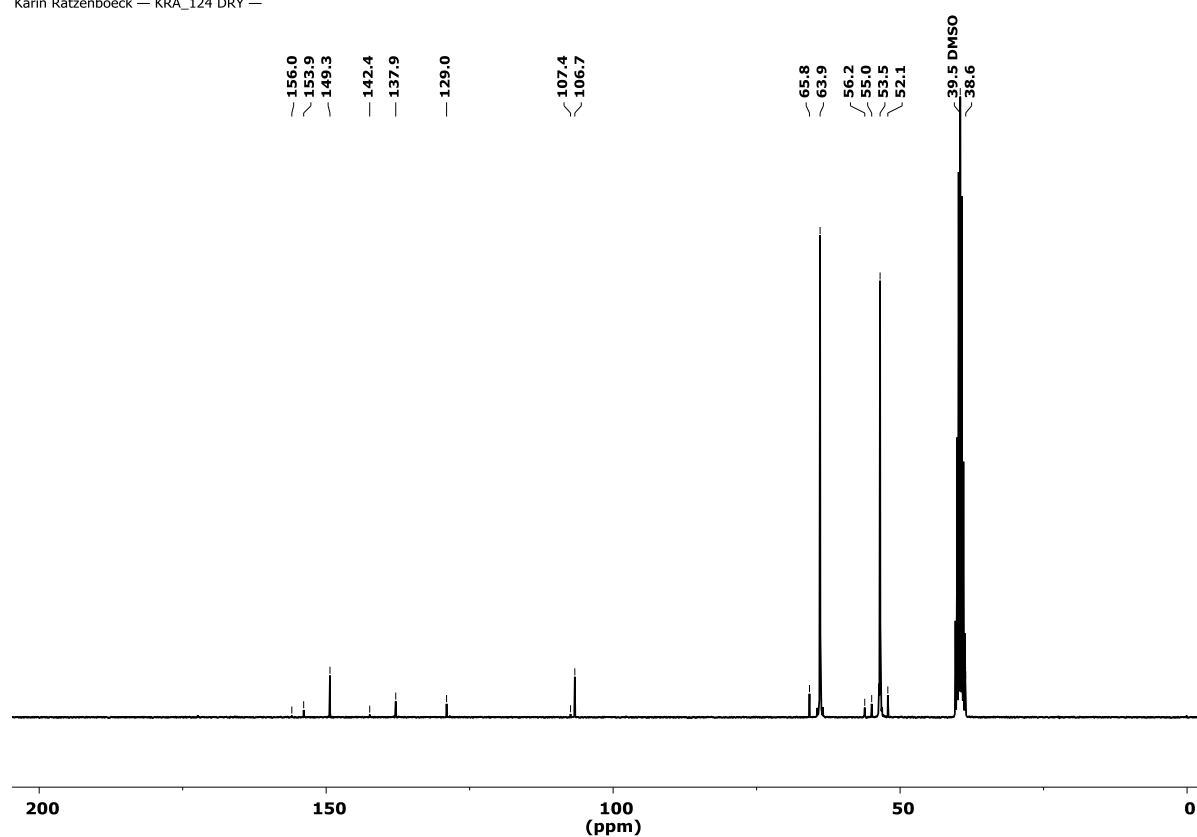


Figure S5. ¹³C-NMR spectrum of **PES** (catalyzed by DMAP) under optimized reaction conditions in DMSO-*d*₆.

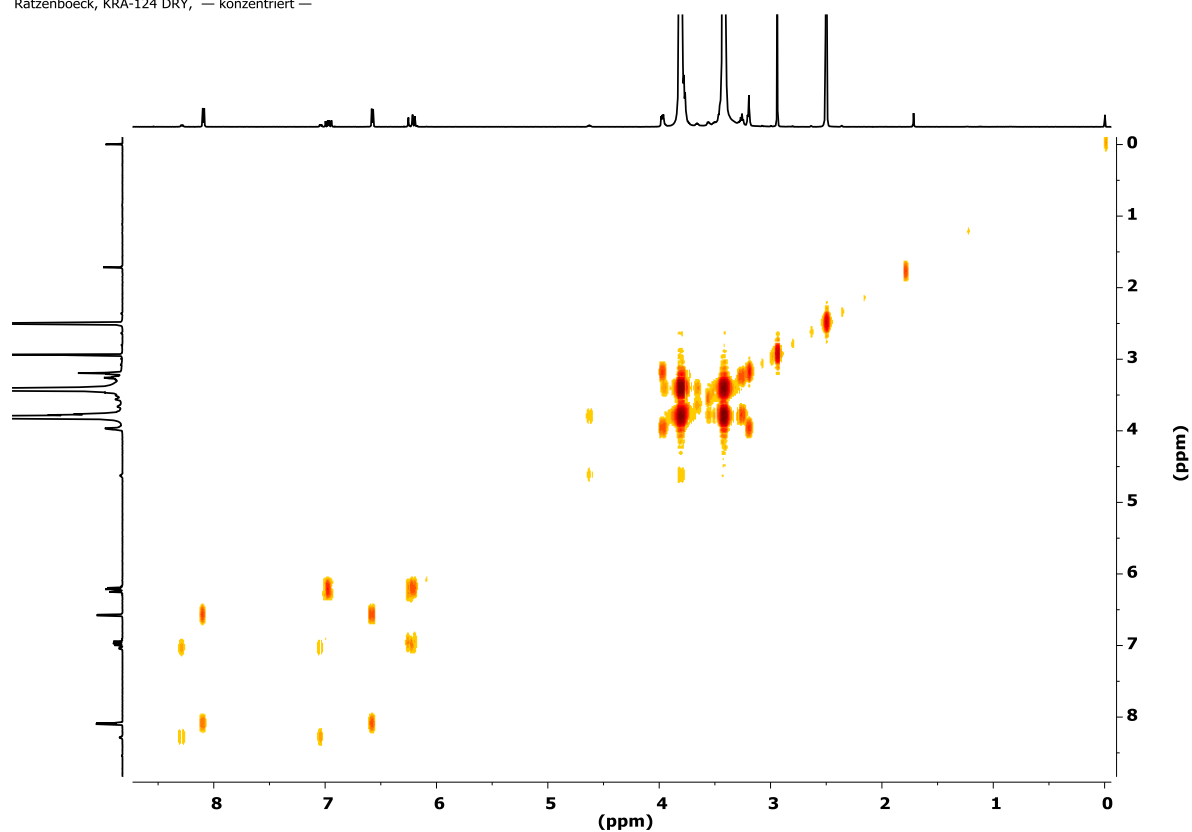


Figure S6. ¹H-¹H-COSY NMR spectrum of **PES** (catalyzed by DMAP) under optimized reaction conditions in DMSO-*d*₆.

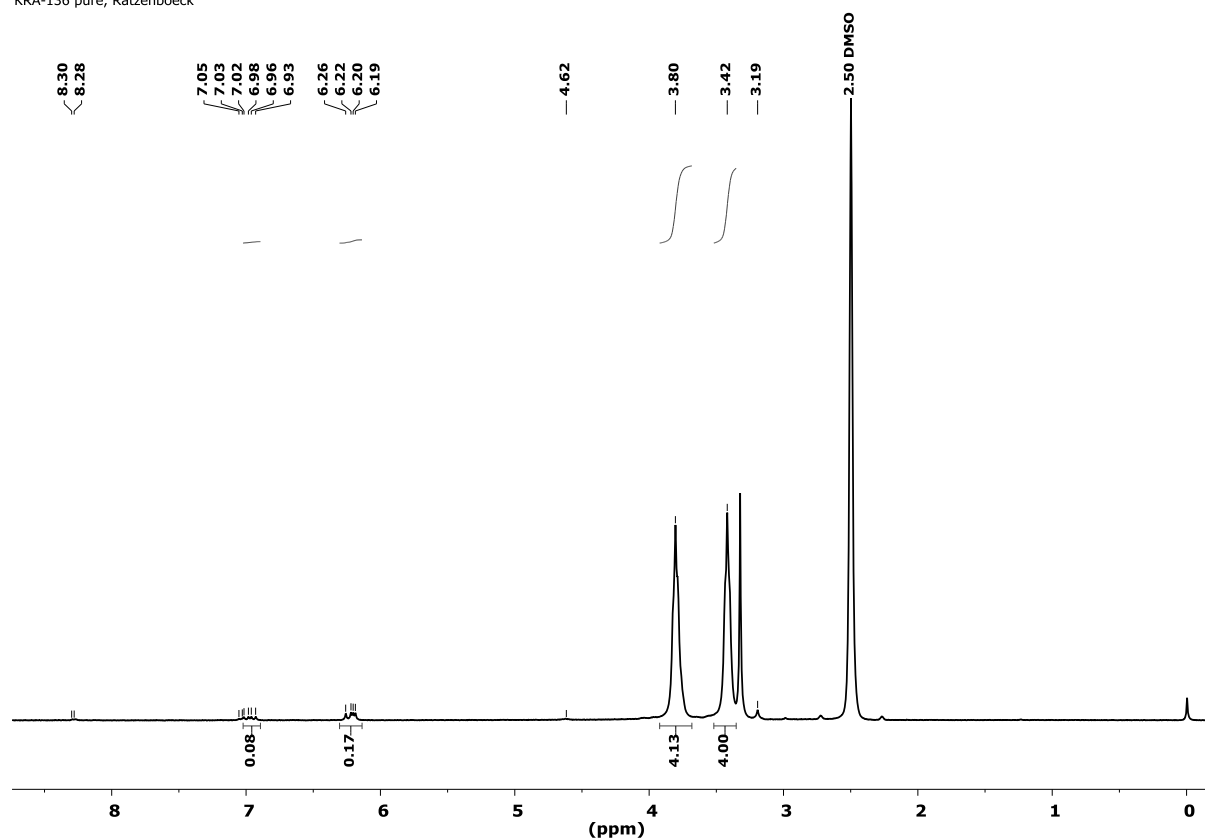


Figure S7. ¹H-NMR spectrum of **PES** (catalyzed by DMAP) under optimized reaction conditions after work-up in DMSO-*d*₆.

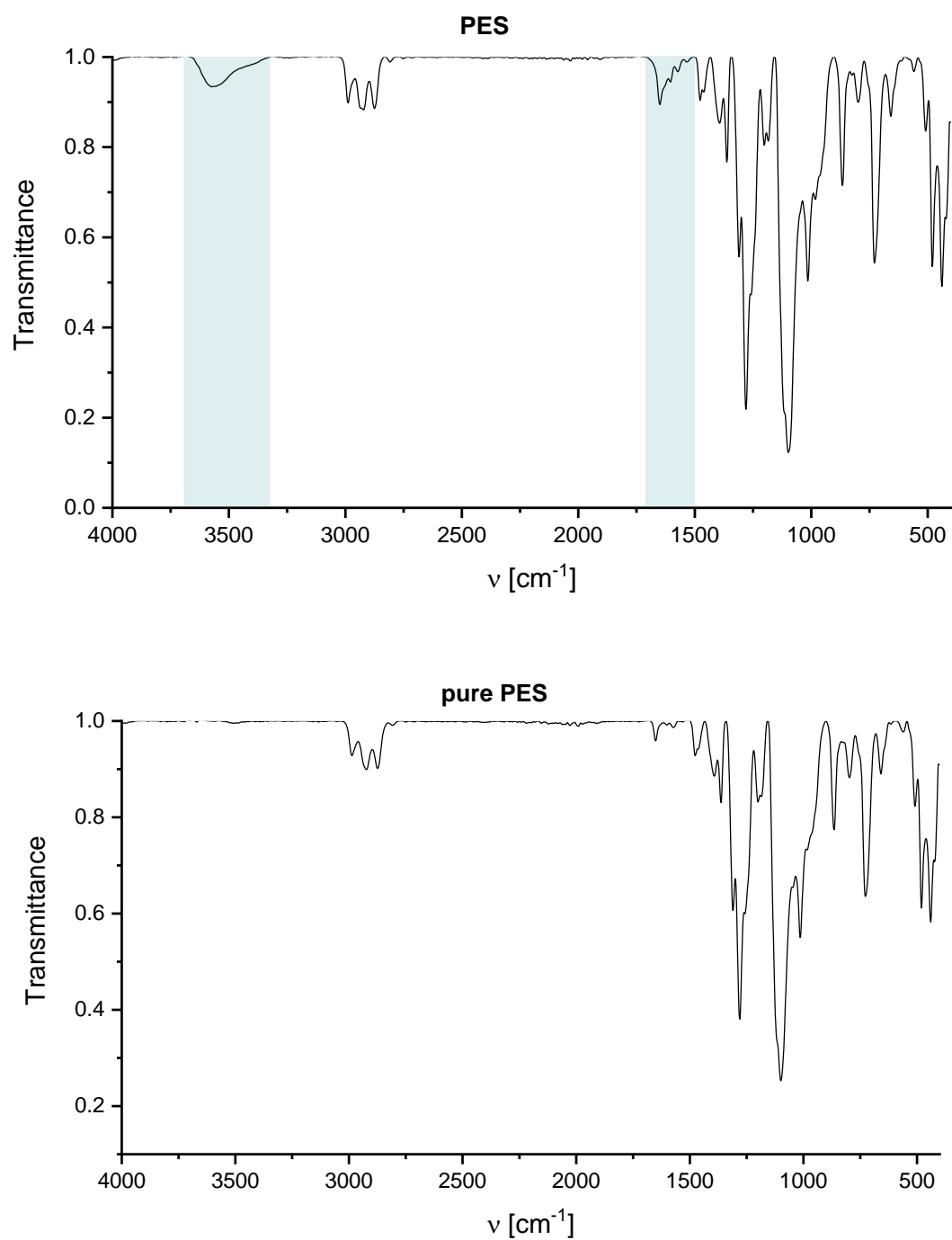


Figure S8. IR spectrum of **PES**; top: crude material (incl. water: 3660 – 3320, 1650 cm⁻¹); bottom: after purification with HCl.

1,4-oxathiane 4,4-dioxide (**1**)

A 4 mL reaction vessel was charged with 5.4 mol% (5.2 mg, 0.046 mmol) KO^tBu. Subsequently, 152 mg (8.44 mmol, 9.9 equiv.) deionized H₂O and 100 mg (0.85 mmol, 1 equiv.) divinyl sulfone were added. The reaction mixture was stirred at 80 °C for 24 h. The crude product was dissolved in methylene chloride (1 mL). The organic layer was washed with brine (1 mL). Further, methylene chloride was removed in vacuo and a colorless powder was obtained.

Alternatively, 1,4-oxathiane 4,4-dioxide (**1**) can be isolated from the reaction mixture of **PES** in which it occurs as side product by extraction with methylene chloride. The solid sample was stirred in methylene chloride overnight. The yellow methylene chloride was then filtered over silica gel and the silica gel was further washed with ethyl acetate. After evaporation of the solvent, 1,4-oxathiane 4,4-dioxide was obtained as colorless crystals.

¹H-NMR (300 MHz, CDCl₃): δ = 4.15 (4H), 3.11 (4H) ppm.

¹³C-NMR (76 MHz, CDCl₃): δ = 66.4, 53.1 ppm.

¹H-NMR (300 MHz, DMSO-*d*₆): δ = 3.97 (4H), 3.20 (4H) ppm.

¹³C-NMR (76 MHz, DMSO-*d*₆): δ = 65.8, 52.1 ppm.

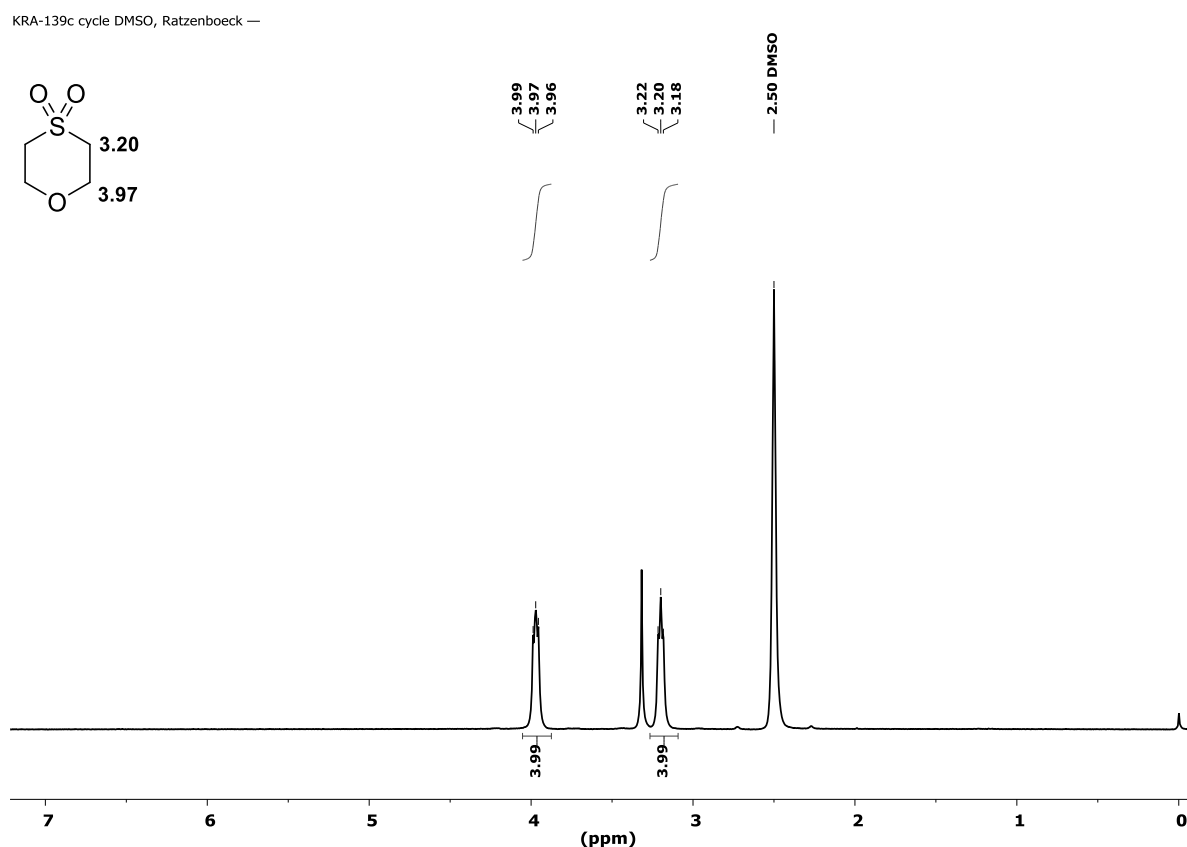


Figure S9. ¹H-NMR spectrum of 1,4-oxathiane 4,4-dioxide (**1**) in DMSO-*d*₆.

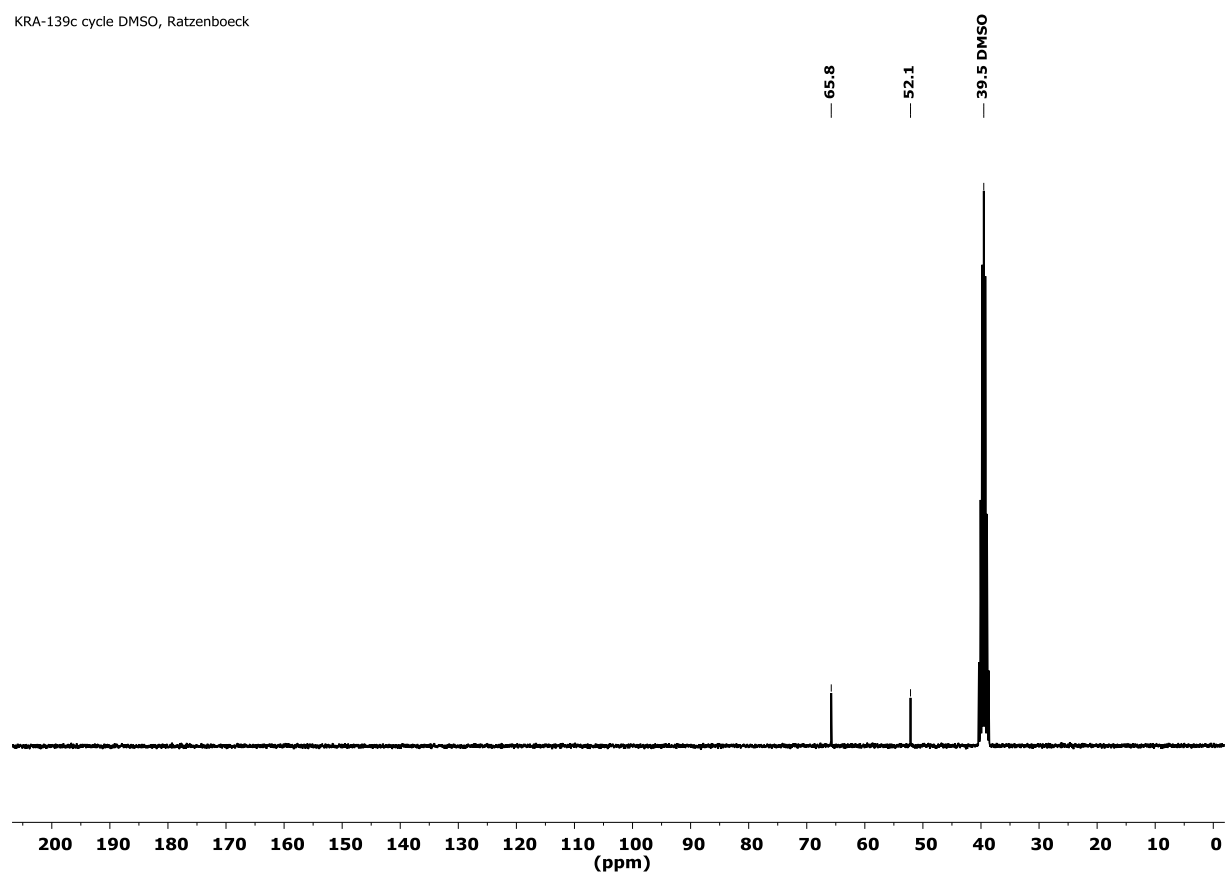


Figure S10. ^{13}C -NMR spectrum of 1,4-oxathiane 4,4-dioxide (**1**) in $\text{DMSO}-d_6$.

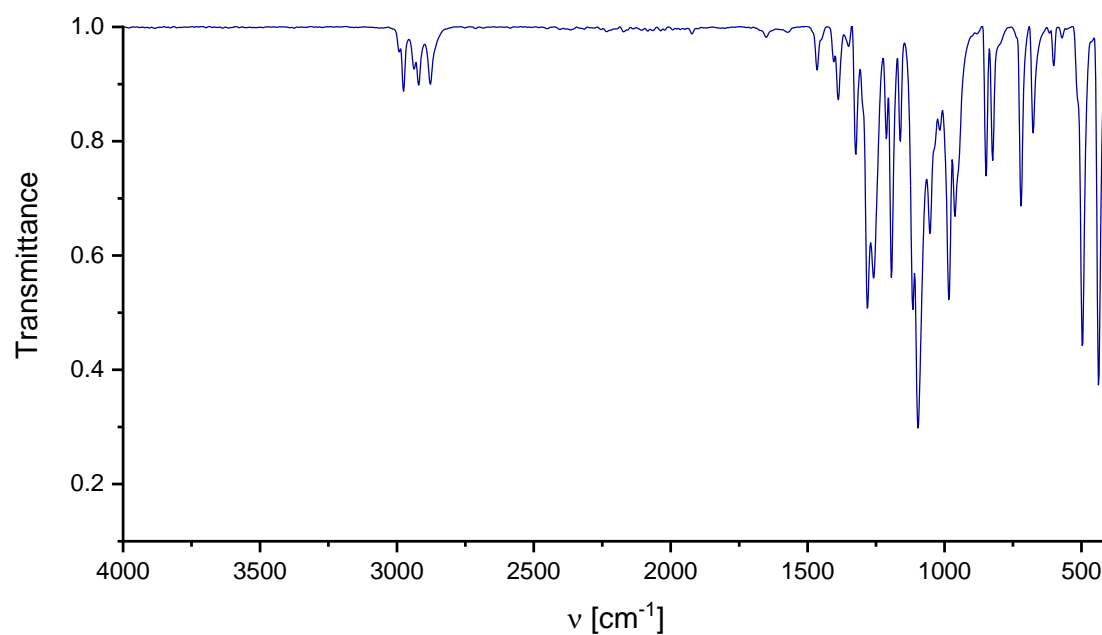


Figure S11. IR spectrum of 1,4-oxathiane 4,4-dioxide (**1**).

4. MALDI-TOF MS

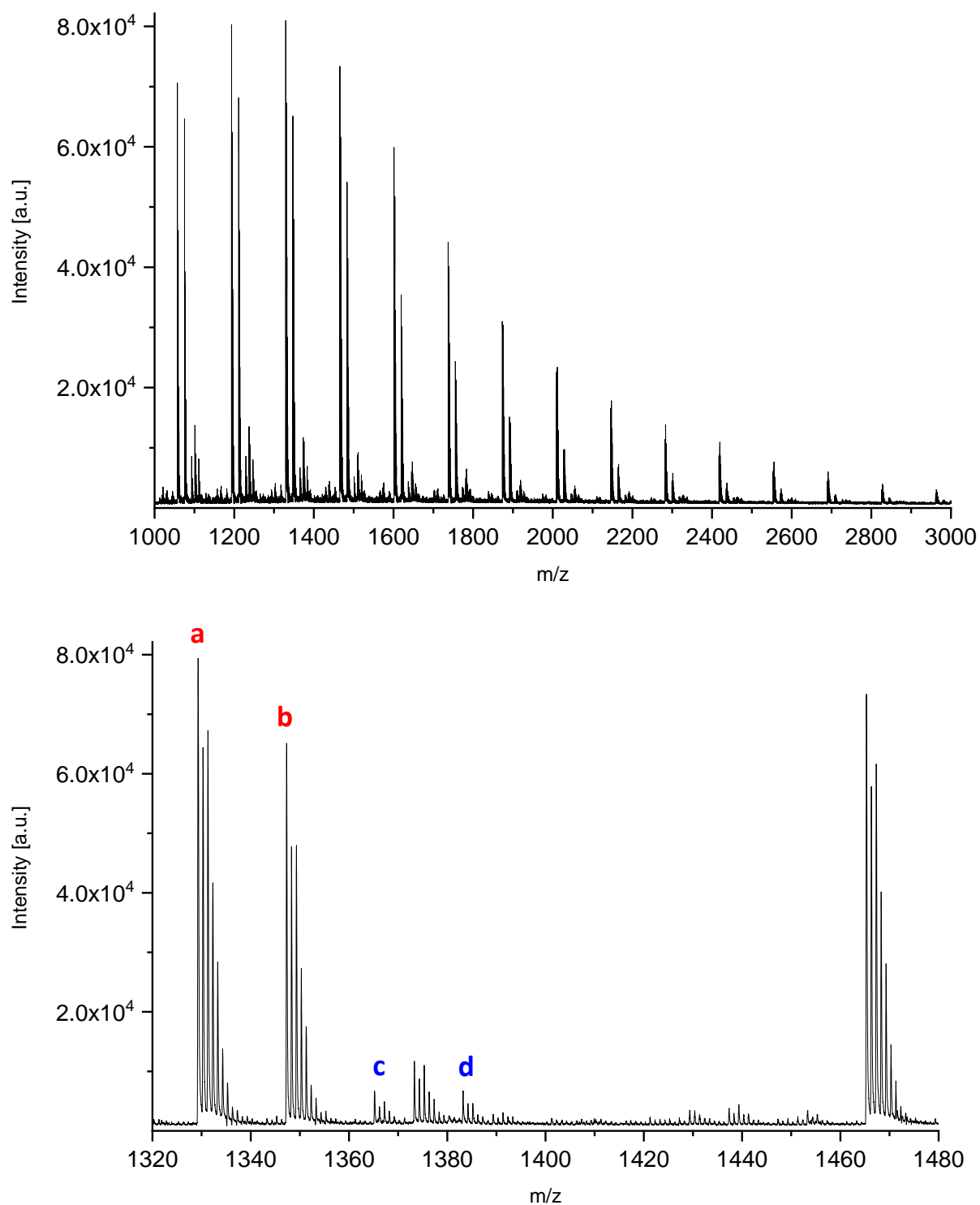


Figure S12. Top: MALDI-TOF MS of **PES** (crude) catalyzed by DMAP; bottom: detail of MALDI-TOF MS with peak assignment (repeat unit = 136.02 Da).

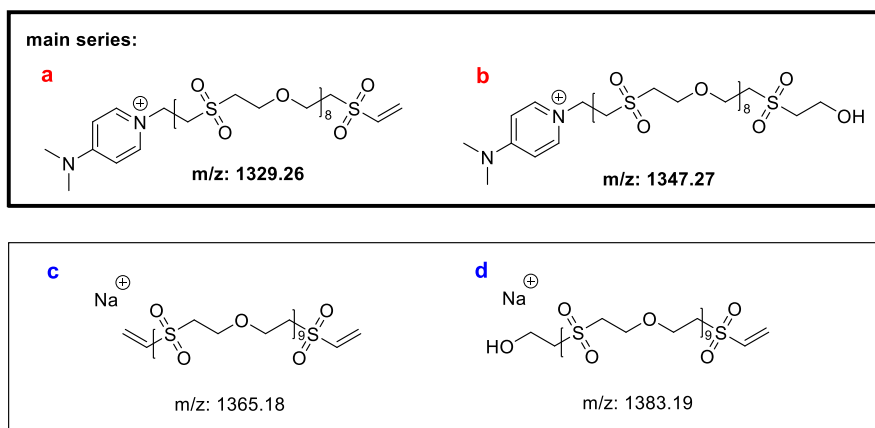


Figure S13. Structures of **PES** (crude) catalyzed by DMAP observed in MALDI-TOF MS.

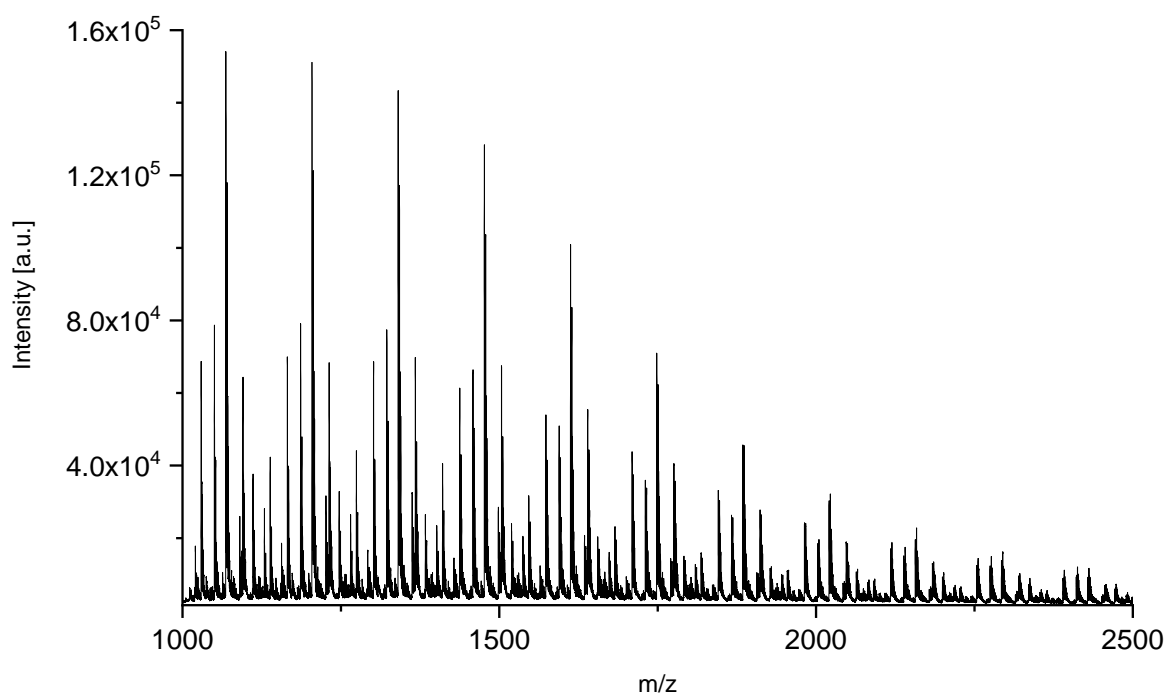


Figure S14. MALDI-TOF MS of **PES** (crude) catalyzed by TMG.

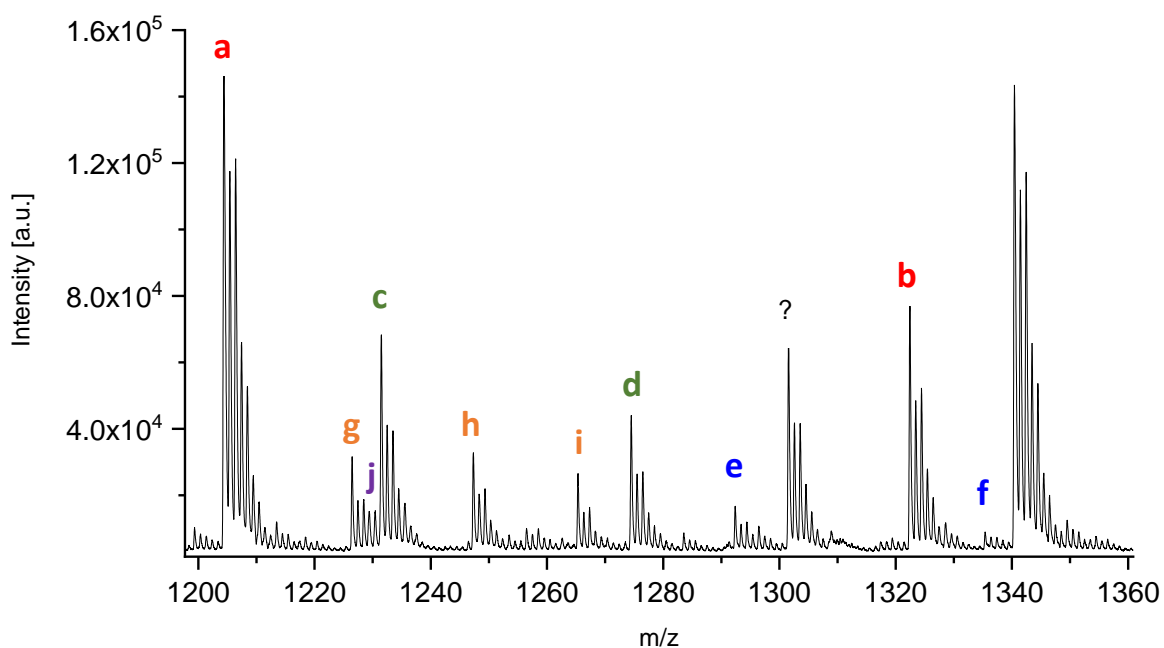


Figure S15. Detail of MALDI-TOF MS of **PES** (crude) catalyzed by TMG with peak assignment (repeat unit = 136.02 Da).

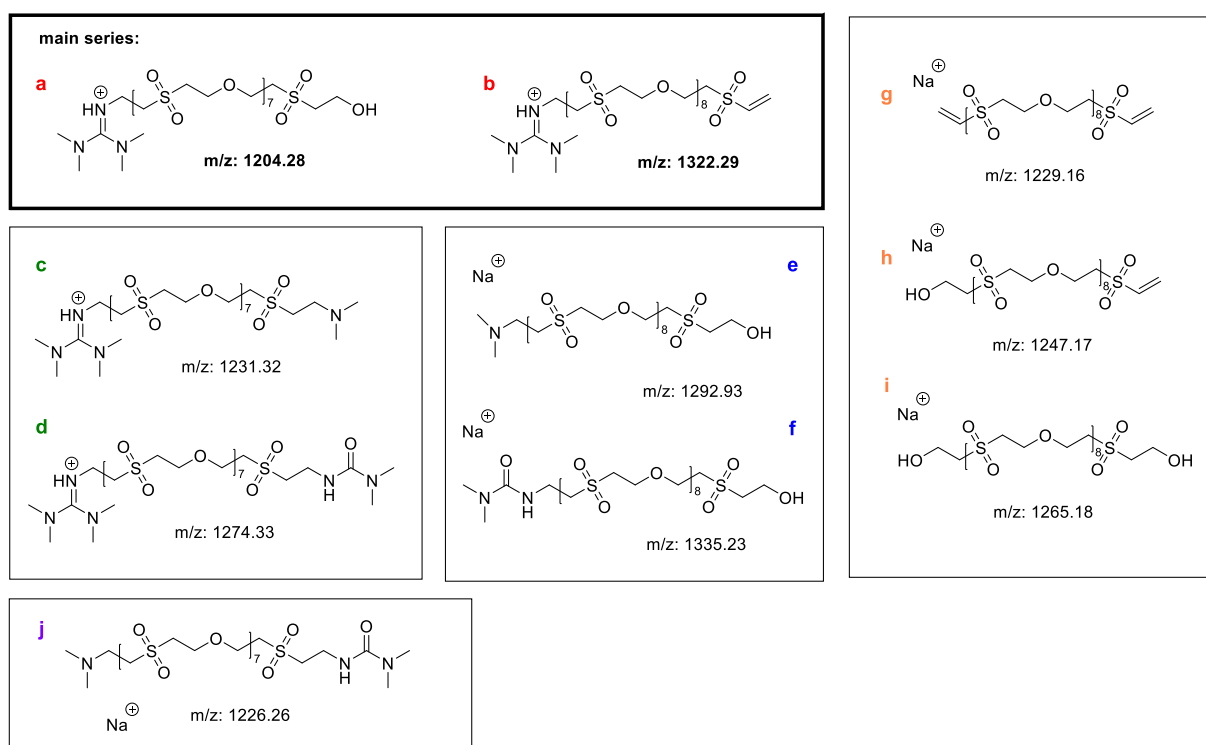


Figure S16. Structures of **PES** (crude) catalyzed by TMG observed in MALDI-TOF MS.

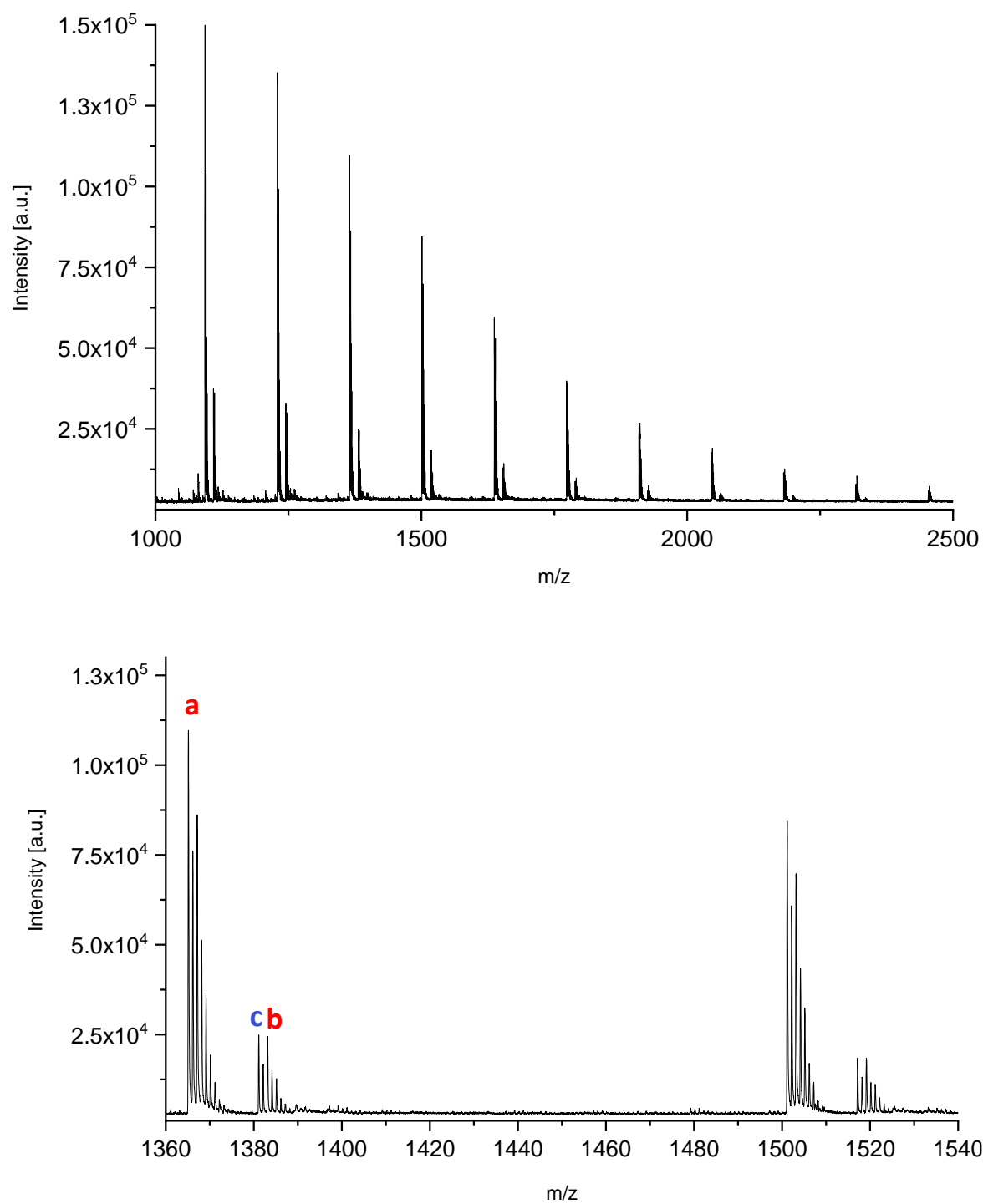


Figure S17. Top: MALDI-TOF MS of **PES** (crude) catalyzed by KO^tBu; bottom: detail of MALDI-TOF MS with peak assignment (repeat unit = 136.02 Da).

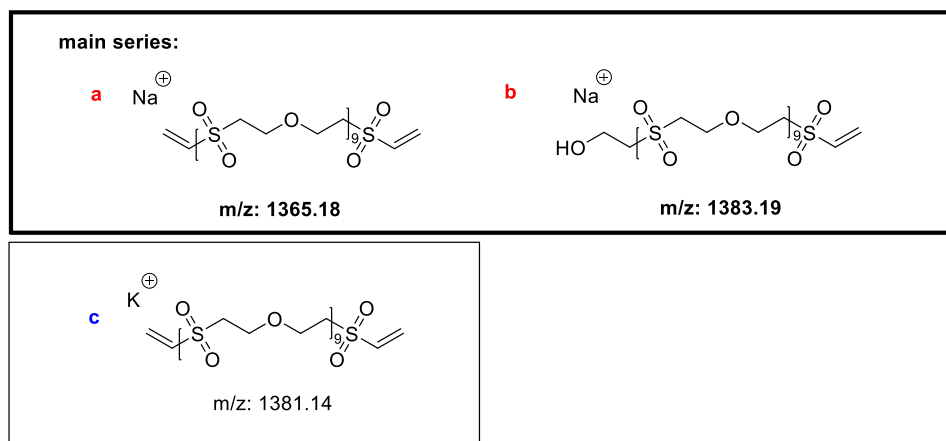


Figure S18. Structures of **PES** (crude) catalyzed by KO^tBu observed in MALDI-TOF MS.

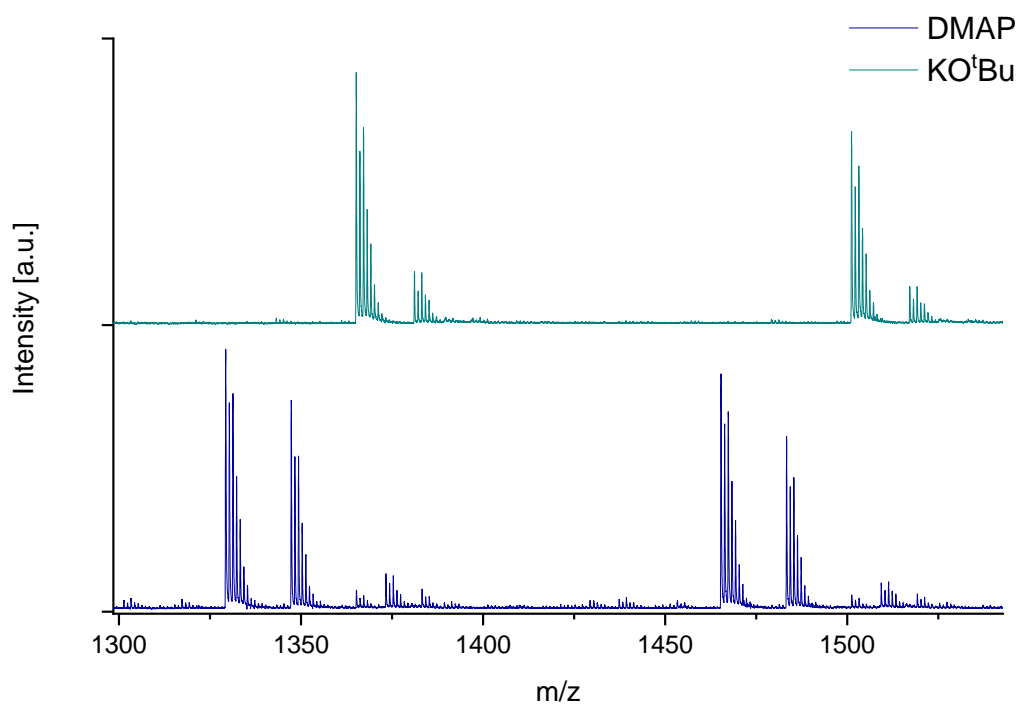


Figure S19. Comparison of MALDI-TOF MES of **PES** (crude) catalyzed by DMAP or KO^tBu (5 mol%).

5. Reaction Progress

In a 10 mL vessel (diameter = 2.5 cm) 4.9 mol% (26.0 mg, 0.213 mmol) DMAP was dissolved in 784 mg (43.6 mmol, 10 equiv.) deionized water. After the addition of 509 mg (4.31 mmol, 1 equiv.) divinyl sulfone, samples were taken after 0.5, 5, 10, 15, 20, 30, 45, 60, 90 min and 24 h. The samples were quenched with 0.5 M HCl (for ^1H -NMR spectroscopy) or conc. acetic acid (for SEC).

In a 10 mL vessel (diameter = 2.5 cm) 4.9 mol% (23.7 mg, 0.211 mmol) KO^tBu was dissolved in 784 mg (43.6 mmol, 10 equiv.) deionized water. After the addition of 509 mg (4.31 mmol, 1 equiv.) divinyl sulfone, samples were taken after 0.5, 15, 30, 45, 60, 120, 240 min and 24 h. The samples were quenched with 0.5 M HCl (for ^1H -NMR spectroscopy) or conc. acetic acid (for SEC).

Monitoring reaction progress

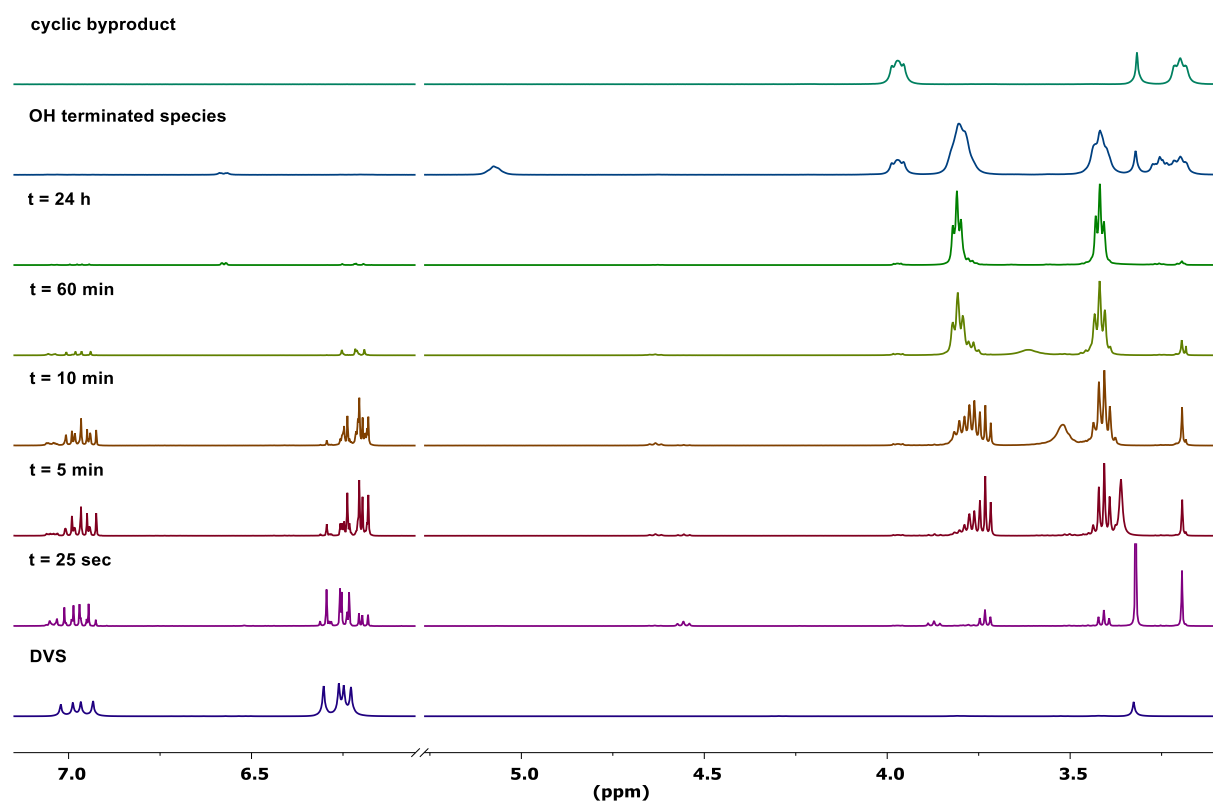


Figure S20. ^1H -NMR spectra of **Figure 1a** in detail; reaction of DVS with water catalyzed by DMAP compared to DVS, cyclic side product **1** and OH-terminated species in DMSO- d_6 .

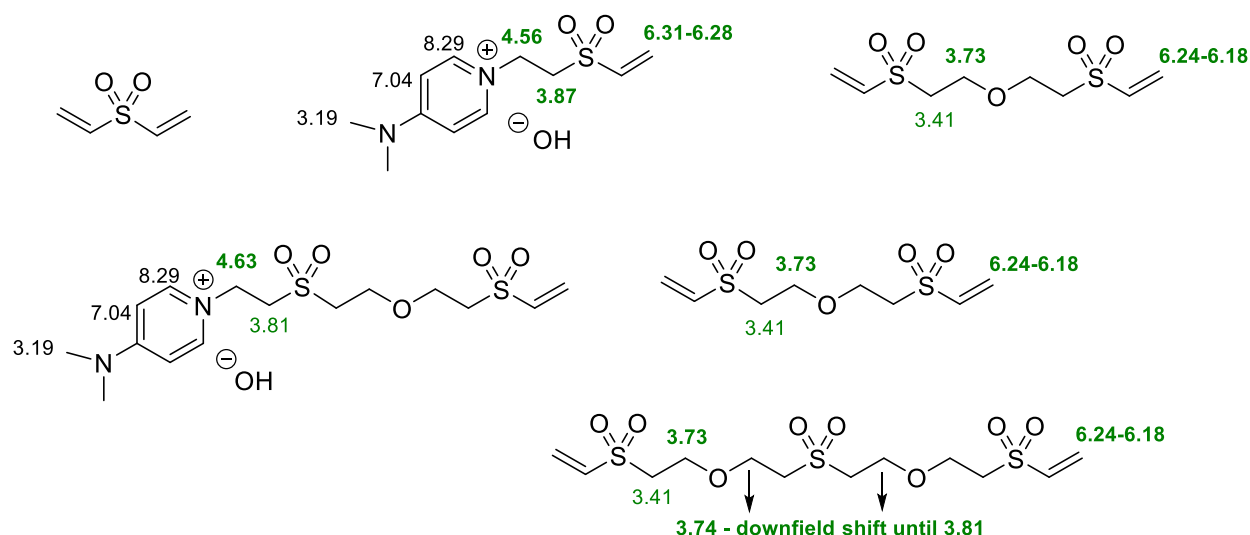


Figure S21. ^1H -NMR shifts (in ppm) in $\text{DMSO}-d_6$ of species observed within the first 10 min in a DMAP catalyzed reaction.

Calculation based on NMR data as follows:

The double bond conversion was calculated after the respective amount of time. Oxa-Michael repeat unit (3.82-3.72 ppm -O-CH₂-repeating unit), cyclic side product **1** (3.97 ppm -O-CH₂-cyclic) and DMAP⁺ terminated species (4.63 ppm -N-CH₂- DMAP⁺ end group) were considered. The remaining double bonds were assigned to DVS and vinyl sulfone end groups. The converted double bonds were related to the oxa-Michael repeat unit, cyclic side product **1** and DMAP⁺ end group.

(6.21 ppm -CH=CH₂ end group, 6.30 ppm peak specific for DVS is equal to 1/4 of total DVS integral)

$$\begin{aligned}
 \int \text{CH}_2 \text{ oxa} - \text{Michael} &= \int -\text{O} - \text{CH}_2 - \text{repeating unit} + \int -\text{O} - \text{CH}_2 - \text{cyclic} + \int -\text{N} - \text{CH}_2 - \text{DMAP}^+ \text{ end group} \\
 &= \int 3.81 \text{ ppm} + \int 3.97 \text{ ppm} + \int 4.63 \text{ ppm}
 \end{aligned}$$

$$\text{Double bond conversion [\%]} = \frac{\int \text{CH}_2 \text{ oxa} - \text{Michael}}{\int -\text{CH} = \text{CH}_2 \text{ end group} + \int \text{CH}_2 \text{ oxa} - \text{Michael}} * 100$$

$$\text{oxa} - \text{Michael RU [\%]} = (\text{DB conversion}) * \frac{\int -\text{O} - \text{CH}_2 - \text{repeating unit}}{\int \text{CH}_2 \text{ oxa} - \text{Michael}}$$

$$\text{cycle [\%]} = (\text{DB conversion}) * \frac{\int -O - CH_{2-cyclic}}{\int CH_2 oxa - Michael}$$

$$\text{DMAP end group [\%]} = (\text{DB conversion}) * \frac{\int -N - CH_{2-DMAP^+ end group}}{\int CH_2 oxa - Michael}$$

$$\text{DVS end groups [\%]} = (1 - \text{DB conversion}) * \int 6.30 \text{ ppm} * 4$$

$$\text{vinyl sulfone end group [\%]} = (1 - \text{DB conversion}) * (1 - \int 6.30 \text{ ppm} * 4)$$

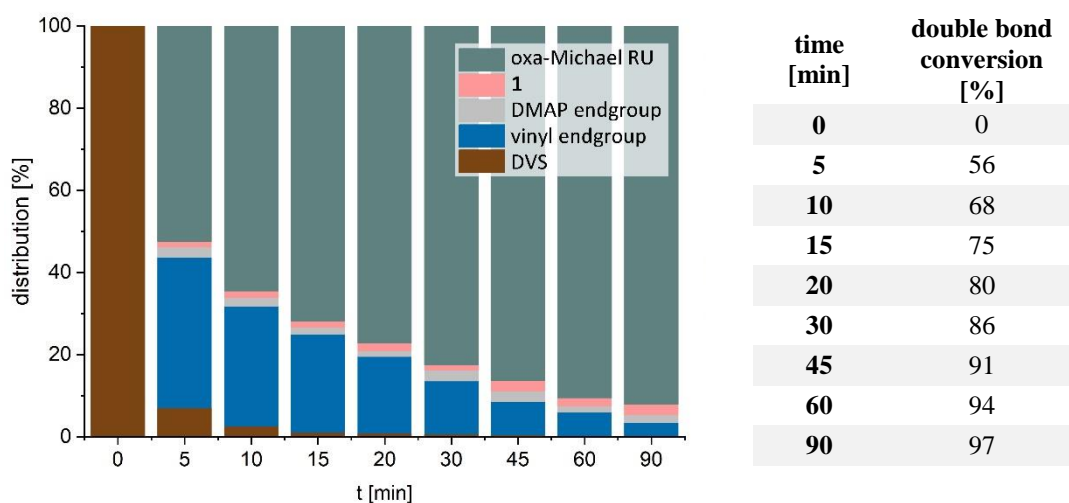


Figure S22. Left: Reaction progress (DMAP catalyzed) showing the development of the relative amount of different chemical entities over time (monitored by ^1H -NMR spectroscopy); right: double bond conversion over time.

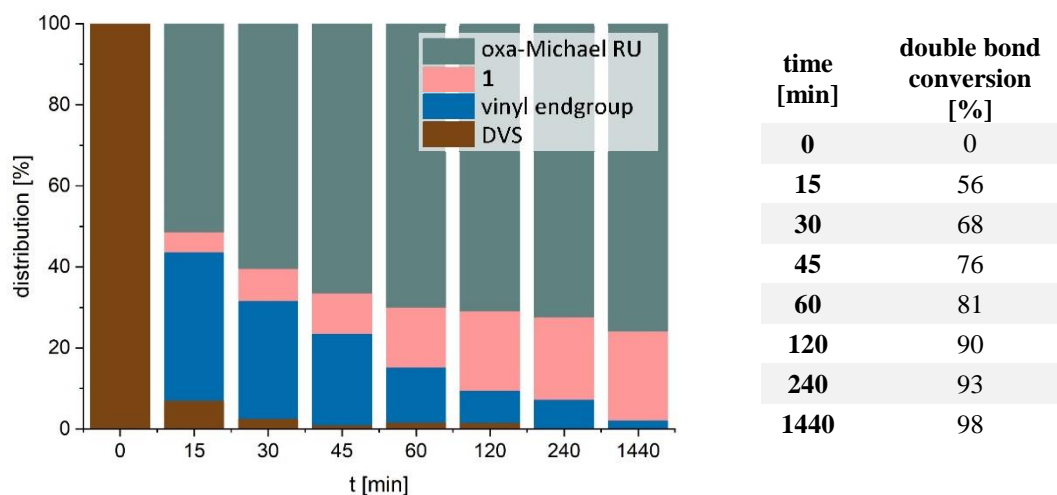


Figure S23. Left: Reaction progress (KOtBu catalyzed) showing the development of the relative amount of different chemical entities over time (monitored by ^1H -NMR spectroscopy); right: double bond conversion over time.

Consumption of unreacted DVS over time:

$$\text{unreacted DVS [\%]} = \frac{\frac{4 * (\int 6.30 \text{ ppm})}{2}}{\int -CH = CH_{2 \text{ end group}}} * 100$$

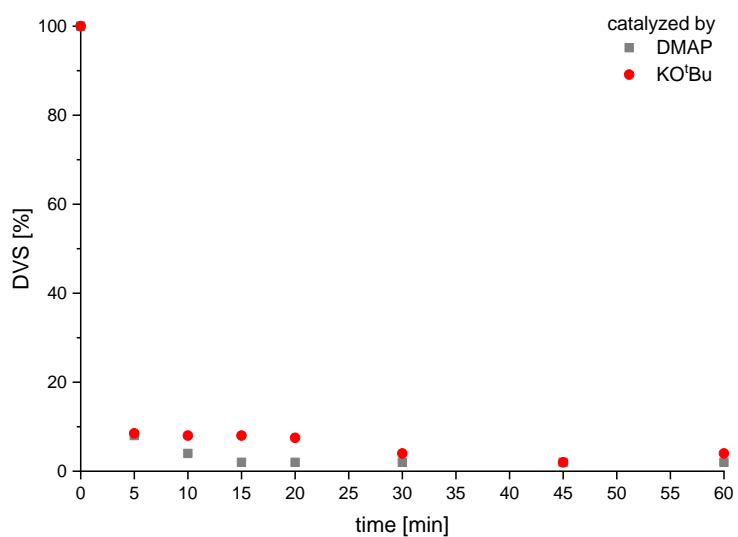


Figure S24. Unreacted divinyl sulfone in reaction mixture catalyzed by DMAP (grey) or KOtBu (red) over time.

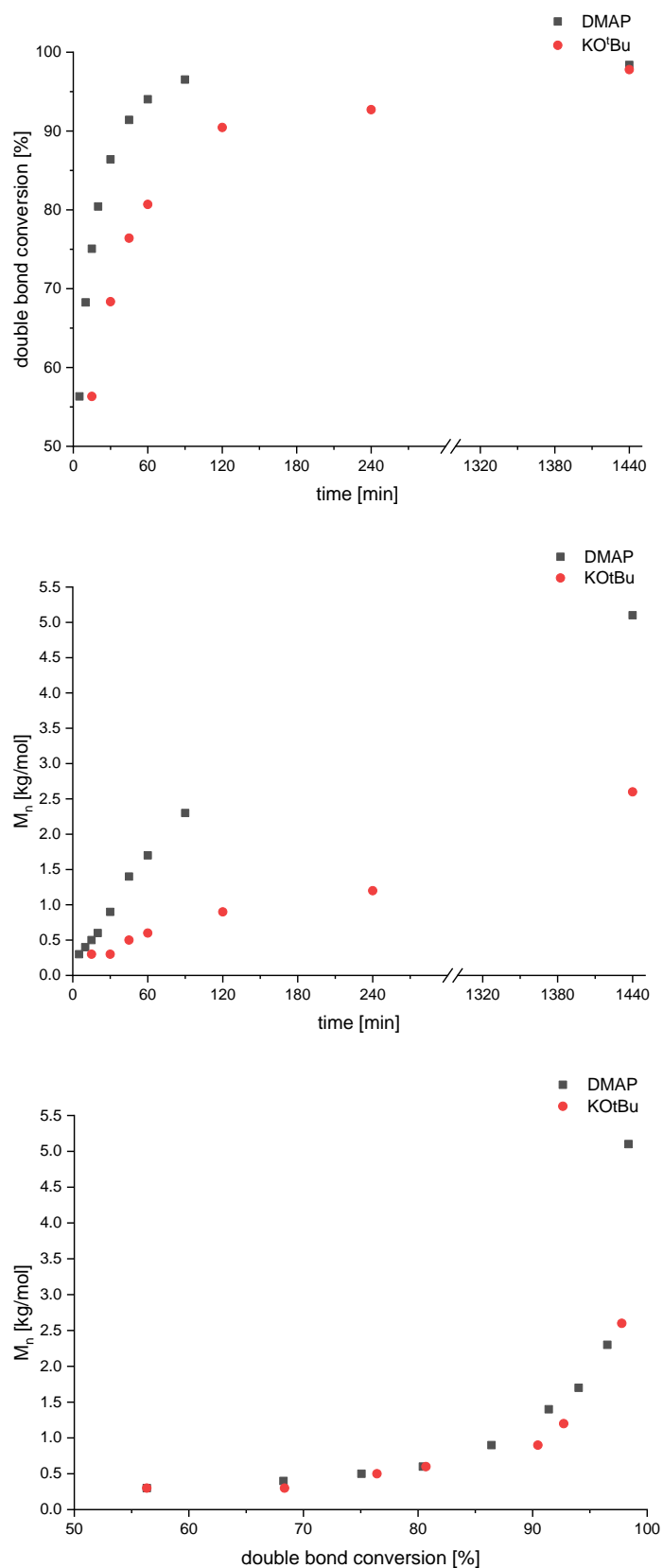


Figure S25. a) Double bond conversion vs reaction time for DMAP and KO^tBu catalyzed reactions; b) molecular mass M_n vs reaction time for DMAP and KO^tBu catalyzed reactions; c) molecular mass M_n vs double bond conversion for DMAP and KO^tBu catalyzed reactions.

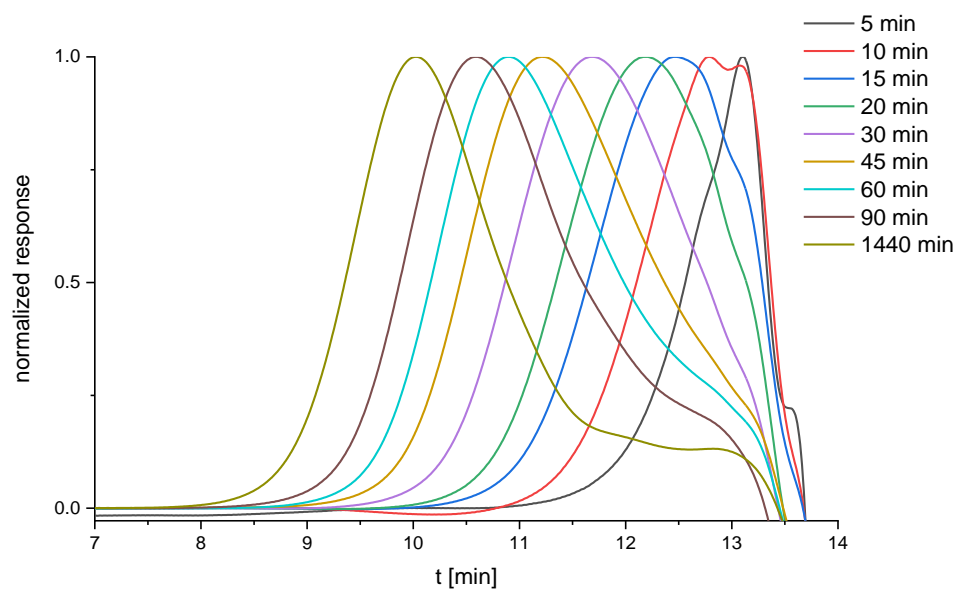


Figure S26. SEC chromatogram of kinetic experiment with DMAP; RI detector.

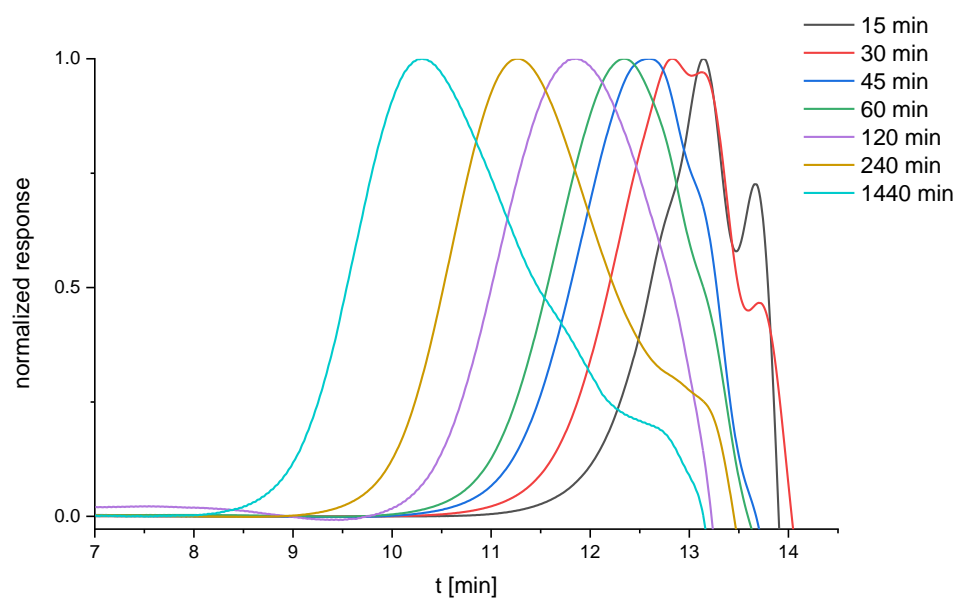


Figure S27. SEC chromatogram of kinetic experiment with KO'Bu; RI detector.

Table S1. SEC results of kinetic experiment in detail.

	5 mol% DMAP			5 mol% KO ^t Bu		
Time [min]	M_w [kg/mol]	M_n [kg/mol]	\bar{D}	M_w [kg/mol]	M_n [kg/mol]	\bar{D}
5	0.4	0.3	1.3			-
10	0.6	0.4	1.5			-
15	0.8	0.5	1.6	0.4	0.3	1.3
20	1.1	0.6	1.8			-
30	1.9	0.9	2.1	0.5	0.3	1.7
45	3.1	1.4	2.2	0.8	0.5	1.6
60	4.3	1.7	2.5	0.9	0.6	1.5
90	6.6	2.3	2.9			-
120	-	-	-	1.6	0.9	1.8
240	-	-	-	2.9	1.2	2.4
1440	15.4	5.1	3.0	9.3	2.6	3.6

6. Synthesis

Synthesis of PES in 1 M solution in DMSO

In a 4 mL reaction vessel 5.2 mol% (5.5 mg, 0.045 mmol) DMAP was dissolved in 149 mg (8.27 mmol, 9.5 equiv.) deionized H₂O and 650 μ L DMSO-*d*₆. After the addition of 103 mg (0.87 mmol, 1 equiv.) divinyl sulfone, the reaction mixture was stirred at room temperature for 1 h. A sample of the colorless solution was analyzed by ¹H-NMR spectroscopy. No polymerization could be observed.

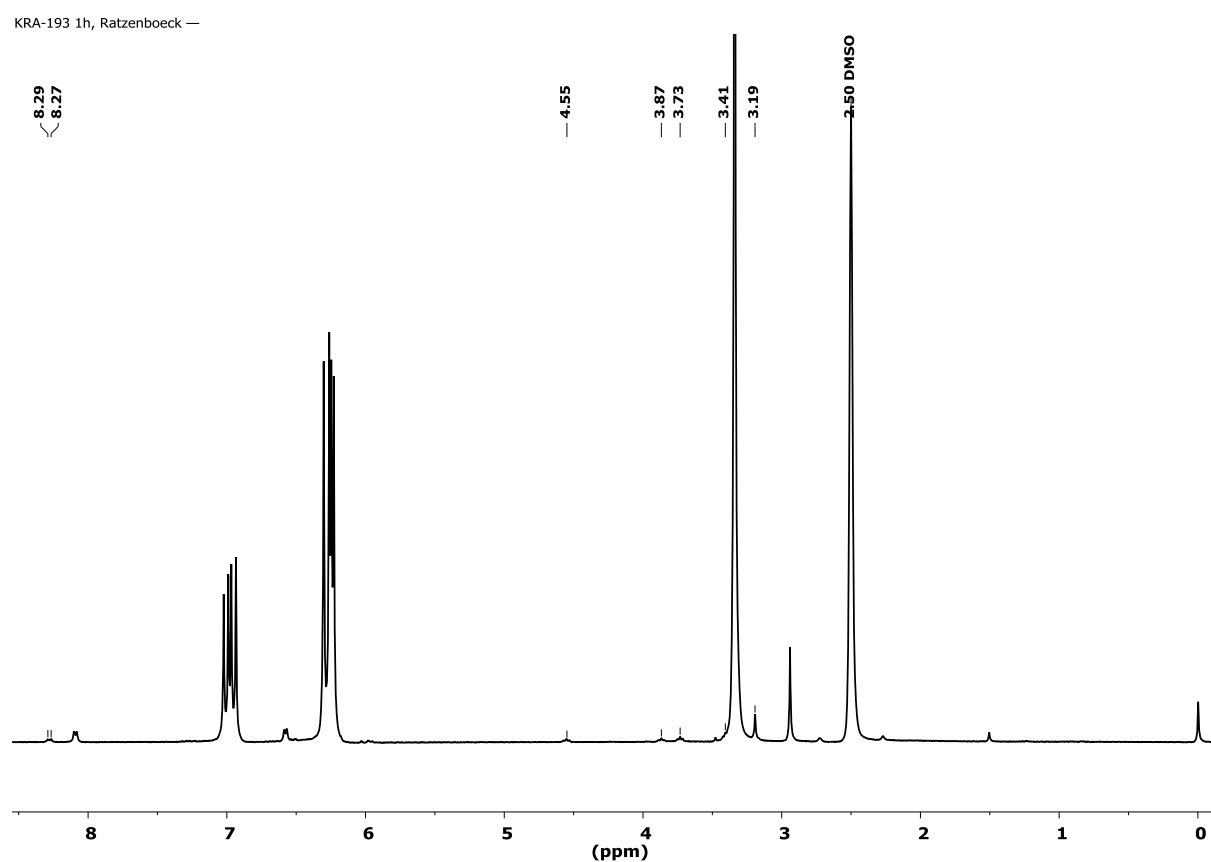
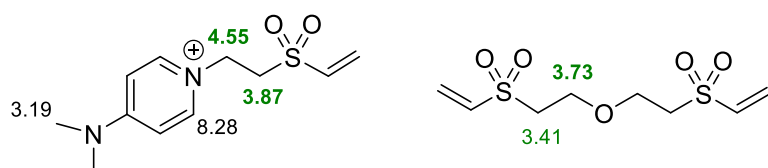


Figure S28. ¹H-NMR spectrum of reaction progress in solution after 1 h in DMSO-*d*₆.

observed species after 1 h reaction time:



Bis-(2-methanesulfonyl-ethyl) ether

In a 4 mL reaction vessel 5 mol% (11.4 mg, 0.093 mmol) DMAP was dissolved in 170 μ L (9.44 mmol, 5.0 equiv.) deionized water. 199 mg (1.87 mmol, 1.0 equiv.) methyl vinyl sulfone was added, and the mixture was stirred at room temperature. ^1H -NMR spectroscopy revealed a conversion of 94% after 1 h (96% bis-(2-methanesulfonyl-ethyl) ether, 4% DMAP end capped species) and full conversion after 2.5 h. For isolation, the product was acidified with 0.5 mL 1 M HCl and was further recrystallized from water. Colorless needles (112 mg, 52%) were obtained.

In case of KO^tBu as catalyst the reaction was performed in analogy to the above description.

^1H -NMR (300 MHz, CDCl_3): δ = 3.97 (t, $-\text{O}-\text{CH}_2-$, 4H), 3.27 (t, $-\text{CH}_2-\text{SO}_2-$, 4H), 2.99 (s, CH_3 , 6H) ppm.

^{13}C -NMR (75 MHz, CDCl_3): δ = 65.0 ($-\text{CH}_2-\text{SO}_2-$), 54.9 ($-\text{O}-\text{CH}_2-$), 42.9 (CH_3) ppm.

^1H -NMR (300 MHz, $\text{DMSO}-d_6$) : δ = 3.80 (t, $-\text{O}-\text{CH}_2-$, 4H), 3.40 (t, $-\text{CH}_2-\text{SO}_2-$, 4H), 2.99 (s, CH_3 , 6H) ppm.

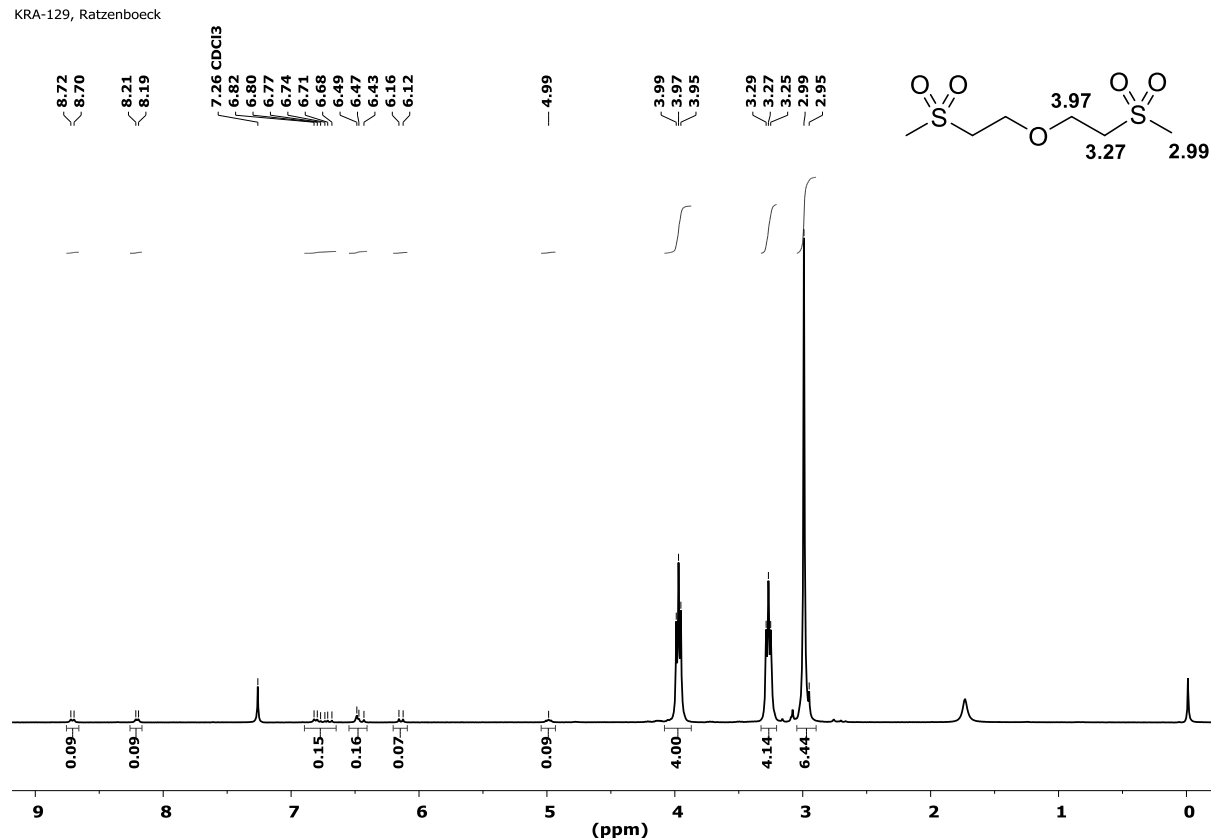


Figure S29. ^1H -NMR spectrum of bis-(2-methanesulfonyl-ethyl) ether in CDCl_3 with TMS after 1 h reaction time.

$^1\text{H-NMR}$ (300 MHz, CDCl_3): δ = 8.71 (d, J = 7.6 Hz, $-\text{CH}-$ DMAP $^+$ end group), 8.20 (residual DMAP), 6.81 (d, J = 7.6 Hz, $-\text{CH}-$ DMAP $^+$ end group), 6.72 (residual methyl vinyl sulfone), 6.49 – 6.43 (residual DMAP + methyl vinyl sulfone), 6.14 (residual methyl vinyl sulfone), 4.99 ($-\text{N}-\text{CH}_2-$ DMAP $^+$ end group), **3.97** (t, $-\text{O}-\text{CH}_2-$, **4H**), **3.27** (t, $-\text{CH}_2-\text{SO}_2-$, **4H**), **2.99** (s, CH_3 , **6H**), 2.95 (residual DMAP) ppm.

Exact masses:

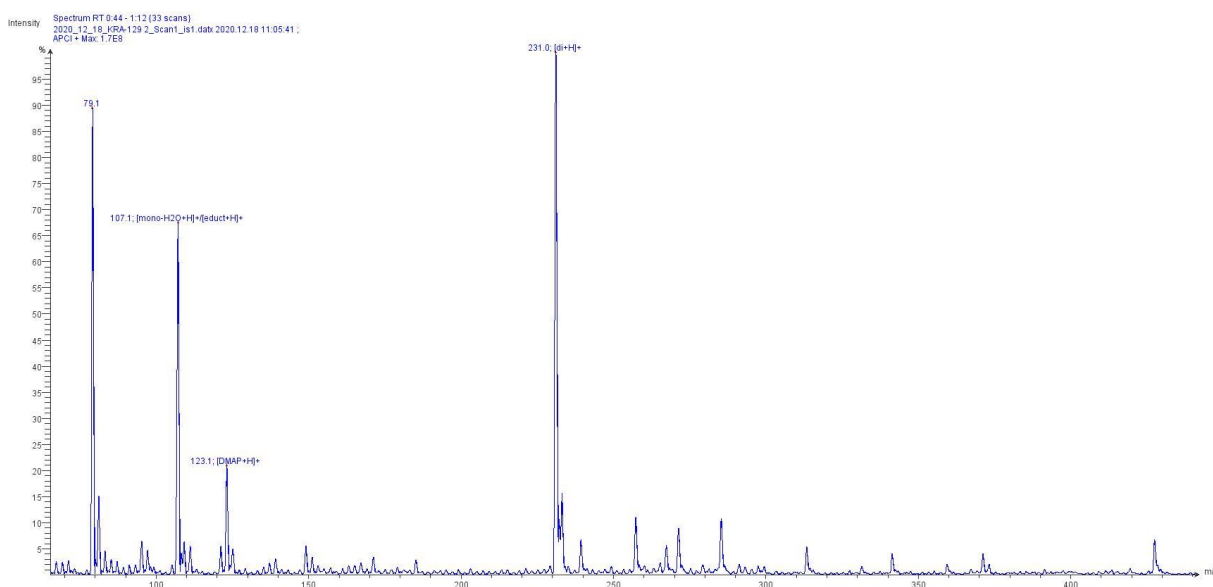
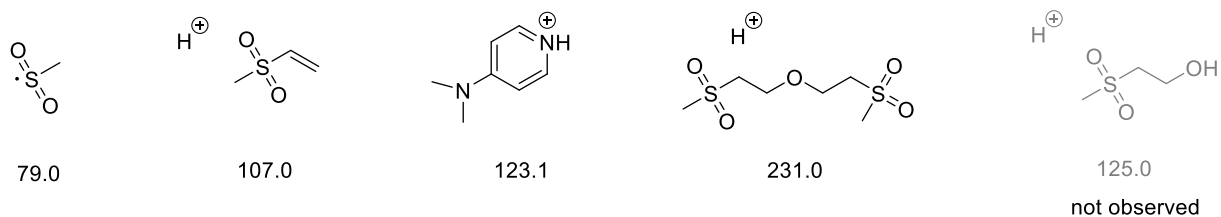


Figure S30. Low-resolution MS of the reaction mixture of bis-(2-methanesulfonyl-ethyl) ether (before work-up).

KRA-305 1h, Ratzenboeck

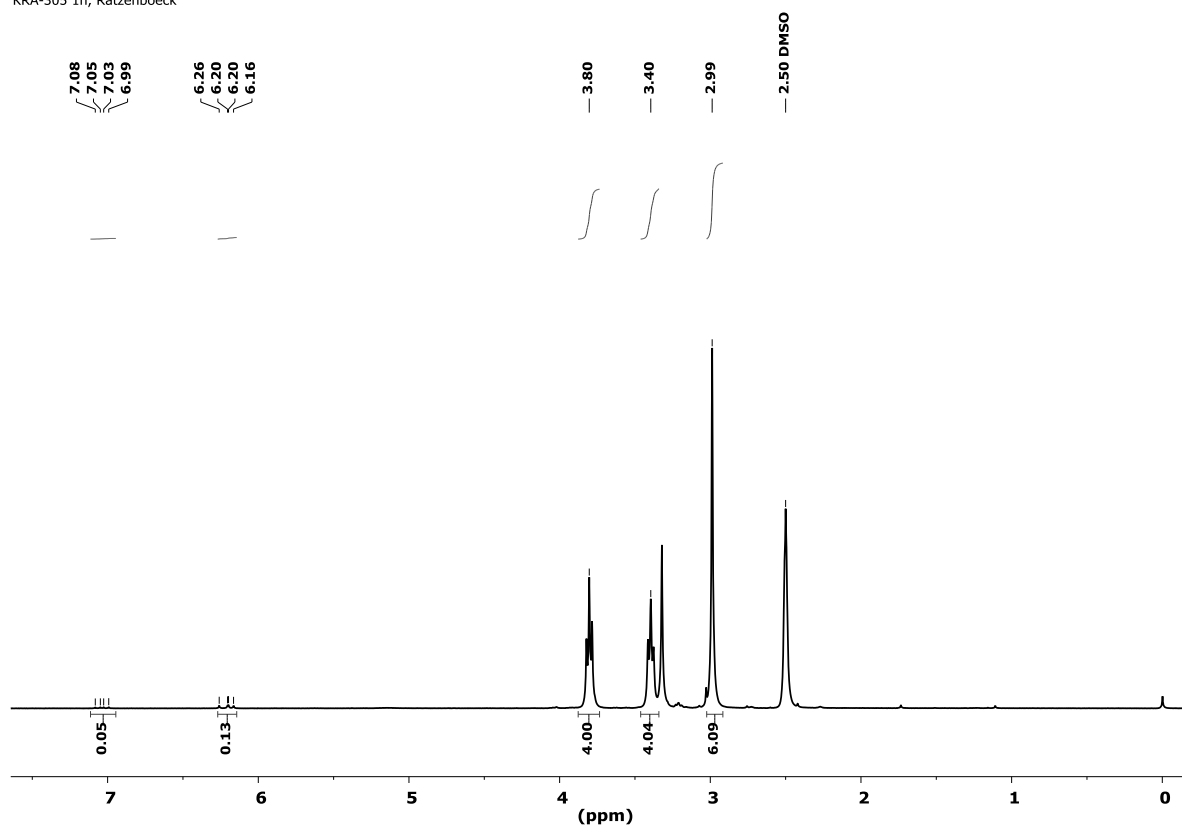


Figure S31. ¹H-NMR spectrum of bis-(2-methanesulfonyl-ethyl) ether prepared by 5 mol% KO^tBu in DMSO-*d*₆ after 1 h reaction time; 3.33 ppm denotes residual water.

KRA-129_2 pure, Ratzenboeck —

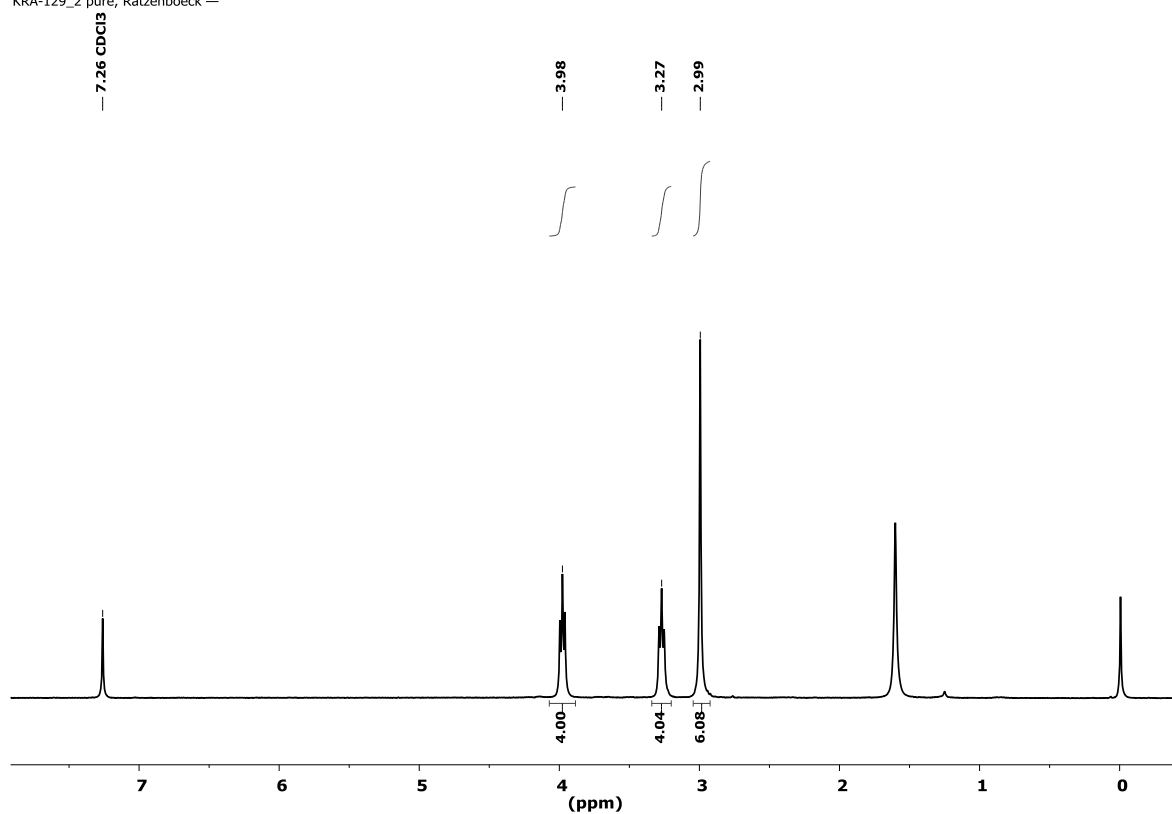


Figure S32. ¹H-NMR spectrum of isolated bis-(2-methanesulfonyl-ethyl) ether in CDCl₃ with TMS; 1.56 ppm residual water.

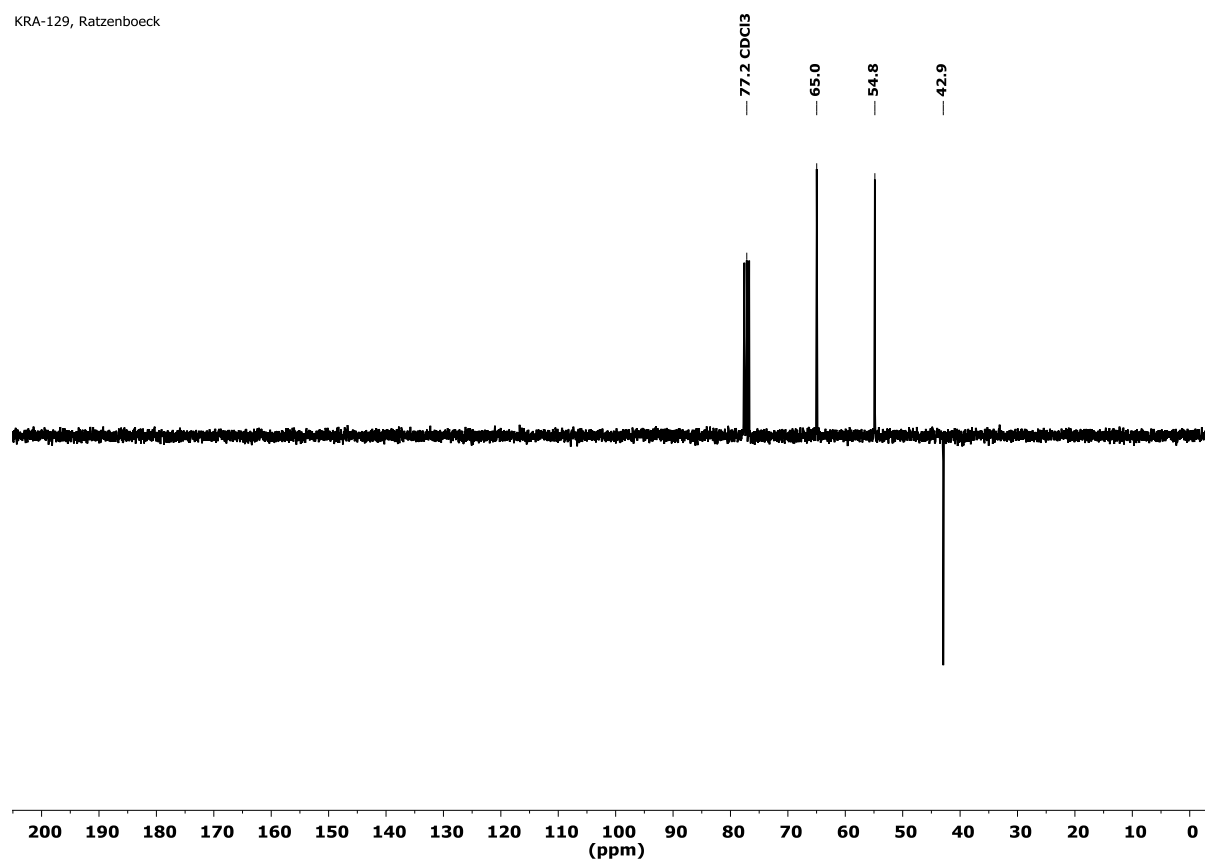


Figure S33. ^{13}C /APT-NMR spectrum of isolated bis-(2-methanesulfonyl-ethyl) ether in CDCl_3 .

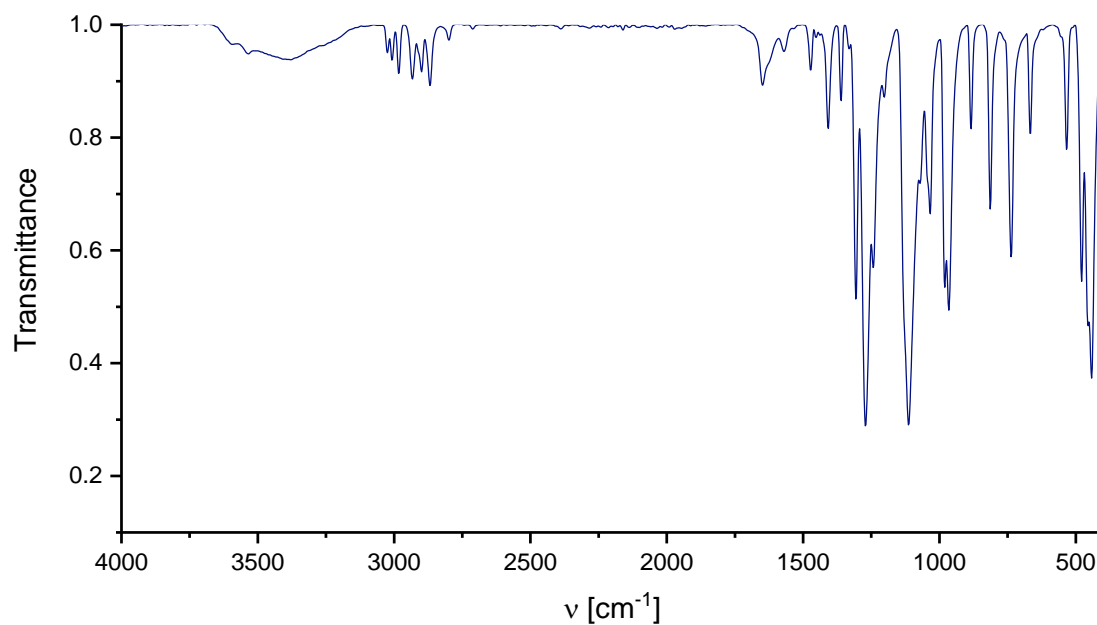


Figure S34. IR spectrum of isolated bis-(2-methanesulfonyl-ethyl) ether.

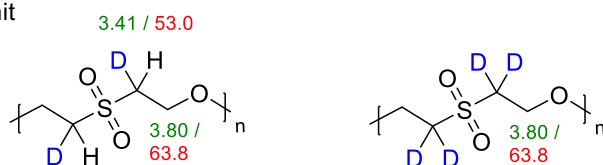
Synthesis of PES with D₂O

In a 4 mL reaction vessel 5.0 mol% (5.3 mg, 0.043 mmol) DMAP was dissolved in 188 mg (9.39 mmol, 11 equiv.) D₂O. After the addition of 101 mg (0.85 mmol, 1 equiv.) divinyl sulfone, the reaction mixture was stirred at room temperature for 1 h. An off-white product was obtained.

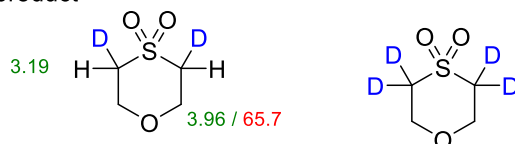
¹H-NMR (500 MHz, DMSO-*d*₆): δ = 8.30 (d, J = 6.4 Hz, -CH- DMAP⁺ end group), 7.04 (d, J = 7.2 Hz, -CH- DMAP⁺ end group), 7.00 – 6.92 (m, -CH=CH₂ end group), 6.25 – 6.17 (m, -CH=CH₂ end group), 4.64 (t, -N-CH₂- DMAP⁺ end group), 3.96 (s, -O-CH₂- cyclic), 3.80 (s, -O-CH₂-), 3.78 (m, -CH₂-OH end group), 3.41 (m, -CHD-SO₂-), 3.26 (t, -CHD-CH₂-OH end group), 3.19 (s, -CH₃ DMAP⁺ end group, -CHD-SO₂- cyclic) ppm.

¹³C-NMR (125 MHz, DMSO-*d*₆): δ = 65.7 (-O-CH₂-cyclic), 63.8 (-O-CH₂-), 53.0 (-CHD-SO₂- / -CD₂-SO₂-) ppm.

repeating unit



cyclic side product



end groups

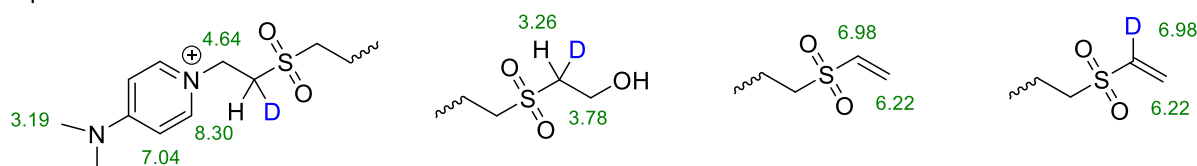
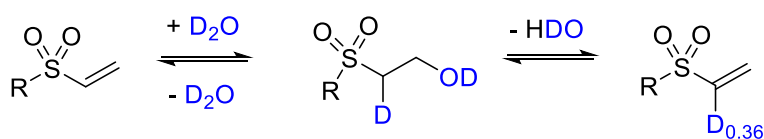


Figure S35. Species identified by NMR spectroscopy in the polymerization of DVS and D₂O.



Scheme S1. Partial deuteration of vinyl group as attack and elimination of hydroxide is a fast, reversible process.

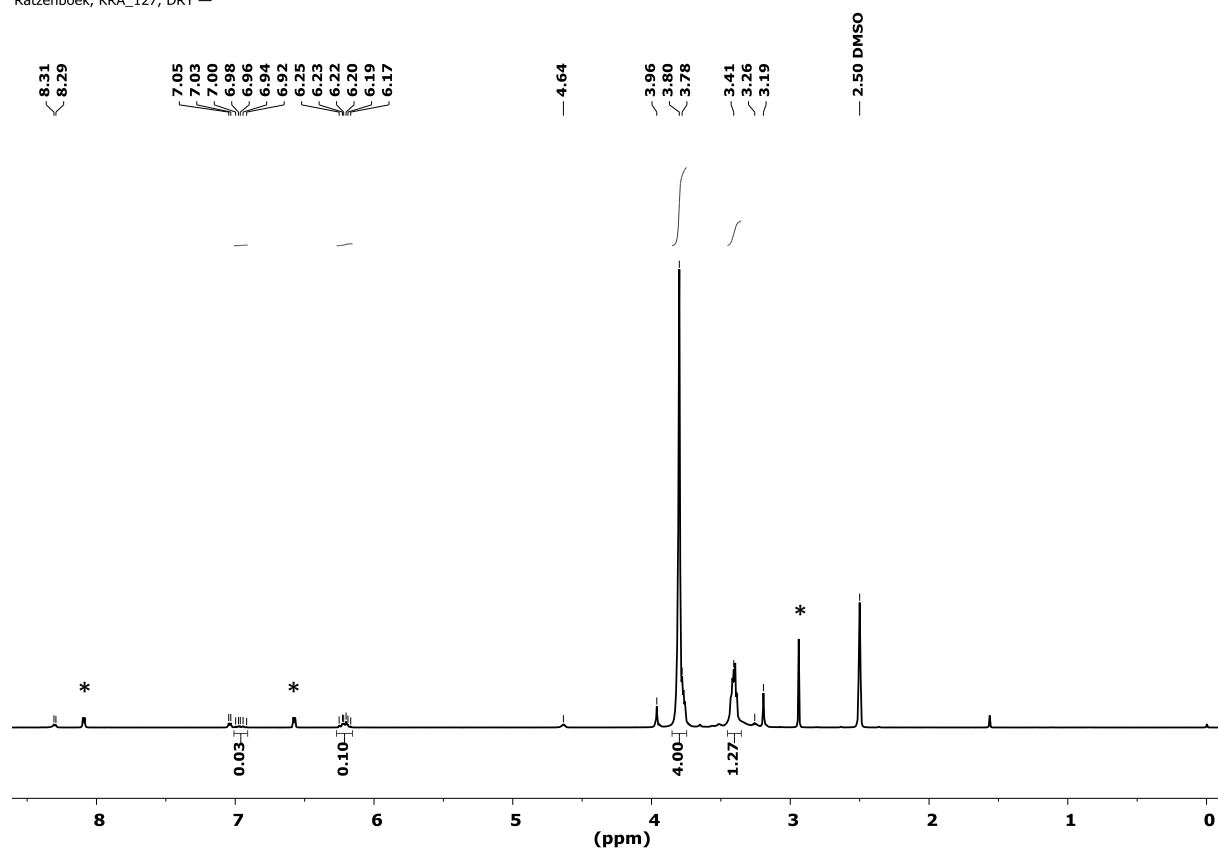


Figure S36. ^1H -NMR spectrum of synthesis of PES with D_2O in $\text{DMSO}-d_6$; * denotes residual DMAP.

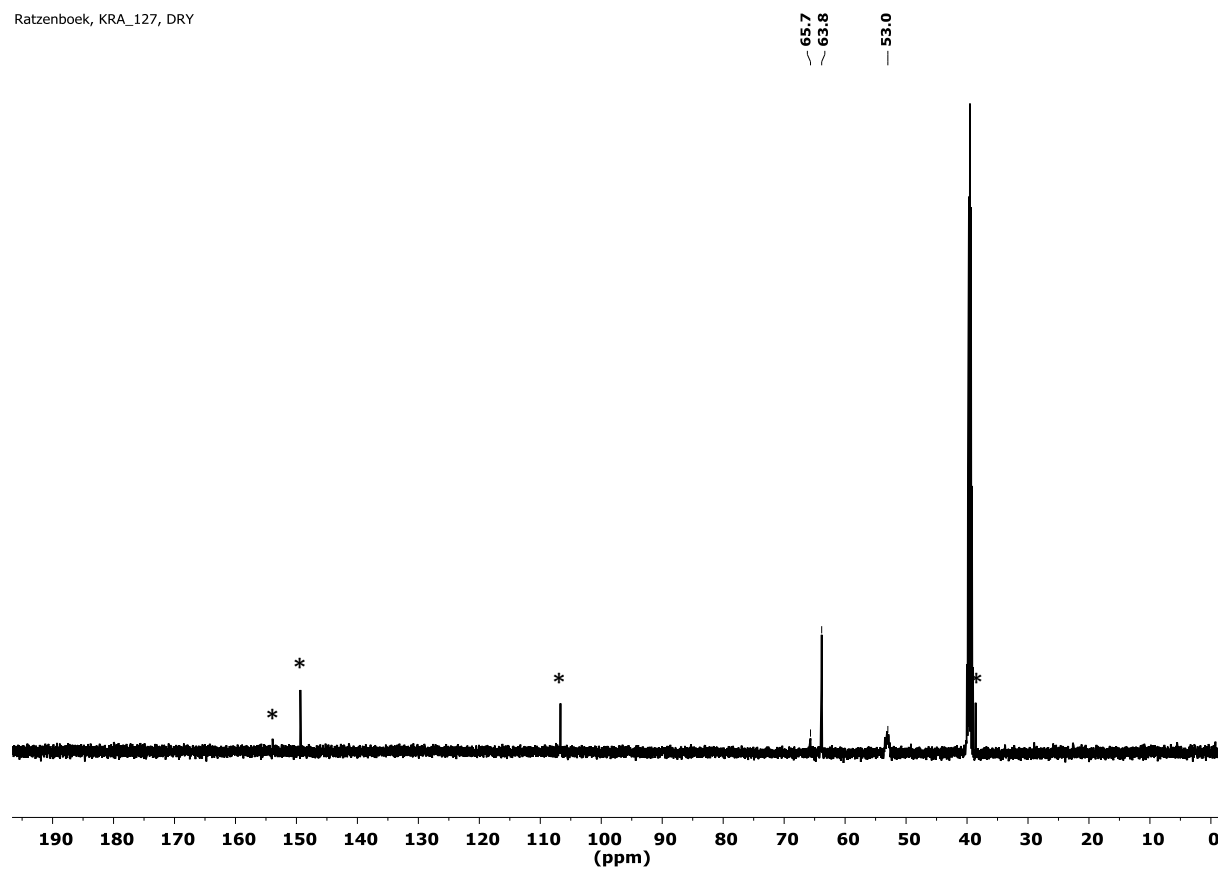


Figure S37. ^{13}C -NMR spectrum of synthesis of PES with D_2O in $\text{DMSO}-d_6$; * denotes residual DMAP.

Reactivity of DVS with D₂O

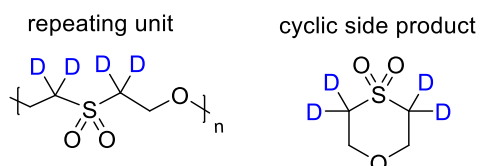
To evaluate if deuterium exchange of D₂O and the vinyl proton next to the sulfone group is possible if no base or nucleophiles are present, 666 mg (33.3 mmol, 100 equiv.) D₂O and 39.3 mg (0.33 mmol, 1 equiv.) divinyl sulfone were stirred for 20 h at room temperature and at 80 °C to ensure miscibility. In both cases, ¹H-NMR spectra after 5 min and 20 h reaction time showed an identical integral proton ratio of the vinyl groups and no incorporation of deuterium.

Synthesis of PES monitored in D₂O

A NMR tube was charged with 5.2 mol% (2.1 mg, 0.017 mmol) DMAP or 4.9 mol% (1.8 mg, 0.016 mmol) KO^tBu. Thereupon, 666 mg (33.3 mmol, 100 equiv.) D₂O and 39.3 mg (0.33 mmol, 1 equiv.) divinyl sulfone were added. ¹H-NMR spectroscopy was measured after 5 min and 1 h. After about 1 h the off-white product precipitated from D₂O. It was dissolved in DMSO-*d*₆ and analysed by ¹H-NMR spectroscopy (Figure S41).

¹H-NMR (300 MHz, DMSO-*d*₆): δ = 6.22 – 6.19 (d, -CD=CH₂ end group), 3.95 (s, -O-CH₂- cyclic), 3.78 (s, -O-CH₂-) ppm.

¹H-NMR (300 MHz, D₂O): δ = 6.45 – 6.35 (m, -CD=CH₂ end group), 4.17 (s, -O-CH₂- cyclic), 3.97 (s, -O-CH₂-) ppm.



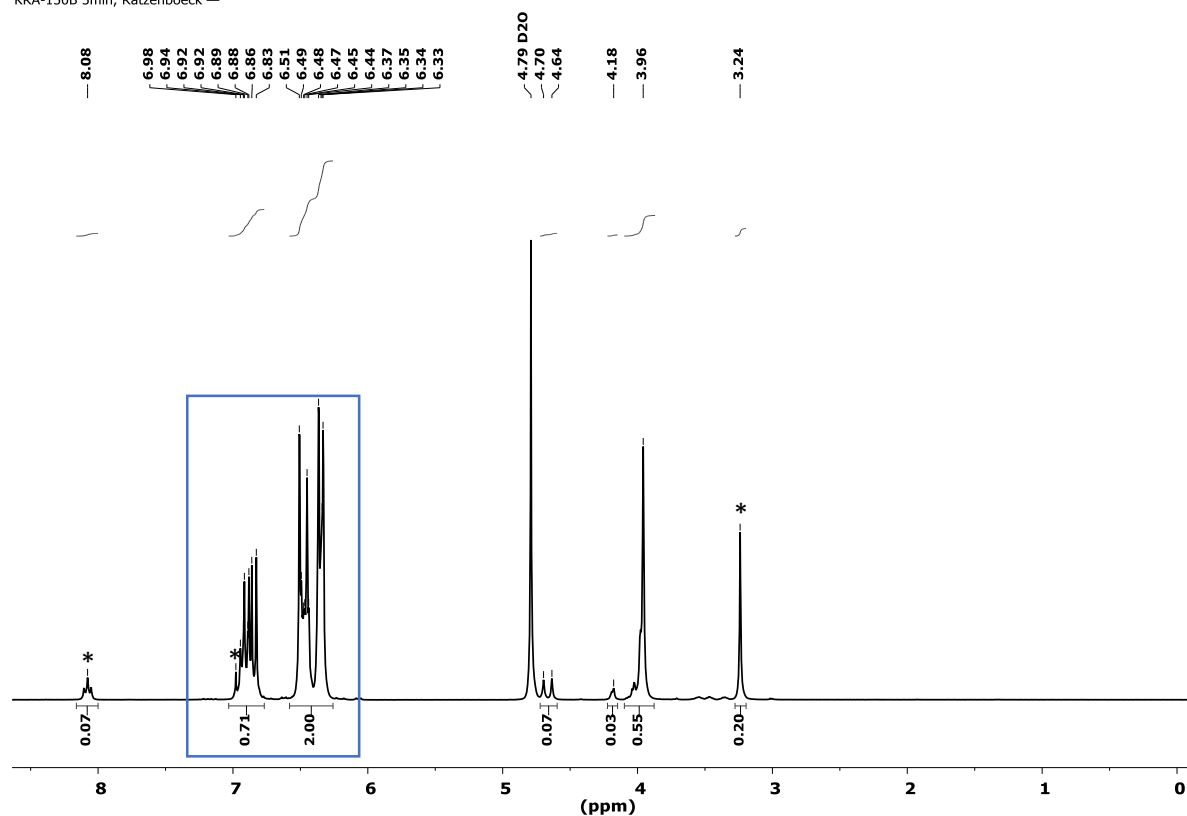


Figure S38. ^1H -NMR spectrum after 5 min of synthesis of **PES** in D_2O catalyzed by DMAP, * denotes DMAP; signals of DMAP and DVS overlap (6.98-6.83 ppm); $0.71-0.07 = 0.64$; integral ratio 0.64:2.

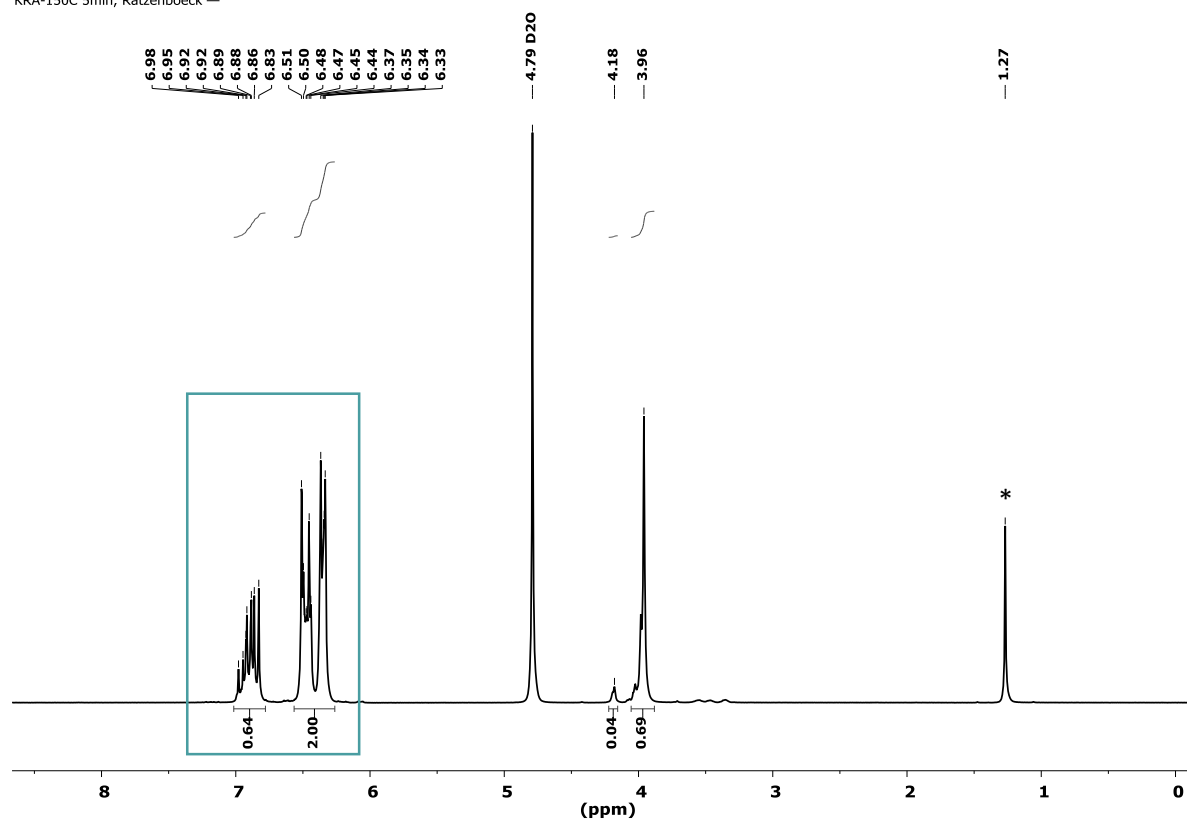


Figure S39. ^1H -NMR spectrum after 5 min of synthesis of **PES** in D_2O catalyzed by KO^tBu , * denotes KO^tBu ; integral ratio 0.64:2.

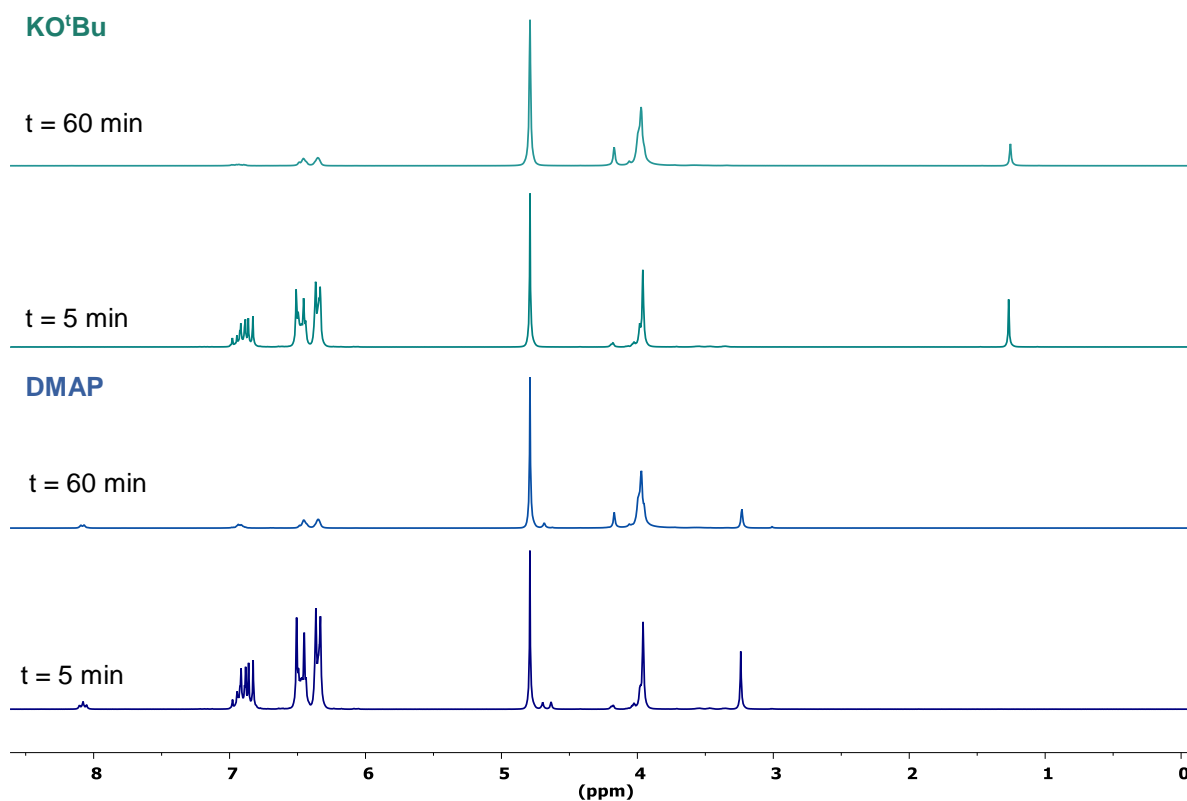


Figure S40. Comparison of ^1H -NMR spectrum of the synthesis of **PES** in D_2O after 5 min and 60 min catalyzed by DMAP (bottom) or KO^tBu (top).

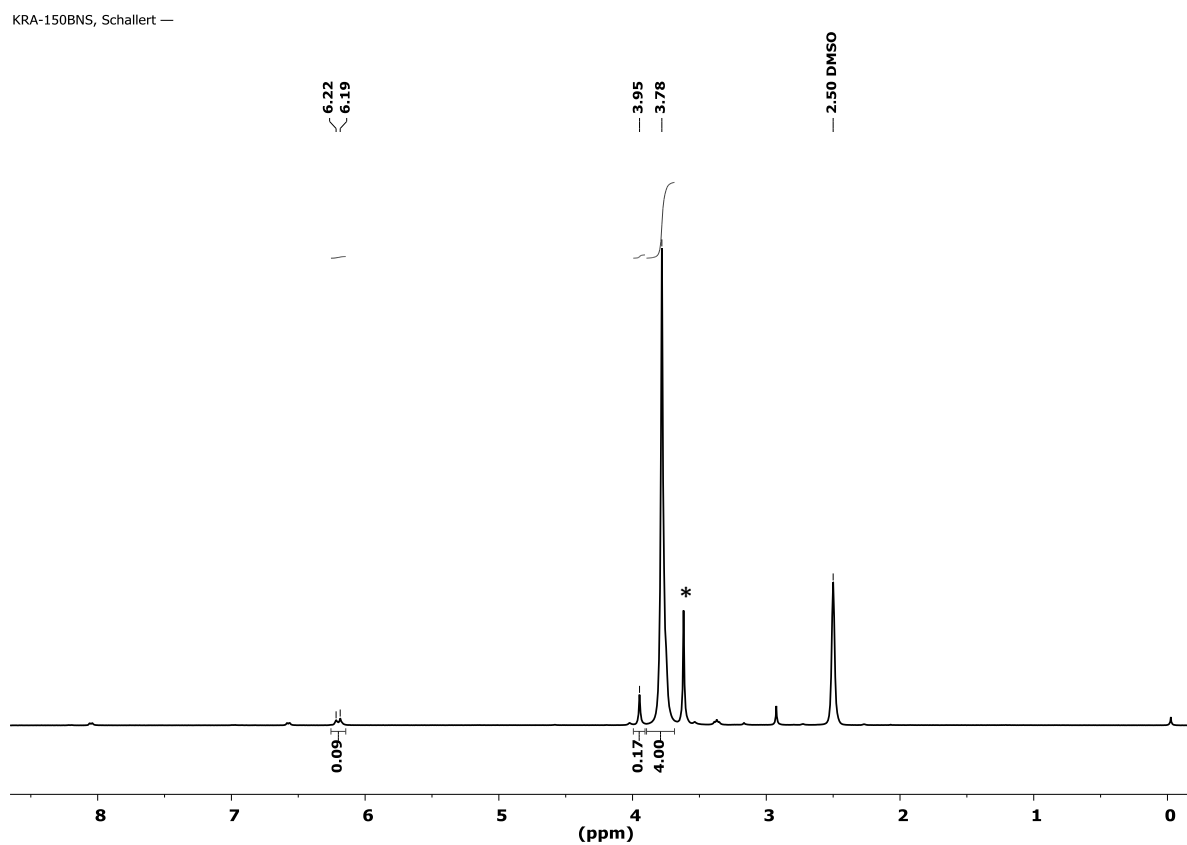


Figure S41. ^1H -NMR spectrum of polymer obtained by synthesis of **PES** with 100 equiv. D_2O in $\text{DMSO}-d_6$, * denotes HDO.

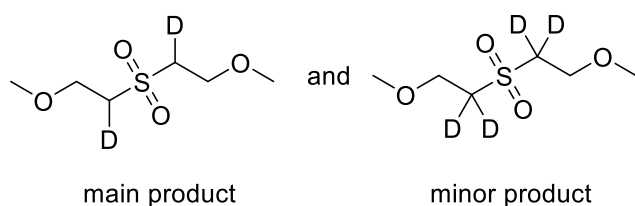
To demonstrate the acidity of the proton in the α -position to the sulfone group, bis-(2-methoxyethyl)-sulfone was synthesized and stirred with D₂O under basic conditions. By ¹H-NMR spectroscopy partly deuterated bis-(2-methoxyethyl)-sulfone in the α -position to the sulfone group was observed.

Reaction of bis-(2-methoxyethyl)-sulfone with D₂O

Bis-(2-methoxyethyl)-sulfone was synthesized according to modified literature procedure using 2.5 mol% DBU as catalyst.^[1] In a 4 mL reaction vessel 5.5 mol% (2.9 mg, 0.026 mmol) KO^tBu, 86 mg (0.47 mmol, 1 equiv.) bis-(2-methoxyethyl)-sulfone and 50 μ L (2.77 mmol, 5.9 equiv.) D₂O were stirred for 50 min. Partly deuterated bis-(2-methoxyethyl)-sulfone was obtained.

¹H-NMR (300 MHz, CDCl₃): δ = 3.81 (t, -O-CH₂-, 4H), 3.38 (s, -CH₃, 6H), 3.31 (m, -CHD-SO₂-, 1.7H) ppm.

¹³C-NMR (76 MHz, CDCl₃): δ = 66.2 – 66.1 (-O-CH₂-), 59.2 (CH₃), 55.0, 54.8, 54.5 (-CHD-SO₂- / -CD₂-SO₂-) ppm.

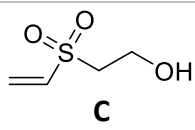
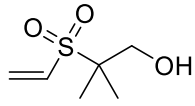
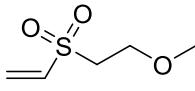


pK_a values

For the calculation of pK_a values we used the prediction platform provided by the Luo group.^[2] For water in water a pK_a of 13.32 could be retrieved. The pK_a of compound **C** (Scheme 1) was calculated by the same method. In general, Luo's pK_a calculations are in good agreement with experimental values for e.g. alcohols (see Table S2). Concerning compound **C**, it can also be seen that the acidity of similar compounds remains high e.g. if the α -carbon is substituted with methyl groups. However, the protons at α -position are of similar acidity than the OH group (as revealed by calculating the pK_a of the methanol adduct).

In the context of our work it is important to consider the acidities in a non-protic (polar) solvent like DMSO (which might be the best approximation for DVS). Such pK_a values in DMSO can also be retrieved with Luo's method. Also in this case calculated values are in agreement with measured values. It is demonstrated by both experiments and calculations that alcohols are more acidic than water using DMSO as solvent. The only exception is *t*-BuOH which is less acidic than water. The acidity of **C** in DMSO is found to be distinctly higher than that of water.

Table S2. Calculated and experimental pK_a values in H₂O or DMSO.

	calc. pK _a (H ₂ O) ^[2]	exp. pK _a (H ₂ O) ^[3,4]	calc. pK _a (DMSO) ^[2]	exp. pK _a (DMSO) ^[3]
H ₂ O	13.32	14 / 15.75	28.23	31.4
MeOH	15.44	15.49	27.92	29.0
EtOH	15.69	15.93	28.15	29.8
<i>i</i> -PrOH	16.78	16.10	29.66	30.3
<i>t</i> -BuOH	16.83	16.04	31.13	32.2
 C	9.49	-	14.64	-
	9.88	-	15.13	-
	10.62	-	20.51	-

7. Computational Details

All calculations were run with the TURBOMOLE program (version 7.4.1)^[5], except for the DLPNO-CCSD(T)/aug-cc-pVTZ calculations which were performed with ORCA (version 4.2.1).^[6] Conformational searches of all structures have been performed with the COSMO-conf programme^[7] with geometries optimized at the PBE^[8]/def2-SVPD level and D3-dispersion^[10] correction. Furthermore, single points were calculated using PBE+D3/def2-TZVPPD.

The lowest-energy structures were then optimized using the B3LYP^[9] functional, the def2-TZVPPD basis set and D3^[10]-dispersion correction. Analytical normal modes were determined using the TURBOMOLE's aoforce program for confirmation of the stationary points and calculation of the frequencies. The frequencies were scaled by a factor of 1.003^[11] to account for anharmonic effects and zero-point vibrational energies and thermal properties (at 25°C) were calculated using the rigid-rotor harmonic oscillator (RRHO) approximation using the abovementioned B3LYP+D3/def2-TZVPPD.

At these minima, we also calculated single point energies using MP2/aug'-cc-pVTZ and MP2/aug'-cc-pVQZ, representing a mixed scheme in which diffuse functions are used on all atoms except hydrogen. Single point energies were also calculated with DLPNO-CCSD(T) with the aug-cc-pVTZ basis set. Both Hartree-Fock and correlation energies were extrapolated to the basis set limit by using the respective l^{-5} ^[12] and l^{-3} ^[13] extrapolation formulae:

$$HF/aug'-cc-pVTQZ = E(HF_{QZ}) + \frac{E(HF_{QZ}) - E(HF_{TZ})}{(\frac{4}{3})^5 - 1}$$

$$MP2corr/aug'cc-pVTQZ = E(MP2 - HF)_{QZ} + \frac{E(MP2-HF)_{QZ} - E(MP2-HF)_{TZ}}{(\frac{4}{3})^3 - 1}$$

Our best estimate of the energy results in:

$$E = HF/aug'-cc-pVTQZ + MP2corr/aug'-cc-pVTQZ + \Delta(CCSD(T)-MP2)/aug-cc-pVTZ + \Delta[T,ZPVE](B3LYP/def2-TZVPPD)$$

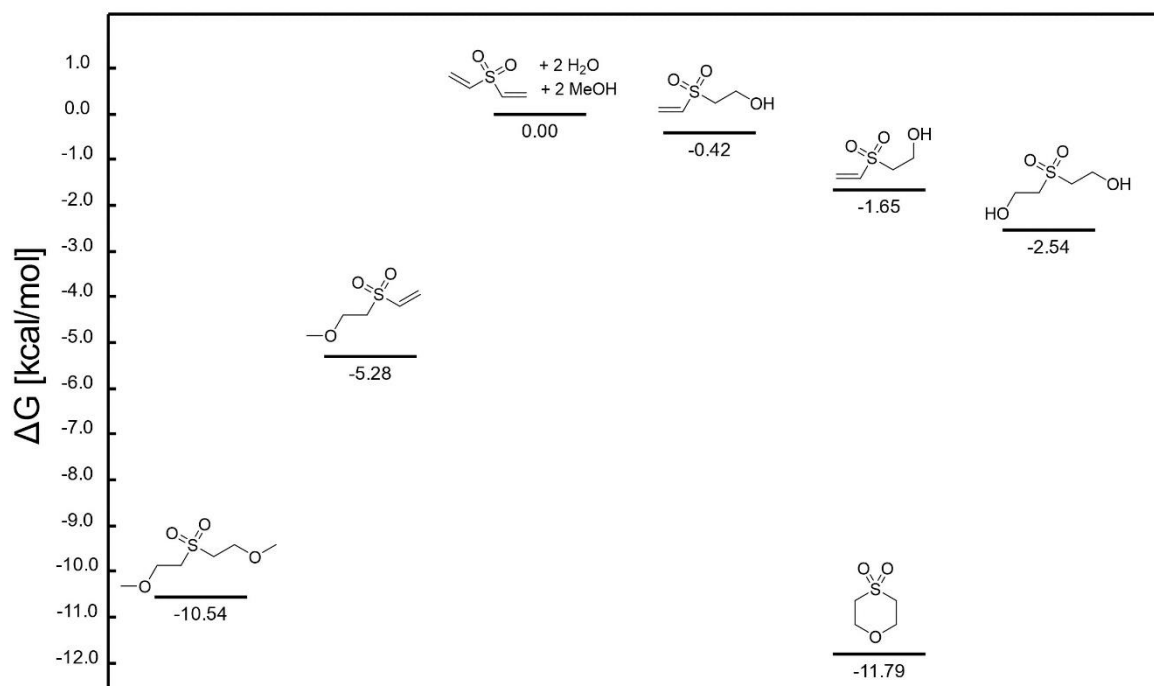


Figure S42. Relative stabilities of model compounds; additional H₂O and MeOH molecules were omitted in the illustration.

Gibbs' free energies of several alcohol and ether model structures were calculated using the abovementioned post-Hartree Fock scheme. Generally, oxa-Michael products of divinyl sulfone and methanol were found to be more much more stable than those with water as Michael donor. Thus, the formation of an ether (-5.28 kcal/mol) is thermodynamically favored over the formation of 2-hydroxyethyl vinyl sulfone (-0.42 kcal/mol). The energy difference of below 1 kcal/mol between divinyl sulfone and 2-hydroxyethyl vinyl sulfone also supports experiments in which reversibility of the reaction was observed. By conformational analysis of all structures, it was found that intramolecular hydrogen bonding leads to a stabilization of 2-hydroxyethyl vinyl sulfone lowering the Gibbs' free energy to -1.65 kcal/mol. However, since the reaction is performed in water, intermolecular hydrogen bonding interactions can also be expected for divinyl sulfone and 2-hydroxyethyl vinyl sulfone. These would stabilize the structures and potentially favor the linear structure over the one with intramolecular hydrogen bonding.

Moreover, di-hydration of divinyl sulfone leading to HES is thermodynamically favored (-2.54 kcal/mol). In experiments at room temperature, HES could not be observed as 2-hydroxyethyl vinyl sulfone immediately reacts with vinyl sulfone species. Additionally, the formation of 1,4-oxathiane 4,4-dioxide (**1**) is thermodynamically strongly favored (-11.79 kcal/mol). However, as already noted **1** was only observed as minor side product.

Table S3. Energies obtained from DFT, MP2 and DLPNO-CCSD(T) calculations of model structures.

	DFT				MP2 TZ			MP2 QZ			Extrapolation			DLPNO-CCSD(T)			Total Energy + chem. pot [kJ/mol]	kcal/mol
	E (el) [Hartree]	E [kJ/mol]	Chem. Pot	Total Energy	E (HF TZ)	Delta MP2-HF	E (MP2 TZ)	E (HF QZ)	Delta MP2-HF (QZ)	E (MP2 QZ)	exchange	correlation	E MP2 extrapol	E MP2	E CCSDT	Delta	E MP2 + ΔCCSD(T)	
DVS	-704,53800	-1849764,529	167,26	-1849597,269	-702	-1,4678	-704	-702,284888	-1,647633191	-703,932522	-0,01059984	-0,13124837	-704,0743698	-704	-704	-0,0907	-704,1651	-1.848.618,1
H2O	-76,432409	-200673,2889	7,94	-200665,3489	-76,0599945	-0,282044439	-76,3420389	-76,0654272	-0,316705539	-76,3821327	-0,00169031	-0,02529324	-76,40911625	-76,3280059	-76	-0,0132	-76,4223	-200.638,8
HES	-857,453244	-2251243,491	308,74	-2250934,751	-854	-2,04888	-856	-854	-2	-857	-0,01353429	-0,17867632	-856,9448565	-856,289158	-856,405881	-0,1167	-857,0616	-2.249.906,4
Difference	-0,050423	-132,384699	125,60000	-6,784699	-0,044601	-0,017021	-0,061621	-0,043167	-0,012692	-0,055859			-0,052254	-0,056127	-0,055765	0,000362	-0,051892	-10,64
kJ/mol					-117,10		-161,79	-113,33		-146,66			-137,19	-147,36	-146,41	0,95	-136,24	-2,54

	DFT				MP2 TZ			MP2 QZ			Extrapolation			DLPNO-CCSD(T)			Total Energy + chem. pot [kJ/mol]	kcal/mol
	E (el) [Hartree]	E [kJ/mol]	Chem. Pot	Total Energy	E (HF TZ)	Delta MP2-HF	E (MP2 TZ)	E (HF QZ)	Delta MP2-HF (QZ)	E (MP2 QZ)	exchange	correlation	E MP2 extrapol	E MP2	E CCSDT	Delta	E MP2 + ΔCCSD(T)	
DVS	-704,53800	-1849764,529	167,26	-1849597,269	-702	-1,4678	-704	-702,284888	-1,647633191	-703,932522	-0,01059984	-0,13124837	-704,0743698	-704	-704	-0,0907	-704,1651	-1.848.618,1
H2O	-76,432409	-200673,2889	7,94	-200665,3489	-76,0599945	-0,282044439	-76,3420389	-76,0654272	-0,316705539	-76,3821327	-0,00169031	-0,02529324	-76,40911625	-76,3280059	-76	-0,0132	-76,4223	-200.638,8
Vinylsulfonylethanol	-780,996048	-2050498,698	236,47	-2.050.262,23	-778	-2	-780	-778	-2	-780	-0,01205498	-0,15488701	-780,5077946	-779,931482	-780,035067	-0,1036	-780,6114	-2.049.263,7
Difference	-0,023188	-60,880460	61,270000	0,389540	-0,021348	-0,007873	-0,029222	-0,020592	-0,005606	-0,026198			-0,024309	-0,026457	-0,026148	0,000309	-0,023999	-1,74
kJ/mol					-56,05		-76,72	-54,07		-68,78			-63,82	-69,46	-68,65	0,81	-63,01	-0,42

	DFT				MP2 TZ			MP2 QZ			Extrapolation			DLPNO-CCSD(T)			Total Energy + chem. pot [kJ/mol]	kcal/mol
	E (el) [Hartree]	E [kJ/mol]	Chem. Pot	Total Energy	E (HF TZ)	Delta MP2-HF	E (MP2 TZ)	E (HF QZ)	Delta MP2-HF (QZ)	E (MP2 QZ)	exchange	correlation	E MP2 extrapol	E MP2	E CCSDT	Delta	E MP2 + ΔCCSD(T)	
DVS	-704,53800	-1849764,529	167,26	-1849597,269	-702	-1,4678	-704	-702,284888	-1,647633191	-703,932522	-0,01059984	-0,13124837	-704,0743698	-704	-704	-0,0907	-704,1651	-1.848.618,1
H2O	-76,432409	-200673,2889	7,94	-200665,3489	-76,0599945	-0,282044439	-76,3420389	-76,0654272	-0,316705539	-76,3821327	-0,00169031	-0,02529324	-76,40911625	-76,3280059	-76	-0,0132	-76,4223	-200.638,8
Vinylsulfonylethanol stab.	-780,996048	-2050505,125	237,82	-2.050.267,31	-778	-2	-780	-778	-2	-780	-0,01206103	-0,15496752	-780,5102869	-779,933795	-780,037367	-0,1036	-780,6139	-2.049.263,9
Difference	-0,025636	-67,307528	62,620000	-4,687528	-0,022618	-0,008880	-0,031498	-0,021881	-0,006723	-0,028604			-0,026801	-0,028771	-0,028449	0,000322	-0,026479	-6,90
kJ/mol					-59,38		-82,70	-57,45		-75,10			-70,37	-75,54	-74,69	0,84	-69,52	-1,65

	DFT				MP2 TZ			MP2 QZ			Extrapolation			DLPNO-CCSD(T)			Total Energy + chem. pot [kJ/mol]	kcal/mol
	E (el) [Hartree]	E [kJ/mol]	Chem. Pot	Total Energy	E (HF TZ)	Delta MP2-HF	E (MP2 TZ)	E (HF QZ)	Delta MP2-HF (QZ)	E (MP2 QZ)	exchange	correlation	E MP2 extrapol	E MP2	E CCSDT	Delta	E MP2 + ΔCCSD(T)	
DVS	-704,53800	-1849764,529	167,26	-1849597,269	-702	-1,4678	-704	-702,284888	-1,647633191	-703,932522	-0,01059984	-0,13124837	-704,0743698	-704	-704	-0,0907	-704,1651	-1.848.618,1
MeOH	-115,715358	-303810,673	74,45	-303.736.22304	-115,091441	-0,467352136	-115,558793	-115,099063	-0,522518671	-115,621582	-0,00237163	-0,04025666	-115,6642104	-115,527356	-116	-0,0332	-115,6974	-303.689,1
DVS MeOH	-820,283823	-2153655,179	304,22	-2.153.350,96	-817	-2	-819	-817	-2	-820	-0,01272986	-0,16948432	-819,7722803	-819,14042	-819,262859	-0,1224	-819,8947	-2.152.329,4
Difference	-0,030462	-79,976814	62,510000	-17,466814	-0,026345	-0,013163	-0,039508	-0,025568	-0,010394	-0,035962			-0,033700	-0,036046	-0,034569	0,001477	-0,032223	-22,09
kJ/mol					-69,17		-103,73	-67,13		-94,42			-88,48	-94,64	-90,76	3,88	-84,60	-5,28

	DFT				MP2 TZ			MP2 QZ			Extrapolation			DLPNO-CCSD(T)			Total Energy + chem. pot [kJ/mol]	kcal/mol
	E (el) [Hartree]	E [kJ/mol]	Chem. Pot	Total Energy	E (HF TZ)	Delta MP2-HF	E (MP2 TZ)	E (HF QZ)	Delta MP2-HF (QZ)	E (MP2 QZ)	exchange	correlation	E MP2 extrapol	E MP2	E CCSDT	Delta	E MP2 + ΔCCSD(T)	
DVS	-704,53800	-1849764,529	167,26	-1849597,269	-702	-1,4678	-704	-702,284888	-1,647633191	-703,932522	-0,01059984	-0,13124837	-704,0743698	-704	-704	-0,0907	-704,1651	-1.848.618,1
MeOH	-115,715358	-303810,673	74,45	-303.736.22304	-115,091441	-0,467352136	-115,558793	-115,099063	-0,522518671	-115,621582	-0,00237163	-0,04025666	-115,6642104	-115,527356	-116	-0,0332	-115,6974	-303.689,1
DVS MeOH2	-936,03189	-2457547,26	441,86	-2.457.105.400	-932	-2	-935	-932,534071	-2,714014179	-935,248086	-0,01486689	-0,20767374	-935,4706262	-934,704506	-934,858469	-0,1540	-935,6246	-2.456.040,5
Difference	-0,061468	-161,385294	125,7000	-35,685294	-0,052587	-0,026946	-0,079532	-0,051056	-0,021344	-0,072400			-0,067836	-0,072776	-0,069610	0,003166	-0,064670	-44,09
kJ/mol					-138,07		-208,81	-134,05		-190,09			-178,10	-191,07	-182,76	8,31	-169,79	-10,54

	DFT				MP2 TZ			MP2 QZ			Extrapolation			DLPNO-CCSD(T)			Total Energy + chem. pot [kJ/mol]	kcal/mol
	E (el) [Hartree]	E [kJ/mol]	Chem. Pot	Total Energy	E (HF TZ)	Delta MP2-HF	E (MP2 TZ)	E (HF QZ)	Delta MP2-HF (QZ)	E (MP2 QZ)	exchange	correlation	E MP2 extrapol	E MP2	E CCSDT	Delta	E MP2 + ΔCCSD(T)	
DVS	-704,538004	-1849764,529	167,26	-1849597,269	-702	-1,4678	-704	-702,284888	-1,647633191	-703,932522	-0,01059984	-0,13124837	-704,0743698	-704	-704	-0,0907	-704,1651	-1.848.618,1
H2O	-76,432409	-200673,2889	7,94	-200665,3489	-76,0599945	-0,282044439	-76,3420389	-76,0654272	-0,316705539	-76,3821327	-0,00169031	-0,02529324	-76,40911625	-76,3280059	-76	-0,0132	-76,4223	-200.638,8
Oxathiane	-781,014613	-2050553,866	253,67	-2.050.300,20	-778	-2	-780	-778	-2	-780	-0,01195009	-0,15392476	-780,5339038	-779,9586	-780,060749	-0,1021	-780,6361	-2.049.306,3
Difference	-0,044201	-116,048671	78,470000	-37,578671	-0,043839	-0,014215	-0,058054	-0,042746	-0,010629	-0,053375			-0,050418	-0,053576	-0,051830	0,001746	-0,048672	-49,318259
kJ/mol					-115,10		-152,42	-112,23		-140,14			-132,37	-140,66	-136,08	4,58	-127,79	-11,79

8. SEC Chromatogram with Different Detectors

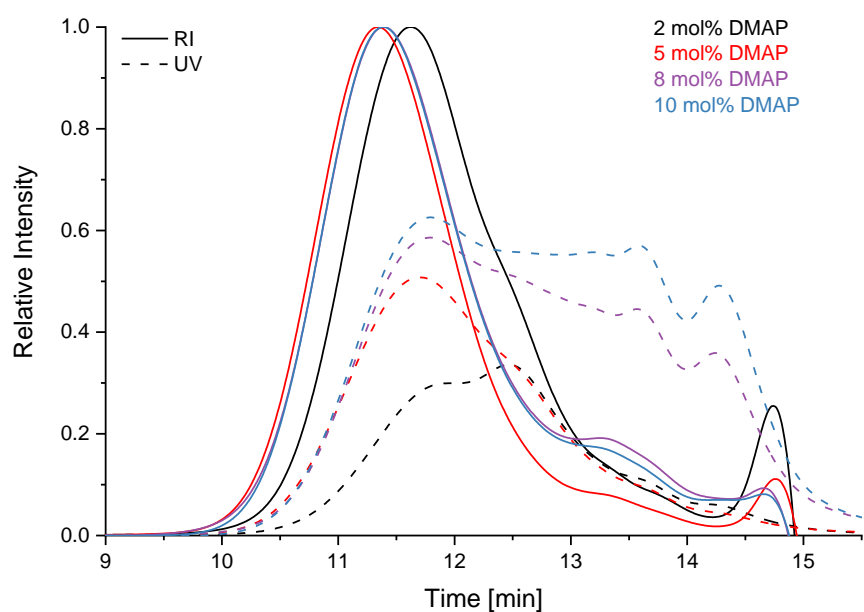


Figure S43. SEC chromatograms of **PES** samples prepared with 2, 5, 8 and 10 mol% DMAP; RI (full) and UV detector (dashed).

9. Bulk NMR Experiments

Bulk NMR experiments with a benzene-*d*₆ insert capillary were carried out.

Interface

A NMR tube containing a capillary insert with benzene-*d*₆ was filled with 200 μ L divinyl sulfone and 200 μ L water (Figure S44). The NMR coil was positioned at the interface of the DVS and water layer resulting in a spectrum in which both shifts of the bulk divinyl sulfone layer as well as of the bulk water layer can be observed. Shifts for bulk water are in accordance with Oka et al.^[14]

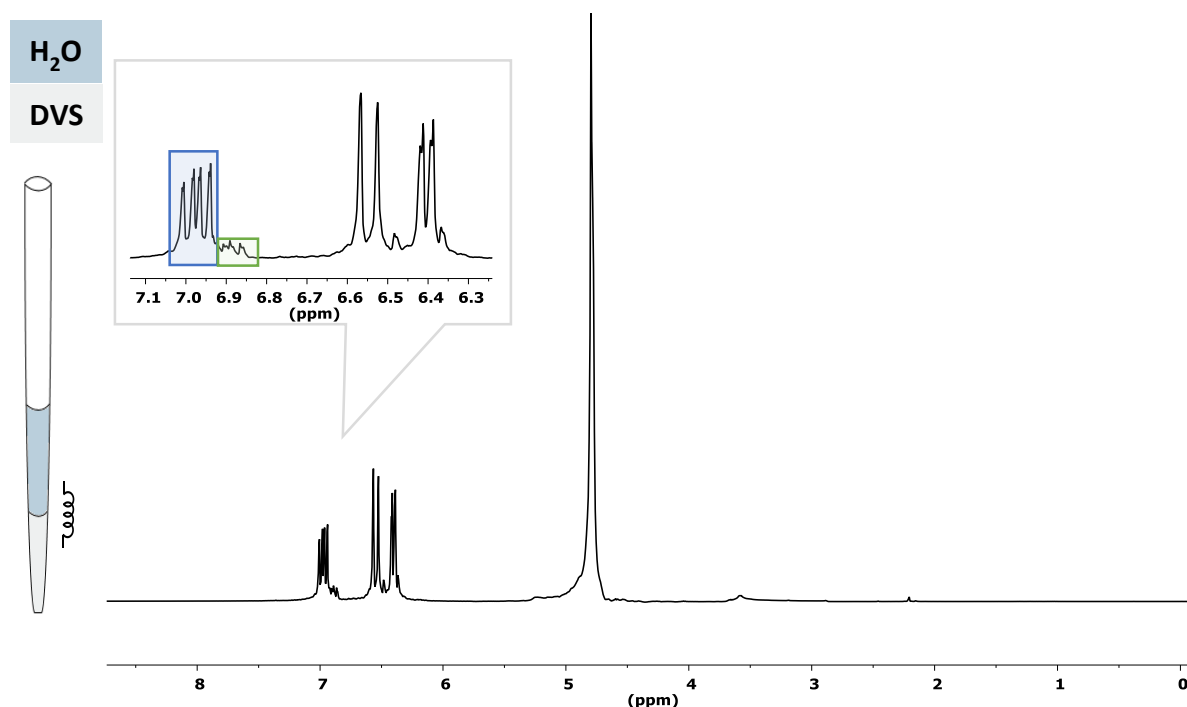


Figure S44. Initial ¹H-NMR spectrum at the interface of water and DVS layer; DVS layer (blue) as well as DVS dissolved in water (green) observed.

After the addition of 5 mol% DMAP dissolved in water the bulk reaction mixture was not shaken in order to still observe the interface of the two layers. Hardly any water dissolved in the DVS layer (Figure S45, bottom). After shaking the NMR tube water dissolved in DVS is observed (Figure S45, top).

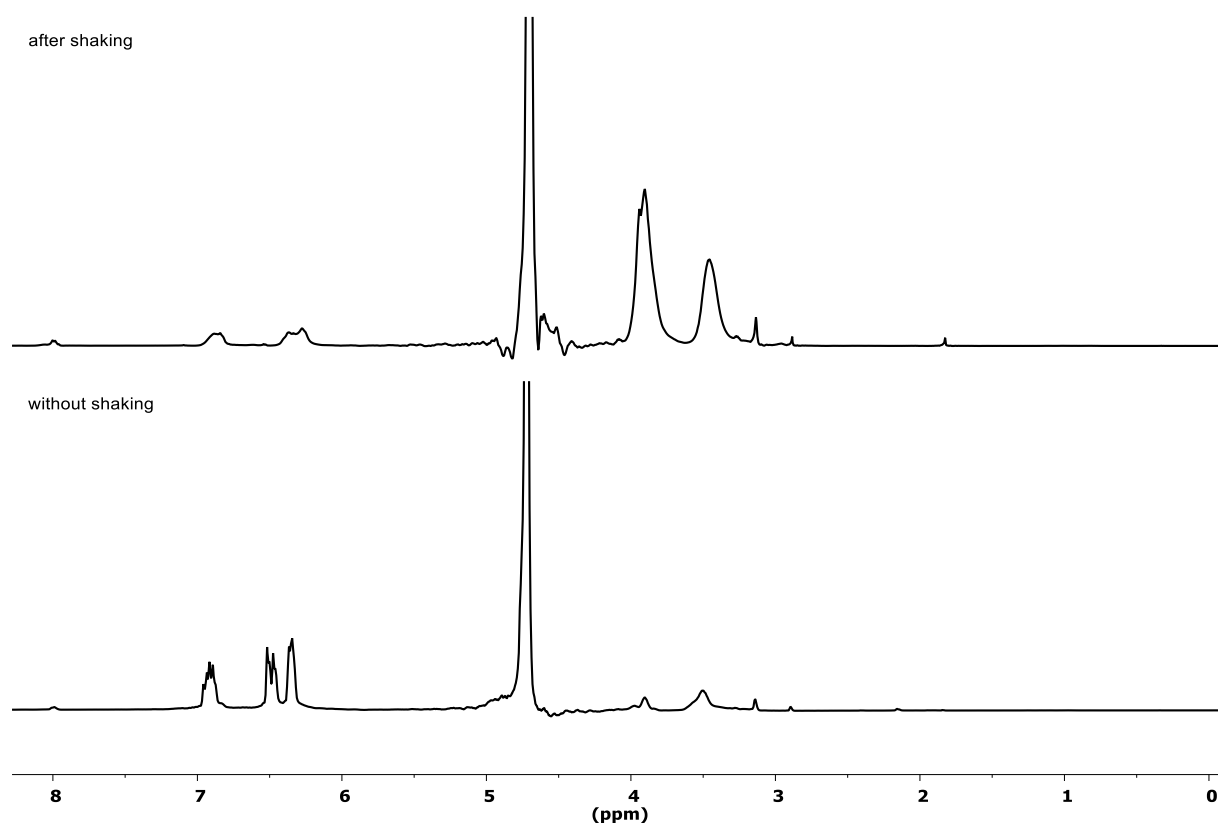


Figure S45. Comparison of ^1H -NMR spectrum after the addition of DMAP without shaking (bottom) and after shaking (top).

DVS layer

A NMR tube containing a capillary insert with benzene-*d*₆ was filled with 400 μ L divinyl sulfone and 172 μ L water in which 5.1 mg DMAP were dissolved. Only after shaking the NMR tube water dissolved in DVS and minor product formation was observed (Figure S46, bottom). After 24 h without stirring only a low amount of product formed in the DVS layer (Figure S46, top).

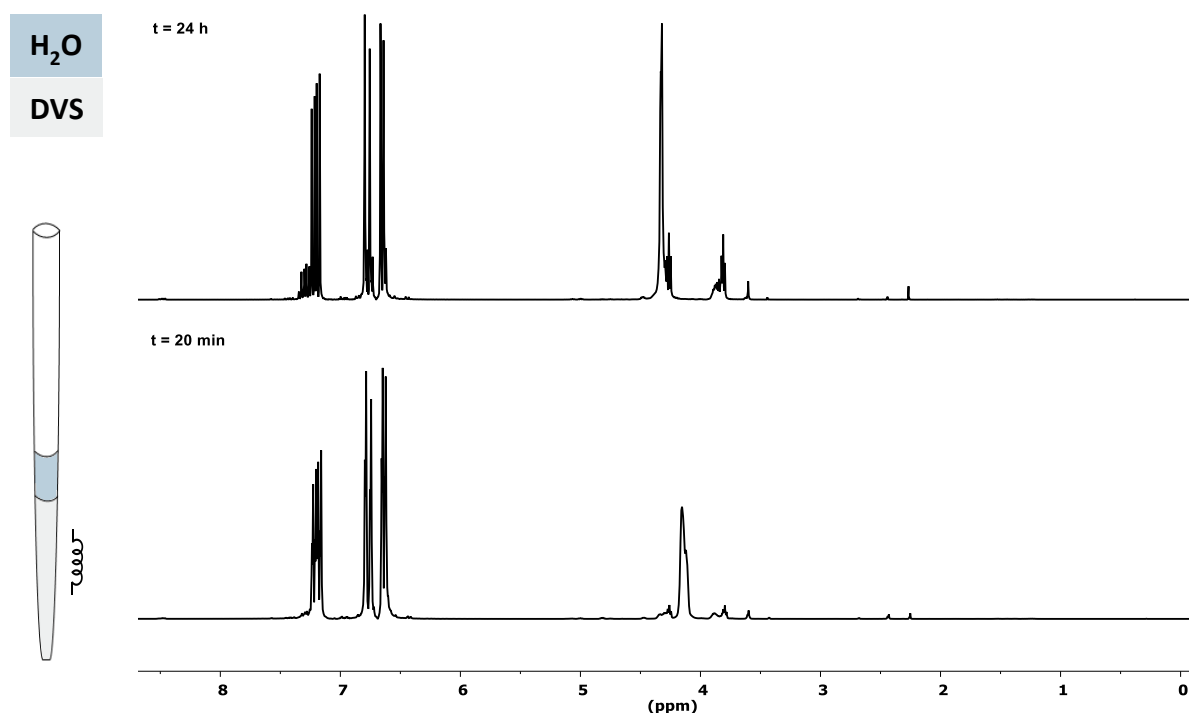


Figure S46. Comparison of ¹H-NMR spectrum after 20 min after shaking (bottom) and 24 h reaction time without stirring (top).

Water layer

A NMR tube containing a capillary insert with benzene- d_6 was filled with 50 μL divinyl sulfone and 350 μL water (Figure S47, bottom). Thereafter, 5.5 mg DMAP dissolved in 40 μL water was added (Figure S47, top) without shaking. Once catalyst is present hardly any unreacted DVS in the water layer can be detected. However, minor product formation can be observed. After 1.3 h (without stirring) still only small amounts of product as well as **1** were detected in the reaction mixture (Figure S48, top).

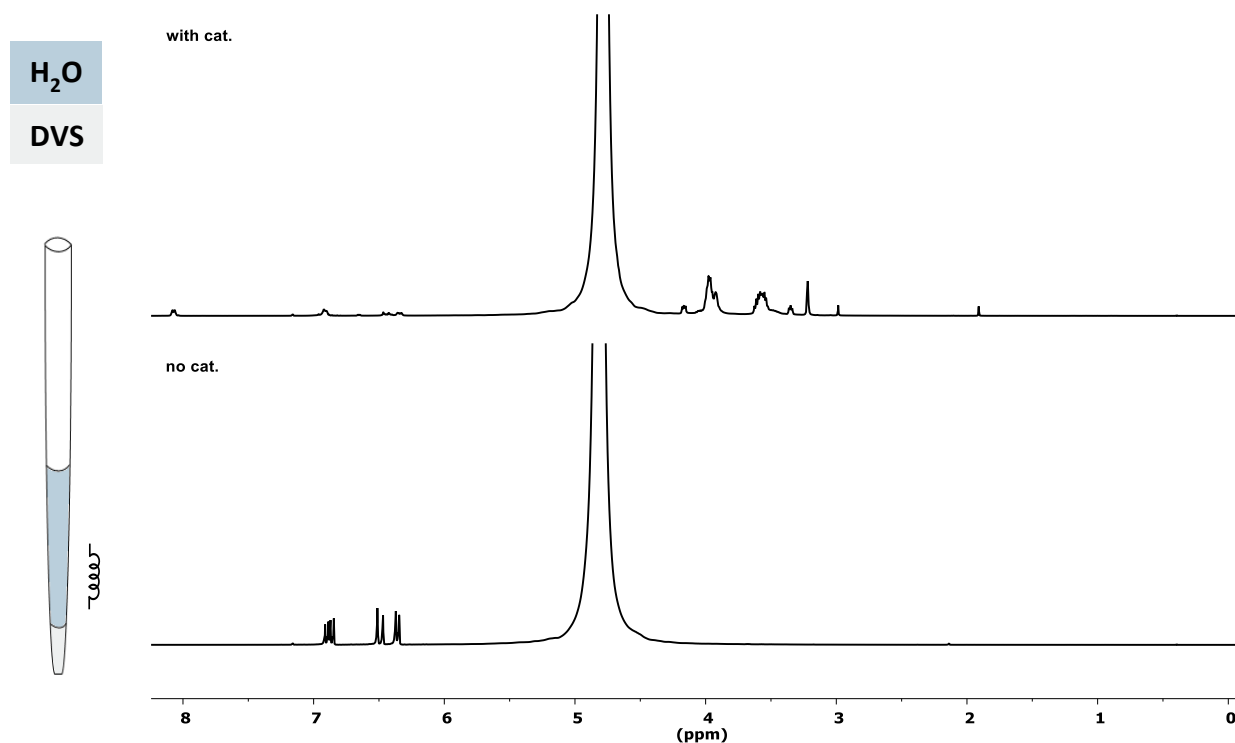


Figure S47. Comparison of ^1H -NMR spectrum before (bottom) and after the addition of DMAP (top).

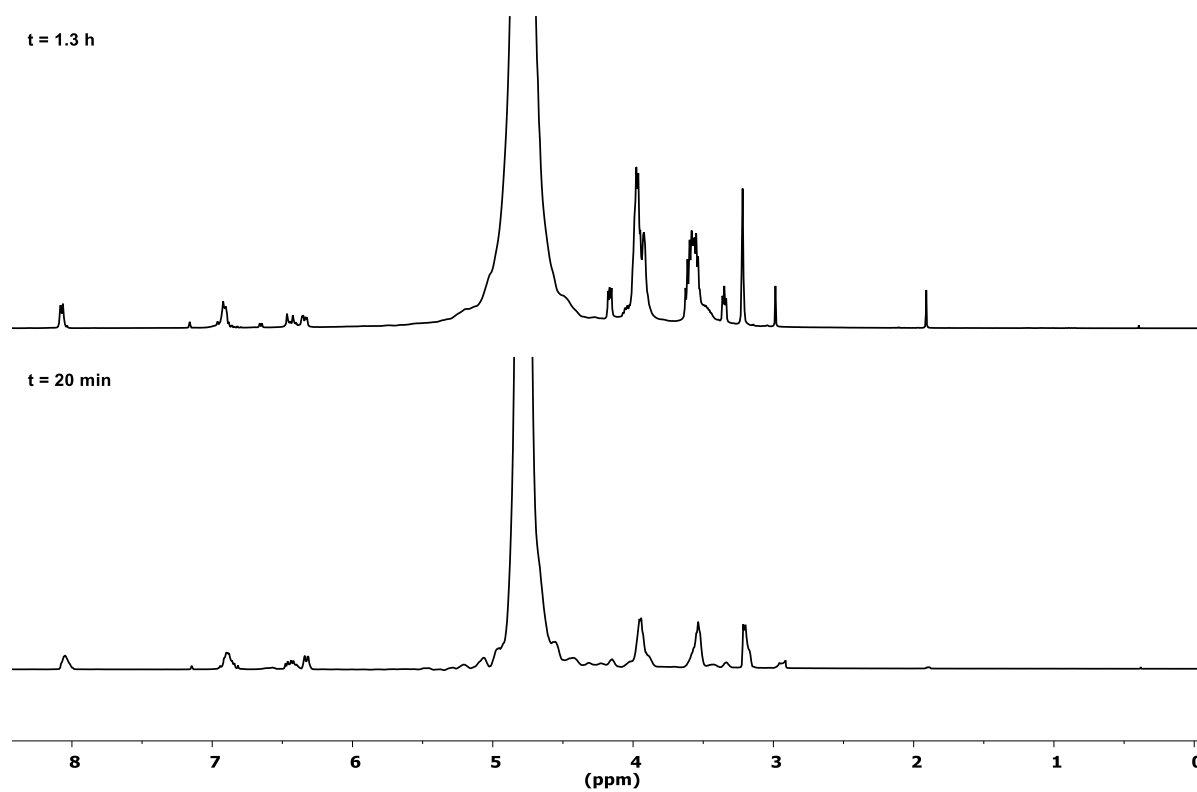


Figure S48. Comparison of ¹H-NMR spectrum after 20 min (bottom) and 1.3 h (top) reaction time showing only a small increase in product formation.

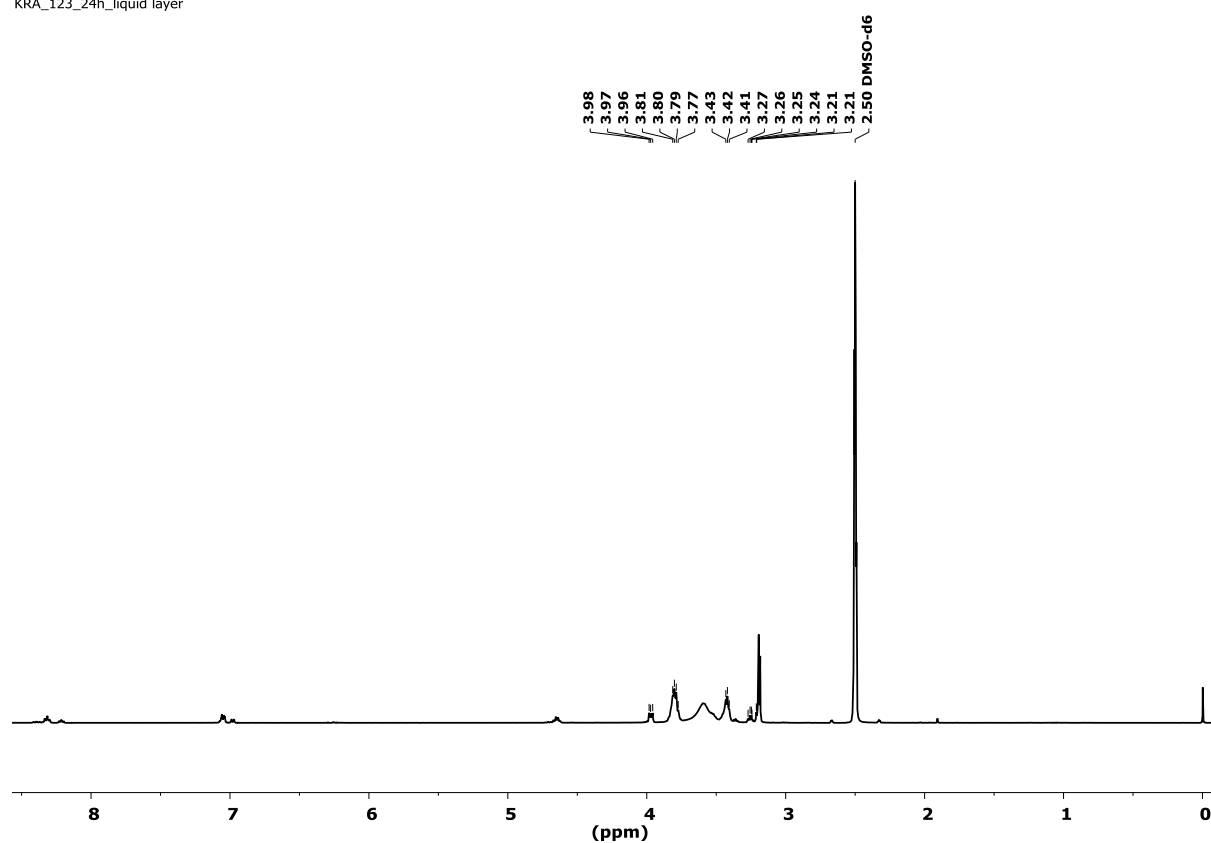


Figure S49. ^1H -NMR spectrum of liquid layer on top of precipitated polymer catalyzed by DMAP after 24 h reaction time in $\text{DMSO-}d_6$.

Result: OH-terminated oligomers, coordinated DMAP^+ species, cyclic side product (**1**)

1,4-oxathiane 4,4-dioxide (**1**) prepared from bis(2-hydroxyethyl) sulfone (HES)

In a 4 mL reaction vessel 4.7 mol% (4.7 mg, 0.084 mmol) KOH was dissolved in 428 mg (1.80 mmol) bis(2-hydroxyethyl) sulfone solution (65 wt% in water). The solution was put into an oven at 80 °C overnight. Exclusively 1,4-oxathiane 4,4-dioxide (**1**) was obtained as a brownish, off-white solid.

KRA-162, Ratzenboeck —

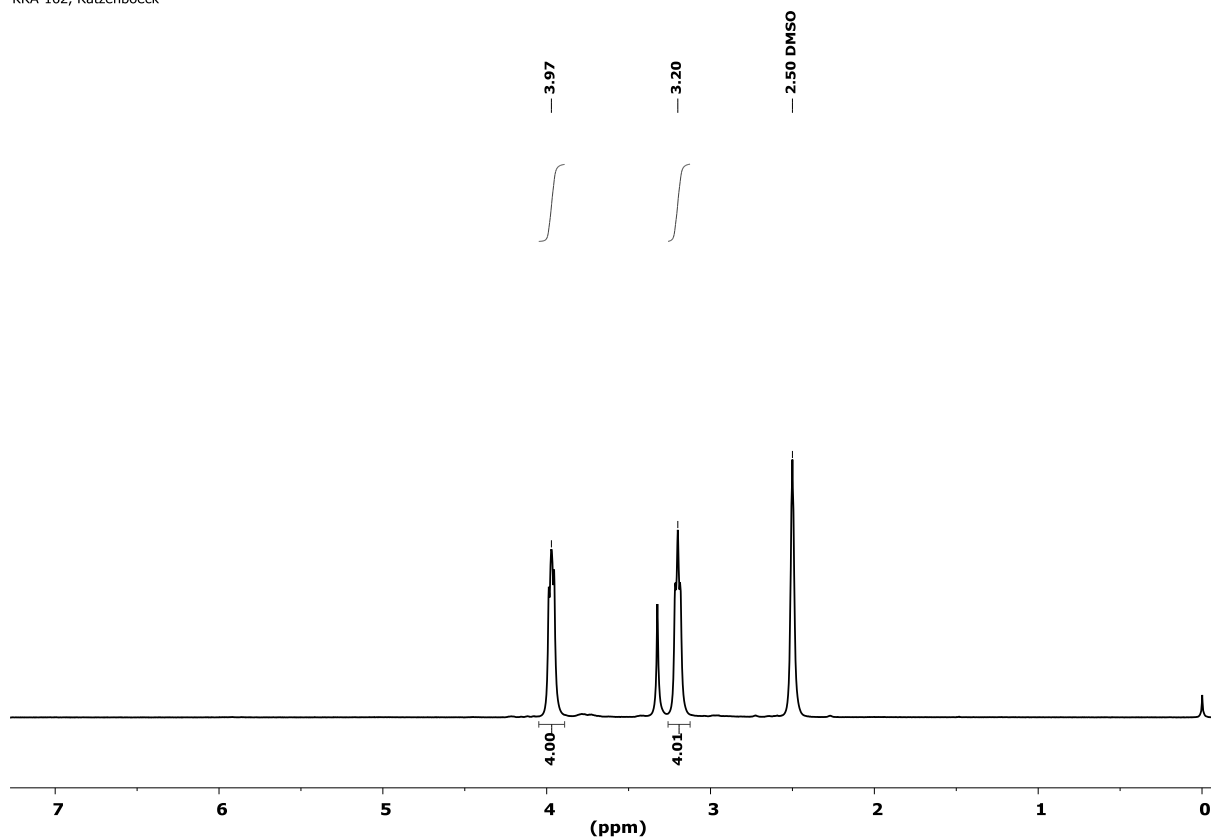


Figure S50. ¹H-NMR spectrum of 1,4-oxathiane 4,4-dioxide (**1**) prepared from 2-hydroxyethyl sulfone in DMSO-*d*₆.

10. Properties

PES	= semi-crystalline PES (without acidic work-up)
amorphous PES	= PES melted at 120 °C for 1 h (without work-up)
pure PES	= PES after acidic work-up

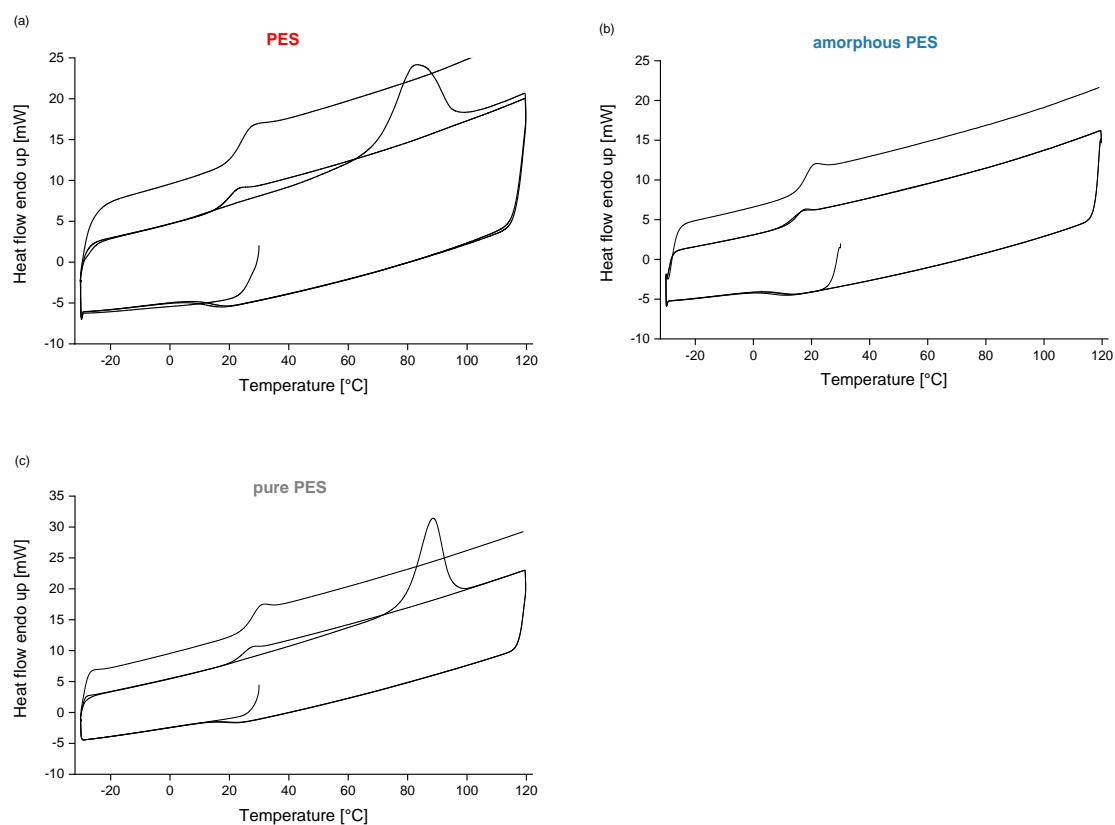


Figure S51. DSC spectra of **PES** (a), amorphous **PES** (b) and pure **PES** (c).

Table S4. DSC data of polymer; heating and cooling rate of 20 °C/min for the 1st and 2nd run and 40 °C/min for the 3rd run.

	T_g [°C]	T_g [°C]	T_g [°C]	T_m [°C]
	2nd heat run	3rd heat run	2nd cooling run	1st heat run
PES	18.7	22.8	11.4	82
amorphous PES	13.3	16.8	7.1	-
pure PES	23.6	26.6	16.2	88

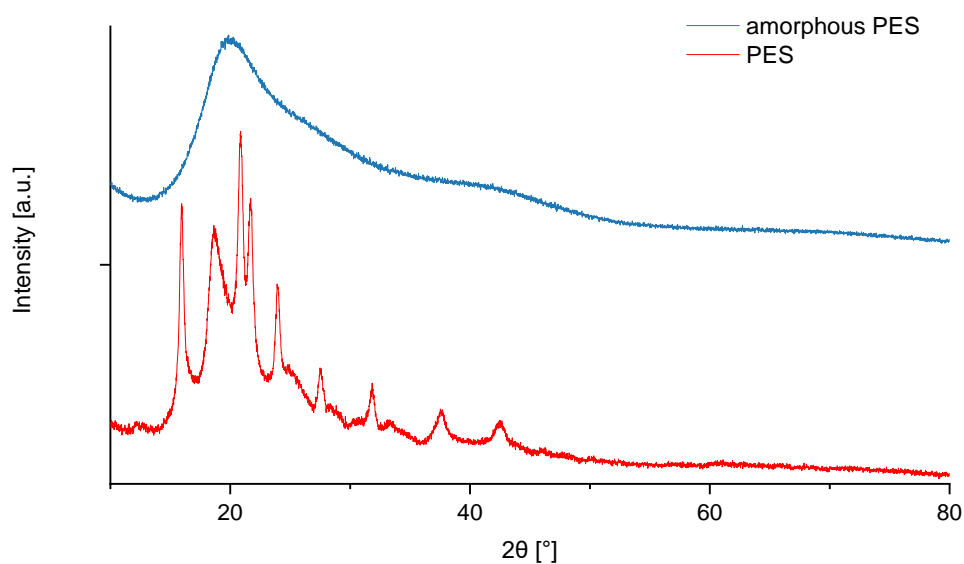


Figure S52. XRD spectrum of **PES** (crude powder) (bottom) and amorphous **PES** (after melting at 120 °C) (top).

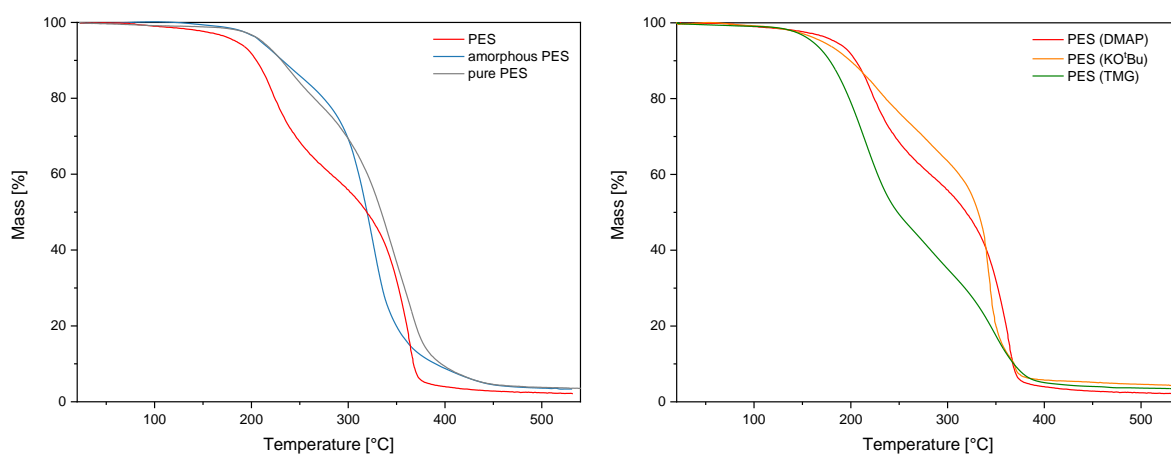


Figure S53. Thermogravimetric analysis of **PES** and pure **PES** compared to amorphous **PES** (left). Comparison of thermogravimetric analysis of **PES** prepared with DMAP, TMG and KO'Bu (right).

Table S5. Degradation onset temperature ($T_{d\ 95\%}$) determined of various polymer samples by TGA.

Sample	Temperature [°C] Mass loss 5%
PES (DMAP)	184
pure PES	211
amorphous PES	209
PES (TMG)	161
PES (KO'Bu)	171

11. Electrochemical Application

For the preparation of a solid polymer electrolyte (SPE) **PES** was synthesized on a large scale. A 50 mL round bottom flask was charged with 5.0 mol% (198 mg, 1.62 mmol) DMAP, 6.01 g (334 mmol, 10 equiv.) deionized water and 3.85 g (32.6 mmol, 1 equiv.) divinyl sulfone. The reaction mixture was stirred and kept at room temperature by cooling with a water bath. After 24 h reaction time, the supernatant was removed and the precipitated product was dried in vacuo. The yellow crude material (yield = 4.42 g (95%)) was used without further purification.

Sample preparation by solvent-free melt process:

The crude polymer (**PES**) was ground into a fine powder in mortar and pestle and dried in high vacuum. The dried polymer was mixed thoroughly with LiTFSI salt (pre-dried at 100 °C in vacuum) in stoichiometric ratios (0-20 wt.%) inside an argon filled glovebox with H₂O and O₂ levels < 0.1 ppm. The mixture was placed on a Teflon plate and transferred into an oven for melting at 120 °C overnight ($t \geq 16$ h). Thereafter, the melted electrolyte was slowly cooled down to room temperature and pressed into a uniform layer (thickness: 0.9-1.0 mm). Thereof, membranes were punched into discs of 12 mm diameter and further characterized. The obtained polymer membrane could easily be peeled-off the Teflon plate. The materials characteristics are soft, slightly sticky and formable.

Five different compositions of polymer membranes containing 0 wt.%, 5 wt.%, 10 wt.%, 15 wt.% and 20 wt.% LiTFSI were prepared.

The material of the SPE can be reused upon deformation or cutting. By putting it into an oven at 80 °C, the material again melts into a uniform piece which again can be pressed and cut into a membrane.

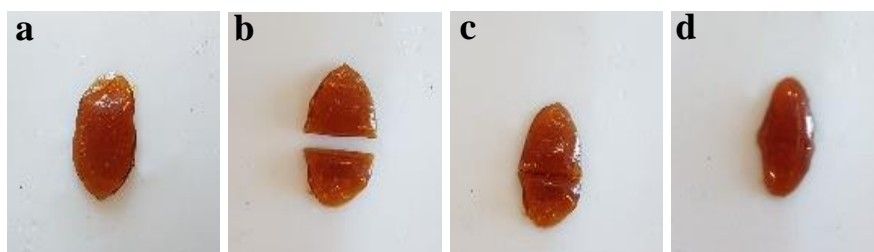


Figure S54. a) Membrane of SPE b) after cutting membrane in two pieces c) two pieces were aligned d) uniform melt after heating the material at 80 °C for 15 min.

Characterization

- PES** = semi-crystalline PES (without work-up)
- amorphous PES** = PES melted at 120 °C for 1 h (without work-up)
- SPE** = melted PES with 15 wt.% LiTFSI

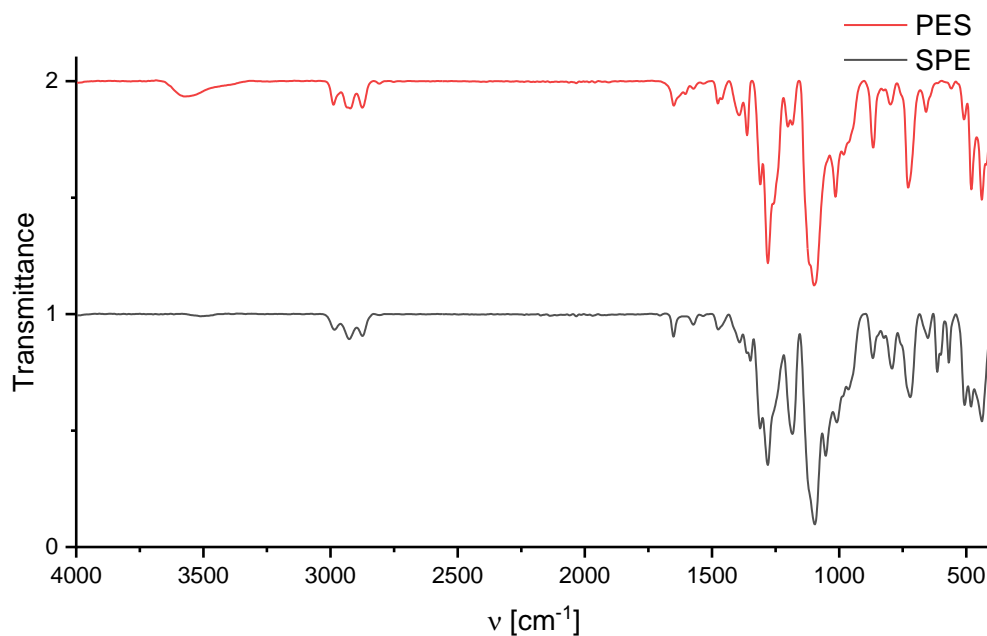


Figure S55. IR spectrum of semi-crystalline **PES** (top) and polymer electrolyte SPE (melted **PES** with 15 wt.% LiTFSI) (bottom). Bands at 1184 and 1053 cm^{-1} correspond to LiTFSI salt.

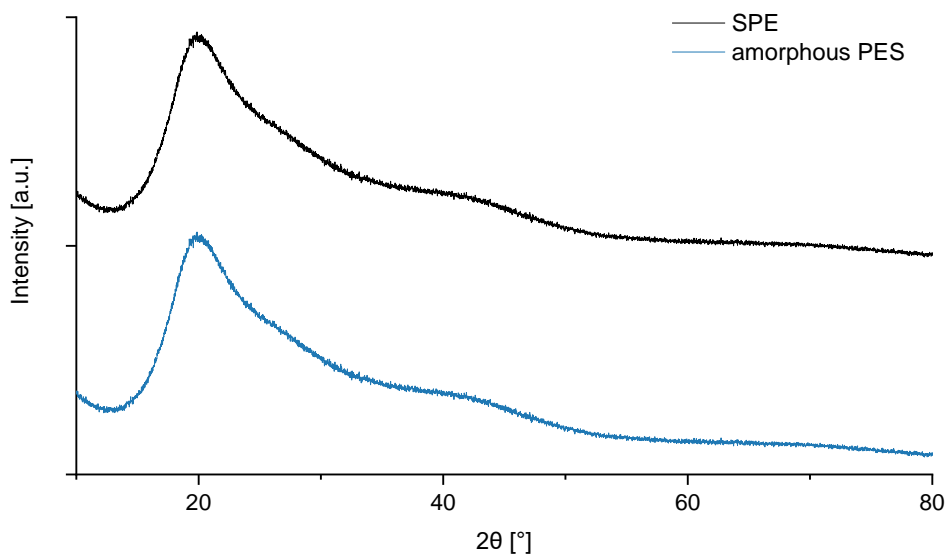


Figure S56. XRD spectrum of amorphous **PES** (bottom) and SPE (melted **PES** with 15 wt.% LiTFSI) (top).

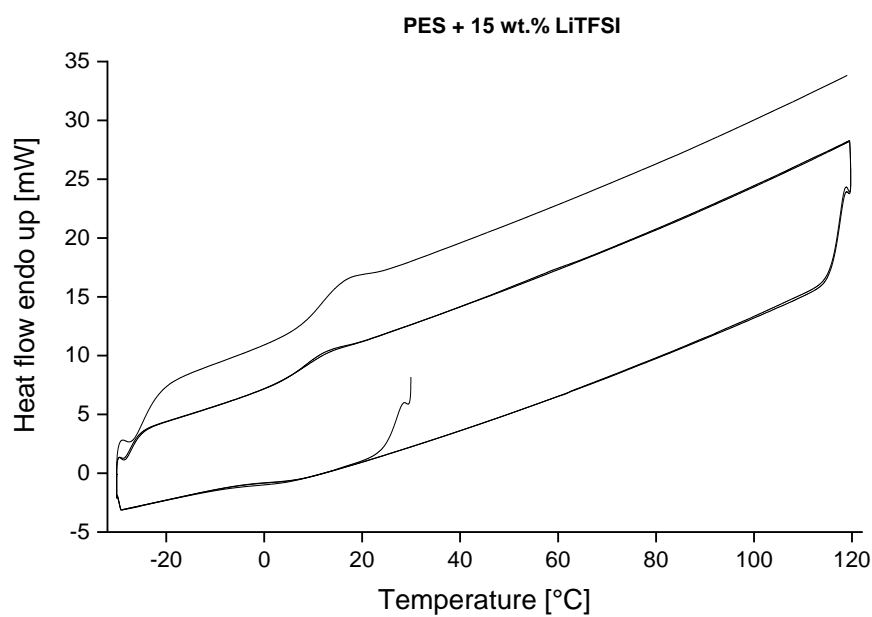


Figure S57. DSC spectrum of polymer electrolyte SPE (melted **PES** with 15 wt.% LiTFSI).

Table S6. DSC data of polymer electrolyte SPE (melted **PES** with 15 wt.% LiTFSI); heating and cooling rate of 20 °C/min for the 1st and 2nd run and 40 °C/min for the 3rd run.

	T_g [°C]	T_g [°C]	T_g [°C]	T_m [°C]
	2nd heat run	3rd heat run	2nd cooling run	1st heat run
amorphous PES	13.3	16.8	7.1	-
SPE	7.6	10.6	- 3.0	-

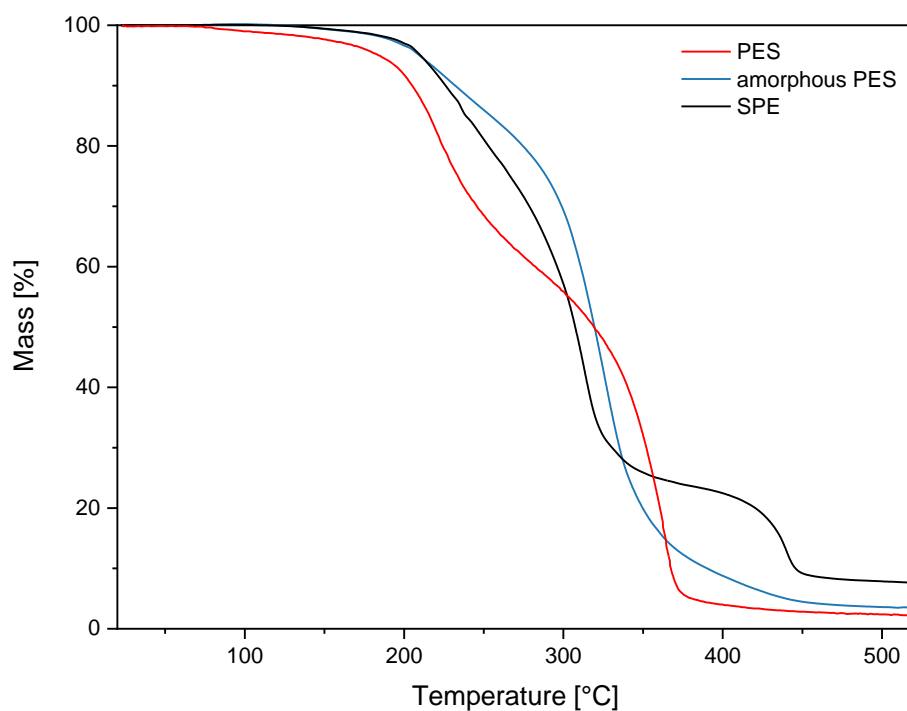


Figure S58. Thermogravimetric analysis of polymer electrolyte SPE compared to **PES** (red) and amorphous **PES** (blue).

Table S7. Degradation onset temperature ($T_{d\ 95\%}$) determined of amorphous **PES** and polymer electrolyte SPE by TGA.

Sample	Mass loss [%]	Temperature [°C]
amorphous PES	5	209
SPE	5	210

Electrochemical Impedance Spectroscopy (EIS)

The dried solid polymer membranes (discs of 12 mm diameter) were assembled into stainless steel Swagelok-type symmetrical cells inside an argon-filled glove box. EIS measurements were performed in a frequency range of 1 MHz to 1 Hz at 25 °C for all the compositions and from 25 °C to 100 °C for a membrane containing 15 wt.% LiTFSI, using Biologic VMP-300 impedance analyzer.

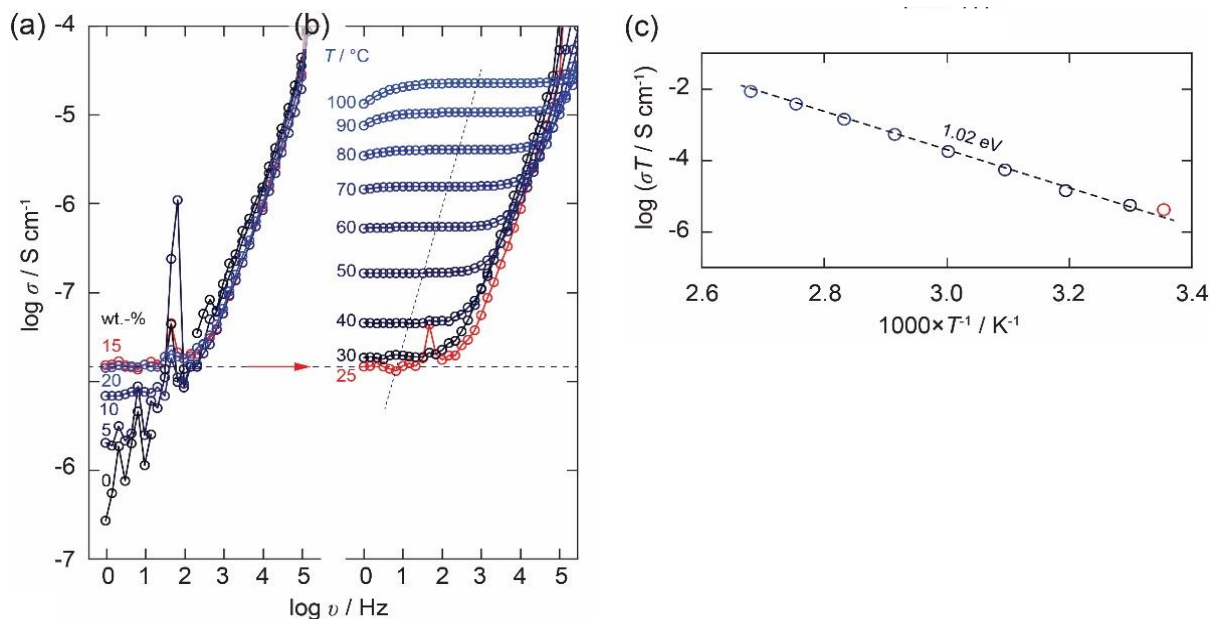


Figure S59. (a) Conductivity isotherms $\sigma'(\nu)$ of **PES** as a function of the salt concentration ranging from 0 to 20 wt.%. (b) Conductivity isotherms of **PES** incl. 15 wt.% LiTFSI recorded in a temperature range from 25 to 100 °C. (c) Arrhenius plot of the temperature dependence of the Li-ion conductivity of **PES** with 15 wt.% LiTFSI.

The real part of the complex conductivity as a function of the frequency is shown in Figure S59a. In general, such isotherms reveal three characteristic regions,^[15] (i) the electrode polarization towards low frequencies, (ii) the so-called DC conductivity plateau at intermediate frequencies (characterizes long-range ion transport), and (iii) the dispersive regime at high frequencies that is associated with the so-called nearly constant loss regime and is almost independent of temperature.^[16] The conductivity values, σ_{dc} , can be directly read off from the distinct dc-plateaus.

The corresponding Arrhenius plot ($\sigma_{\text{dc}}T$, plotted vs. $1000/T$) is shown in Figure S59c showing a linear behavior according to $\sigma_{\text{dc}}T = \sigma_0 \exp(E_a/(k_B T))$. Here, E_a is the activation energy, k_B denotes Boltzmann's constant, T is the absolute temperature and σ_0 represents the Arrhenius pre-factor.

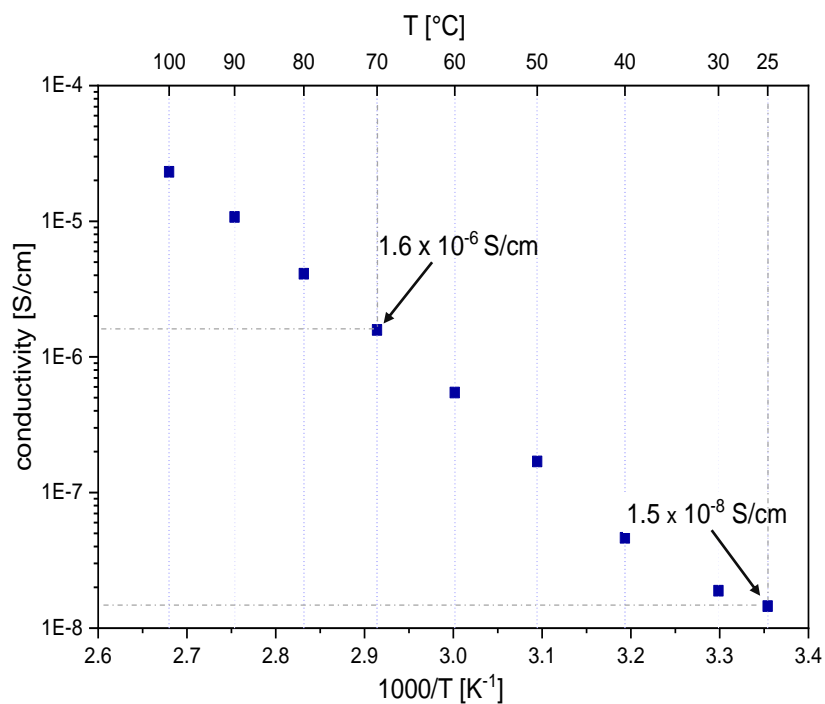


Figure S60. Temperature dependence of the Li-ion conductivity of **PES** with 15 wt.% LiTFSI.

Cell assembling

A two electrode cell was assembled in a Swagelok cell. The setup consisted of a stainless-steel electrode, the **PES** membrane as polymer electrolyte and a lithium metal as a reference electrode. Three cells were tested at 45 °C to confirm the stability of the polymer electrolyte.

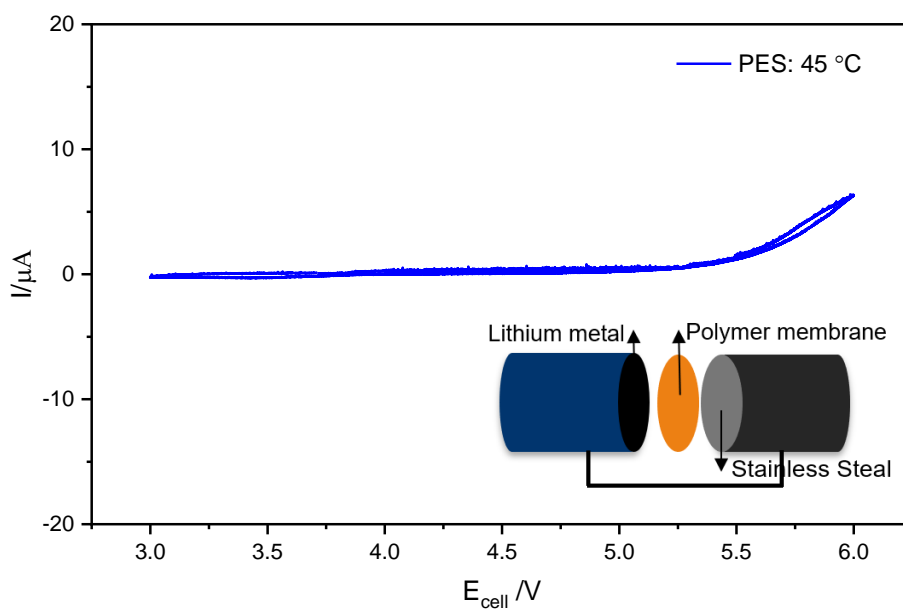


Figure S61. Cyclic voltammetry of **PES** membrane with 15 wt.% LiTFSI at a scan rate 0.1 mV/s.

12. References

-
- ¹ S. Strasser, C. Slugovc, Nucleophile-mediated oxa-Michael addition reactions of divinyl sulfone – a thiol-free option for step-growth polymerisations, *Catal. Sci. Technol.* **2015**, 5, 5091–5094. DOI: [10.1039/C5CY01527H](https://doi.org/10.1039/C5CY01527H)
- ² calculated using the pK_a prediction platform available at pka.luo-group.com see: Q. Yang, Y. Li, J.-D. Yang, Y. Liu, L. Zhang, S. Luo, J.-P. Cheng, Holistic Prediction of the pK_a in Diverse Solvents Based on a Machine-Learning Approach, *Angew. Chem. Int. Ed.* **2020**, 59, 19282–19291. DOI: [10.1002/anie.202008528](https://doi.org/10.1002/anie.202008528)
- ³ W. N. Olmstead, Z. Margolin, F. G. Bordwell Acidities of water and simple alcohols in dimethyl sulfoxide solution, *J. Org. Chem.* **1980**, 45, 3295–3299. DOI: [10.1021/jo01304a032](https://doi.org/10.1021/jo01304a032)
- ⁴ J. P. Guthrie Hydrolysis of esters of oxy acids: p K_a values for strong acids; Brønsted relationship for attack of water at methyl; free energies of hydrolysis of esters of oxy acids; and a linear relationship between free energy of hydrolysis and p K_a holding over a range of 20 p K units, *Can. J. Chem.* **1978**, 56, 2342–2354. DOI: [10.1139/v78-385](https://doi.org/10.1139/v78-385)
- ⁵ “TURBOMOLE 7.4.1.,” can be found under <https://www.turbomole.org/>
- ⁶ F. Neese, Software Update: The ORCA Program System, Version 4.0., *Wiley Interdiscip. Rev. Comput. Mol. Sci.* **2018**, 8, e1327. DOI: [10.1002/WCMS.1327](https://doi.org/10.1002/WCMS.1327)
- ⁷ COSMOlogic GmbH & Co KG, “COSMOconf 4.1”
- ⁸ J. P. Perdew, K. Burke, M. Ernzerhof, Generalized Gradient Approximation Made Simple, *Phys. Rev. Lett.* **1996**, 77, 3865–3868. DOI: [10.1103/PhysRevLett.77.3865](https://doi.org/10.1103/PhysRevLett.77.3865)
- ⁹ a) A. D. Becke, Density-Functional Exchange-Energy Approximation with Correct Asymptotic Behavior, *Phys. Rev. A* **1988**, 38, 3098–3100. DOI: [10.1103/PhysRevA.38.3098](https://doi.org/10.1103/PhysRevA.38.3098); b) C. Lee, W. Yang, R. G. Parr, Development of the Colle-Salvetti Correlation-Energy Formula into a Functional of the Electron Density, *Phys. Rev. B* **1988**, 37, 785–789. DOI: [10.1103/PhysRevB.37.785](https://doi.org/10.1103/PhysRevB.37.785); c) S. H. Vosko, L. Wilk, M. Nusair, Accurate Spin-Dependent Electron Liquid Correlation Energies for Local Spin Density Calculations: A Critical Analysis, *Can. J. Phys.* **1980**, 58, 1200–1211. DOI: [10.1139/p80-159](https://doi.org/10.1139/p80-159); d) P. J. Stephens, F. J. Devlin, C. F. Chabalowski, M. J. Frisch, Ab Initio Calculation of Vibrational Absorption and Circular Dichroism Spectra Using Density Functional Force Fields, *J. Phys. Chem.* **1994**, 98, 11623–11627. DOI: [10.1021/j100096a001](https://doi.org/10.1021/j100096a001)
- ¹⁰ S. Grimme, J. Antony, S. Ehrlich, H. Krieg, A Consistent and Accurate Ab Initio Parametrization of Density Functional Dispersion Correction (DFT-D) for the 94 Elements H-Pu, *J. Chem. Phys.* **2010**, 132, 154104. DOI: [10.1063/1.3382344](https://doi.org/10.1063/1.3382344)
- ¹¹ M. K. Kesharwani, B. Brauer, J. M. L. Martin, Frequency and Zero-Point Vibrational Energy Scale Factors for Double-Hybrid Density Functionals (and Other Selected Methods): Can Anharmonic Force Fields Be Avoided?, *J. Phys. Chem. A* **2015**, 119, 1701–1714. DOI: [10.1021/jp508422u](https://doi.org/10.1021/jp508422u)
- ¹² J. M. L. Martin, G. De Oliveira, Towards Standard Methods for Benchmark Quality Ab Initio Thermochemistry - W1 and W2 Theory, *J. Chem. Phys.* **1999**, 111, 1843–1856. DOI: [10.1063/1.479454](https://doi.org/10.1063/1.479454)
- ¹³ W. Kutzelnigg, J. D. Morgan, Rates of Convergence of the Partial-Wave Expansions of Atomic Correlation Energies, *J. Chem. Phys.* **1992**, 96, 4484–4508. DOI: [10.1063/1.462811](https://doi.org/10.1063/1.462811)

-
- ¹⁴ K. Oka, T. Shibue, N. Sugimura, Y. Watabe, B. Winther-Jensen, H. Nishide, Long-lived water clusters in hydrophobic solvents investigated by standard NMR techniques, *Sci. Rep.* **2019**, 9, 223. DOI: [10.1038/s41598-018-36787-1](https://doi.org/10.1038/s41598-018-36787-1)
- ¹⁵ K. Funke, C. Cramer, D. Wilmer in *Diffusion in Condensed Matter. Methods, Materials, Models* (Eds.: P. Heitjans, J. Kärger), Springer-Verlag Berlin Heidelberg, Berlin, Heidelberg, **2005**, pp. 857–893. DOI: [10.1007/3-540-30970-5_21](https://doi.org/10.1007/3-540-30970-5_21)
- ¹⁶ J. C. Dyre, P. Maass, B. Roling, D. L. Sidebottom, Fundamental questions relating to ion conduction in disordered solids, *Rep. Prog. Phys.* **2009**, 72, 46501. DOI: [10.1088/0034-4885/72/4/046501](https://doi.org/10.1088/0034-4885/72/4/046501)